Norwegian University
of Life Sciences

Master's Thesis 2024 60 ECTS
Faculty of Chemistry, Biotechnology and Food and science

Unveiling the Potential of Norwegian Fungi: Exploring LDPE Biodegradation for Sustainable Plastic Waste Management

Synnøve Dvergsdal
Biotechnology

Acknowledgement

Words cannot express my gratitude to all the volunteers who took the time to collect samples for me. This project would not have been complete without it. Also, thanks to every media platform spreading the information about the project and the need for samples. Here under Nynorsk press, Norges Bondelag and Bondebladet. A special thanks to Vestland Bondelag who sent e-mails to all the farmers in Western Norway.

I want to thank everyone at NVI and NMBU who helped me by answering my many questions, helped me organise myself at the lab and gave me training. I want to give a special thanks to Else Marie Aasen, who helped me organise the growth project at NMBU; Oscar Daniel Rangel Huerta, who helped me with R-studio coding; and Samantha Kim Pettersen, who helped me organize at the NVI laboratory.

I am grateful to my head supervisor, Ida Skaar, for not only teaching me about the fungal existence but also engaging with ideas, information, and motivation. Thanks to my co-supervisor, Bjørn Christian Schirmer, for also engaging in my master's project, contributing with chemistry facts, and giving me guidance. A special thanks my to co-supervisor Magdalena Monika Owczarek-Koscielniak for always been available to answer my questions (also at weekends) and explaining every little detail during lab training, giving me a much better understanding of how things work.

Lastly, I want to make a special thanks to my partner and family for taking care of dinner and housework in the most hectic periods allowing me to focus on my project.

Abstract

In this thesis we dive into the biodegradation process to investigate the fungal ability to degrade plastic, as previous reports show promising results. In 2020 a study done by NORCE investigated 43 rivers in western Norway and found that 70% of the plastic in the rivers consisted of agricultural plastic were silage plastic wrap dominated (Velle, 2020).

The amount of plastic produced is increasing. By nature, it could take over 1000 years to degrade plastic. While thermal degradation is environmentally hostile, recycling is restricted as the quality of process decreases after each recycling. Therefore, we need more sustainable ways to degrade the plastic.

Few studies have been done on Norwegian fungi's plastic degrading capabilities. Since fungi are very adaptable, it is possible that they can provide the needed enzymes for degradation and utilise plastic as a carbon source.

In this study the aim was to identify and test a low density polyethylene (LDPE) degrading fungus. The research is also a pilot for larger project — *Could fungi be Dr. Jekyll and Mr. Hyde in the plastic litter problem?* (Dr. Jekyll and Mr. Hyde).

Plastic from Norwegian farmers were collected. All collected samples went through metabarcoding. Selected fungi were isolated and identified through morphological characteristics and Sanger sequencing. Seven fungal species meeting the set criteria were isolated and cultured using three distinct media alongside LDPE, subjected to either photodegradation or kept unexposed. After 89 days of cultivation, the LDPE pieces were analysed for biodegradation evidence through weight, wettability, and topography. A possible clustering within fungal diversity was observed in samples originating from forest and samples originating from grassland. The family *Cladosporiaceae* was the most abundant of all taxonomic findings. After cultivation, there were no significant changes in LDPE weight, however several fungal species showed interactions with the plastic. While some fungi could adhere to only cracks, *Alternaria* sp. and *Cladosporium uwebraunianum* adhered to the LDPE surface. *C. uwebraunianum* showed the highest growth both on LDPE pieces with and without glucose available. SEM pictures of the fungus showed strong attachment to the LDPE and indicate that some kind of anchoring between the fungus and LDPE has occurred. This thesis is the first to report that *C. uwebraunianum* show a plastic degrading potential.

Sammendrag

I denne studien dykker vi inn i biodegraderingsprosessen for å undersøke om sopp har mulighet til å bryte ned plastik, siden tidligere studier har vist lovene resultater. I 2020 gjennomførte NORCE en studie der de undersøkte 43 elver på Vestlandet. Deres funn viste at 70% av plasten som de fant i elvene bestod av landbruksplast. Av denne plasten dominerte rundballeplast.

Mengden plastikk som produseres øker. Naturlig nedbrytning av plastikken kan ta over 1000 år. Termisk nedbrytning er ikke miljøvennlig og gjenbruk er begrenset da kvaliteten på plasten synker for hver resirkulering. Derfor trenger vi mer bærekraftige måter å bryte ned plasten på.

I Norge finnes det få studier på norske sopper sine plastnedbrytende egenskaper. Siden sopper er veldig tilpasningsdyktige, er det veldig mulig at de kan skille ut enzymene som trenges for degradering og utnytting av plasten som karbonkilde.

I denne studien var målet å identifisere og teste en low density polyethylene (LDPE) nedbrytende sopp. Studien er også en pilot for ett større prosjekt — *Could fungi be Dr. Jekyll and Mr. Hyde in the plastic litter problem?* (Dr. Jekyll and Mr. Hyde).

Rundballeplast ble samlet inn fra norske bønder og analysert gjennom metabarkoding. Utvalgte arter ble identifisert gjennom morfologiske trekk og sanger sekvensering. Syv sopp arter som oppfylte satte kriterier ble isolert og kultivert sammen med LDPE som enten var eksponert for fotodegradering eller ueksponert. Etter 89 dager med kultivering ble LDPE-bitene analysert for tegn på biodegradering gjennom måling av vekt, fuktbarhet og topografi.

En mulig gruppering i soppdiversiteten ble observert hos prøver som stammet fra skog og prøver som stammet fra gressmark. Metabarcodingen viste at familien *Cladosporiaceae* var den mest hyppige av de taksonomiske funnene. Ingen signifikant vektreduksjon for LDPE- bitene ble observert etter dyrkning, men det ble derimot observert interaksjoner mellom flere av soppene og plastikken. Mens noen sopper bare festet seg til sprekker i plasten, kunne *Alternaria* sp. og *C. uwebraunianum* feste seg til LDPE overflaten. *C. uwebraunianum* viste størst vekst både på LDPE som hadde glukose tilgjengelig og ikke tilgjengelig. SEM bilder viste at soppen var sterkt festet med indikasjoner på at soppen forankret seg i LDPE-biten. Denne studien er den første rapporten om at *C. uwebraunianum* har et plastdegraderings potensial.

Abbreviations

act	–	Partial actin gene
bt2	–	Tubulin β chain II
cal	–	Partial calmodulin gene
DG18	–	Dichloran glycerol 18
EM	–	Electron microscopy
ITS	–	Internal transcribed spacer
LDPE	–	Low density polyethylene
LiP	–	Lignin peroxidase
LSU	–	Large subunit
MPa	–	Megapascal
MnP	–	Manganese peroxidase
MSM	–	Mineral salt media
NSM	–	Nucleotide substitution model
OTU	–	Operational taxonomic unit
PA	–	Polyamide
PCR	–	Polymerase chain reaction
PE	–	Polyethylene
PET	–	Polyethene terephthalate
PP	–	Polypropylene
PS	–	Polystyrene
PVC	–	Polyvinyl chloride
rpb1	–	RNA polymerase I
rpb2	–	RNA polymerase II
SEM	–	Scanning electron microscopy

tef-1α	–	Translation elongation factor 1-α

Table of contents

Table of figures

1. Introduction

1.1 Plastic

Plastic waste is a major challenge for the environment. It spreads chemical pollution, occupies space and may harm wildlife, both in the form of macroplastics, in which animals get entangled, and microplastics, which are ingested. It may also serve as a vector for microorganisms, thereby driving the spread of antibiotics. (Secchi and Zarzur, 1999, Geyer, 2020, Tuvo et al., 2023). But who can imagine a life without plastic nowadays? We have become so dependent on plastic that we trust it with our own lives. People are driving cars at 80 km/h, relying on a belt dominated by plastic to hold if a crash should occur. Plastic is cheap and is used in multiple fields like electronics, packaging, furniture, textiles, and many others (Geyer, 2020). Breaking free from plastic is becoming more challenging as new products with plastic are developed and incorporated into people's daily lives.

Plastic history

In 1907, the first synthetic plastic was developed by Leo Bakeland. This new structure contained the chemical components formaldehyde and phenol (Landmarks., 1993). The not fully synthetic polymer, Bakelite, was thermo-resistant and the polymerisation reaction was irreversible. Due to a shortage of other materials during the Second World War, the need for plastic increased. In the subsequent years, plastic emerged as an alternative to reusable packaging, replacing it with convenient disposable packaging (Geyer, 2020). The commencement of plastic manufacturing is frequently attributed to the 1950s, primarily due to the availability of data from that era. The massive plastic production was driven by the increasing range of applications for plastic materials. Chemical additives had also been introduced to enhance the flexibility of the pure polymer, leading to a diversification of properties. Consequently, this led to the proliferation of polymers and additives, which collectively constitute the plastics we recognise today (Geyer, 2020).

Facts about plastic

Plastic is a term for synthetic organic polymers classified according to various properties (Geyer et al., 2017). It can be categorised based on whether its carbon source is fossil – reported to be predominant, or biogenic in nature. Most of the plastics are made of hydrocarbons. Among important properties plastic can possess the ability to be heated and reshaped. These types are recognised as thermoplastics. While others do not inhabit this ability – these are called thermosets. The best-known thermoplastics are polyethylene (PE), polypropylene (PP), polyvinyl chloride (PVC), polyethene terephthalate (PET), polystyrene (PS) and polyamide

(PA). Since they are all fusible when heated, they are much easier to recycle in contrast to thermosets like polyurethanes (PUR). Packaging is the most common use for plastic. 90% of the plastic being used as packaging consists of PE, PP, or PET. PE and PP are the most commonly produced plastic types globally. In year 2017 PE and PP accounted for 45% of the globally produced plastic (Geyer, 2020).

LDPE

PE has the most basic polymer structure consisting of a repetitive CH_2 chain, and as mentioned earlier, is one of the most common synthetic polymers. There are different forms of PE, like for example low-density polyethylene (LDPE), linear low-density polyethylene (LLDPE) and high-density polyethylene (HDPE). The differences between the different PEs are the branch length and number that decide their properties such as heat tolerance, stiffness, and airtightness. LDPE was the first PE developed (Vasile and Pascu, 2005). It is often used in packaging, as bags and plastic films (Geyer, 2020). The low density originates from the polymer chain branches, the long side branches are preventing tight packing of the polymer (figure 1). One of the LDPE appreciated properties is corrosion resistance that includes resistance to organic solvents, chemicals, and weather. It is still somewhat flexible at low temperatures and has a low water absorption tendency (Vasile and Pascu, 2005).

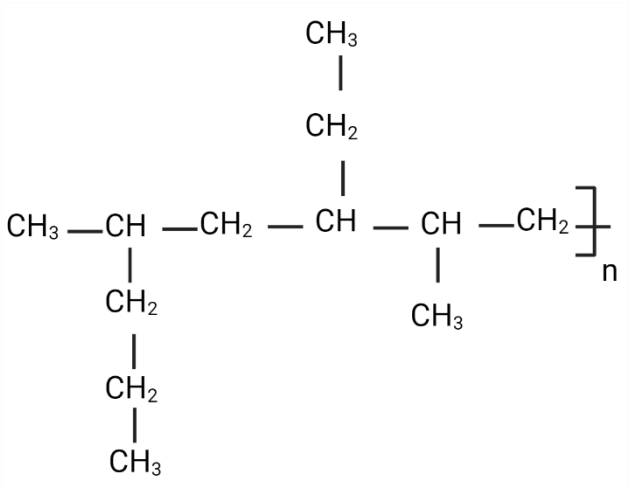

Figure 1: LDPE chemical structure. Figure was created with BioRender.com.

Negative consequences of plastic

The spread of plastic in the environment is an undesirable consequence of the plastic industry (figure 2). The presence of plastic in the nature can cause severe damage to the wildlife, as animals can get stuck in plastic litter and drown or suffocate; they may also accidentally

ingest plastic litter, thereby suffering from energy depletion (Secchi and Zarzur, 1999, Ekanayaka et al., 2022, Wright et al., 2013).

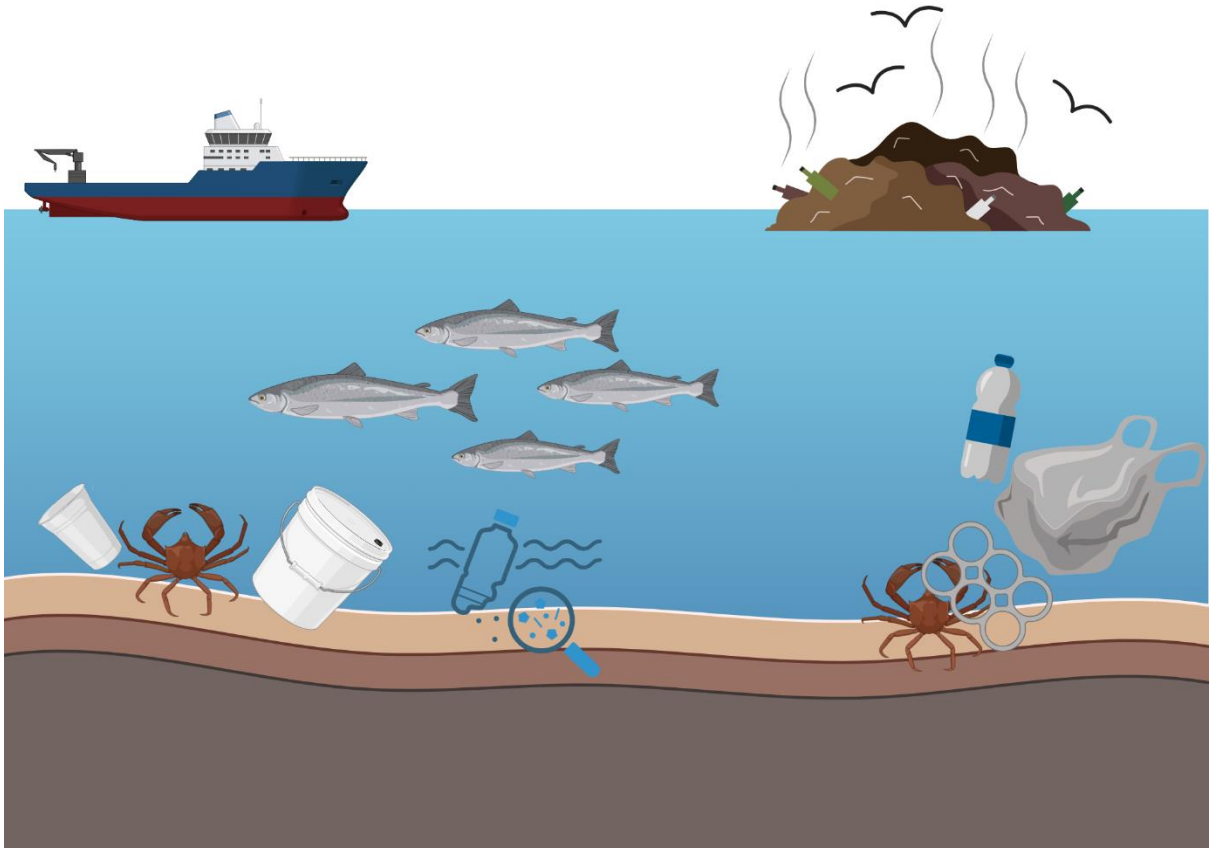

Figure 2: Plastic accumulation in the ocean illustration. Figure was created with BioRender.com.

In society high durability makes plastic preferable, but in nature this trait is undesirable. It has been estimated that natural biodegradation could take 10 to 1000 years, depending on the plastic type (Chamas et al., 2020). In 2015 approximately 79 % of the 6,300 tons of plastics that were generated were accumulated in the natural environment or landfills (Geyer et al., 2017). As early as the 1970s, reports came out about plastic pollution in the sea where the plastic is degraded, accumulated, and eaten by marine organisms (Jambeck et al., 2015, Thompson et al., 2004). Despite plastic already polluting the environment, new plastic continues to be manufactured. The annual plastic production has increased from 1.5 million tons to 335 million tons between the years 1950 and 2016 (Li et al., 2021). In total, the amount of primary plastic produced from 1950 reached 9.2 billion metric tons in 2017 (Geyer, 2020). This corresponds to the volume of 36,682 times the largest cruise chip in the word, the Icon of the Seas. Since plastic production seems to be an increasing trend it is reasonable to believe that the amount of plastic waste will grow and accumulate if no efficient solution is implemented.

Recycling

The plastic use duration time varies from days, to weeks, to years. When it comes to packaging, the plastic is only in use during shipping and storage. Some solutions for reducing the accumulation of plastic waste are degradation and recycling. Recycling is an important part of lowering greenhouse gas emissions by reducing the levels of plastic production (Morris, 1996). Recycled plastics are often referred to as secondary plastics. Even though recycling is a possibility that is favoured by the environment, most of the plastics are disposed of. It has been estimated that, in the period between 1950 and 2017, 76% of all plastic produced was discarded and ended up in either landfills, dumps or the natural environment. In 2017, the generation of primary and secondary plastic waste reached 380 metric tons, of which 18% were recycled, while 26% were incinerated and 56% discarded. This is a progress compared to previous years. The total historical recycling rate of plastic waste so far is 10%; however, this calculated percentage from incinerated and recycled plastics might be overestimated due to restricted information available. The reason why the total historical recycling rate is low could be due to the fact that the formal recycling and incineration of plastic waste didn't start until the 1980s. Now, chemical or mechanical treatment can be used to recycle plastic. While chemical treatment separates polymers to monomers, mechanical treatment results in granules (Geyer, 2020). Chemical treatment gives the most valuable products but has a greater negative environmental impact (gas emissions) and is more expensive (Voss et al., 2022, Geyer, 2020). This could be the cause why the mechanical recycling dominates. There are a few reasons why the reuse of plastic remains low. It is difficult to keep the price for collecting and reprocessing plastic lower than the production itself. Recycling also tends to be more difficult when the plastic is contaminated and mixed with other materials. While thermoplastics can be melted and reused after recycling, plastics like thermosets and the combination of thermosets and thermoplastics present a challenge when it comes to recycling (Geyer, 2020). The plastics will eventually meet their end of use due to reduced quality after recycling or reuse (Zink and Geyer, 2019). This ending point could be incineration, biodegradation or accumulation in the environment or landfills (Geyer, 2020).

Plastic use in agriculture

There are many industries that depend on plastic. In Norway, where agriculture, forestry, and fishing accounted for 11% of the total plastic waste in 2017, plastic is collected after use and then subjected to treatment and recycling. The cost of this recycling strategy is covered by importers and producers as a packaging fee. Silage wrap, consisting mostly of LDPE, and

constitutes the majority of recycled agricultural plastic (Statistisk-sentralbyrå, 2020, Korol et al., 2021). A silage wrap is a plastic foil wrapped around a ball of grass followed by an ensilage process inside the ball that preserves the grass. This is an important way to store and preserve agricultural food in the northern countries. The plastic separates the grass from the environment, preventing spoilage by its ensilage properties and lowering storage costs (Korol et al., 2021). The recycling strategy, however, still faces problems. Even though much of the plastics distributed in Norway is recyclable, imported plastic, lacking this property, is also prevalent. The statistics (provided by Grønt Punkt Norge, 2022) are not sufficient to determine the exact amount of plastic purchased in agriculture due to private imports. According to the numbers available, the material recycling was 77.1% in 2022 (Grønt-punkt-Norge, 2022). The collection of plastic demands a certain amount of energy that varies by the distance from farm to recycling point, but this is the solution that exists today.

1.2 Degradation of PE

As a result of degradation, materials undergo chemical changes that alter their properties and characteristics (Yousif and Haddad, 2013). There are many ways to degrade plastic, including chemical degradation, thermal degradation, photodegradation and irradiation. They all have different active agents.

Photodegradation

Photodegradation uses UV-light or radiation with high energy to degrade polymers. It is an environmentally friendly, but very costly, way to degrade plastic (Shah et al., 2008). Different plastic materials can absorb photons at different wavelengths in the ultraviolet part of the spectre and some are more photostable than others (Shah et al., 2008, Fairbrother et al., 2019). While UV-A and UV-B degrades the polymer directly, visible and infrared light indirectly contributes to degradation by heat. The high energy from UV-radiation can cause oxidation reactions that promote the polymer chains to break, thereby reducing the molecular weight (Shah et al., 2008). The polymer sensitivity for UV-degradations differs between polymer structures. For example, LDPE is less photostable than HDPE (Fairbrother et al., 2019). The polymer sensitivity can also be affected by additives. Industries that sell plastic wrap often use UV-stabilizers combined with LDPE in silage balls to protect the plastic against UV-radiations from the sun (Yousif and Haddad, 2013, Triowrap, 21.05.14). Degradation, by natural UV- radiation from the sun can also promote microbial growth by creating nutrients for bacteria and fungi (Yao et al., 2022).

Biodegradation

The most cost efficient and environmentally friendly way to degrade plastic is through biodegradation (Ekanayaka et al., 2022). Biodegradation is a degrading process in the biosphere where microorganisms are contributing to the process, ensuring that organic compounds are degraded to less complex compounds (Hodzic, 2004). The end-products from aerobic plastic bio-degradation are CO_2 and water, while anaerobic degradation additionally produces methane (Shah et al., 2008). Biodegradation of plastic depends on factors like temperature, type of microbes, and humidity. The biodegradation rate can vary from weeks, decades to centuries, depending on the plastic's degree of hydrophobicity, polymer structure and molecular weight (Geyer, 2020, Wilkes and Aristilde, 2017). Some plastics are produced as biodegradable polymers, but this is a small fraction of the total plastic production (Geyer, 2020). Bacteria and fungi have been reported to degrade different types of plastics like PE, PP and PS (Yuan et al., 2020). Studies have shown that a pretreatment of plastic with UV-light can increase the plastic biodegradation rate (Yamada-Onodera et al., 2001, Albertsson et al., 1987, Taghavi et al., 2021). The plastic absorption of UV-light promotes reactions with oxygen that make it possible for carbonyl groups, hydroxyl group and hydroperoxide groups to form on the polymer backbone in PE (Lee and Li, 2021). This increases the plastic hydrophobicity and lowers the plastic molecular weight, thereby increasing the possibility of interactions with microorganisms. The carboxyl group can further undergo β-oxidation, a process in which fatty acids are degraded and contribute with acetyl-CoA in the krebs cycle (Albertsson et al., 1987, Schulz, 2013).

Enzymes involved in biodegradation

As mentioned above, microorganisms cannot assimilate large polymers and usually require depolymerization to a size lower than 50 carbon atoms (Chen et al., 2020). This may be achieved through hydrolysis or oxidative degradation as a result of depolymerase activity (Yuan et al., 2020). Much of the information about plastic biodegradation are visualizations, and it is poorly explored which enzymes mediate plastic degradation (Chen et al., 2020).

Oxidative degradation

While other plastic types can be degraded through hydrolysis, PE is resistant to this process due to the non-hydrolysable C-C backbone. Therefore, enzymes that are able to degrade PE are found to preform oxidative degradation (Krueger et al., 2015). Enzymes that normally degrade C-C bonds in lignin have been found to also degrade C-C bonds in polyethylene (Chen et al., 2020). Some of the enzymes that have been reported to perform oxidative degradation on

PE are manganese peroxidase (MnP, EC 1.11.1.13), laccase (EC 1.10.3.2) and lignin peroxidase (LiP, EC 1.11.1.14) (Mukherjee and Kundu, 2014). The enzymes that degrade C-C bonds in lignin are not expected to be as efficient in the degrading of PE, due to the high redox potential requirement for cleaving the C-C backbone in PE (Chen et al., 2020). After the formation of phenolic substances in PE from the first biodegradation step, enzymes like laccase (EC 1.10.3.2) can step in and oxidise the produced phenolic compounds. These enzymes are restricted to phenolic substances due to the low redox potential, but through the laccase mediator system they can indirectly cleave C-O and C-C bonds (Abdel-Hamid et al., 2013). The same applies to MnP. This enzyme is restricted to phenolic lignin compounds, but the presence of carboxylic acid can mediate oxidation of non-phenolic lignin through radical formation. In contrast, the enzymes LiP and versatile peroxidase (VP, EC 1.11.1.16), can directly oxidise non-phenolic lignin compounds (Qin et al., 2017). A study by Ericka Santacruz-Juàrez et al. (2021) shows that the enzymes MnP, LiP and laccase can have a synergetic effect on each other in the natural environment. As a side product, the laccase enzyme can produce hydrogen peroxide after degrading PE (Santacruz-Juárez et al., 2021). While laccase uses oxygen as a final electron acceptor, MnP and LiP use hydrogen peroxide (Yao et al., 2022). Laccase can therefore drive the MnP and LiP oxidation in the nature (Chen et al., 2020). VP is an enzyme found in white rot fungi, that functions as a hybrid of both MnP and LiP (Abdel-Hamid et al., 2013). Another fungal enzyme is unspecified peroxygenase (UnP, EC 1.11.2.1) that has shown promising cavital features for potential PE degradation, but this bioreaction process is not yet fully studied (Santacruz-Juárez et al., 2021).

Fungi

As written above, the first step of the biodegradation is focused on weakening the polymer structure and changing the non-reactive chain into a reactive one. Microorganisms can contribute to this process by making cracks and lowering pH of the surrounding. Fungi can also contribute to this step by secreting hydrophobins to lower the polymer hydrophobicity and enlarging the pores in the polymer by using mechanical force of penetrating hyphae (Temporiti et al., 2022). Enzymes like laccase, MnP and LiP can then be extracellularly secreted from fungi and degrade PE to carboxylic acids that can enter the Krebs cycle after β-oxidation (Santacruz-Juárez et al., 2021). A review study by Ekanayaka et al. (2022) confirmed that there have been identified 11 plastic degrading classes of fungi within the phyla *Ascomycota*, *Basidiomycota*, and *Mucormycota*. Most of the plastic degrading fungi can be found in the class *Eurotiomycetes* in the *Ascomycota* phylum. This class contains genera like *Aspergillus* and *Penicillium*. These

genera include species that can degrade PE and/or LDPE (Ekanayaka et al., 2022). studies also showed that *Aspergillus* species can use plastics like PU and LDPE as their sole carbon source, but the PE degradation was more efficient with additional carbon in fungal growth media (Dsouza et al., 2021, Khan et al., 2017).

1.3 Methods

Separation of fungi from plastic surface

To study the fungal diversity in plastics, fungal cells need to be detached from the plastic surface. Plastics with reduced hydrophobicity is often more prone to biofilm formation (Ganesan et al., 2022). A biofilm is a complex microbial community surrounded by a protective extracellular matrix (López et al., 2010). An extracellular matrix is a network consisting of many proteins and other molecules that are secreted by the microbial community (Yue, 2014). Together with bacteria, many fungi are often involved in biofilm creation by secreting extracellular polymeric substances (EPS) (Breitenbach et al., 2022, Di Martino, 2018). Plastics like LDPE can be a platform for biofilm formation (Fanning and Mitchell, 2012, Cholewińska et al., 2022). In order to separate microorganisms and biofilm from the developing on a plastic, sonication can be used. This is a process were ultrasound energy in water results in cavitation. This leads to formation of growing and imploding water bubbles. The mechanical force from this process can disrupt biofilms and cells thereby ensuring that cells detach from the solid surface (Esclapez et al., 2011). Sonication is not only an affordable method for extracting the microbial community from the plastic, but also timesaving, compared to other methods (Battulga et al., 2022, Esclapez et al., 2011).

Fungal identification

For identification of fungi, macroscopical and microscopical approaches can be employed. The macroscopical identification of fungi involves studying the difference in physical traits that can be observed with the naked eye, like colour, shape and size of a colony (Ab Majid et al., 2015). When studying a stained fungal slide under a microscope, more detailed information about the conidia and hyphae can be gained and used for identification. When using microscopic techniques for identifying fungi, fungal slides are often stained for example with lactofuchsin which binds to the fungal cell wall colouring it deep pink. Use of 95% ethanol is a common pretreatment of the slide to make it more receptive towards the staining (Li et al., 2007). It can though be difficult to use morphology alone for identification, and these methods are not completely precise at levels lower than family or genus level and may therefore not support reproducibility. To obtain good resolution and reproducibility in the identification

process, reaching to the species level, molecular identification is used (Raja et al., 2017). Molecular identification can be performed by a DNA barcoding that involves sequencing and analysis of a specific DNA sequences combining conserved and variable fragments, that serve as molecular markers (Yang et al., 2018a). A very popular approach that uses this strategy for a mass identification of complex samples is called metabarcoding.

Metabarcoding is a method for analysing biodiversity through amplification and high throughput sequencing of a specific genetic marker for the specific community members (such as fungi, bacteria, etc.) that are studied. The taxonomical classification is done through comparison with reference databases. One of the advantages that makes this method popular is its low cost (Forsman et al., 2022). The taxonomic resolution of the metabarcoding approach depends on the universal primers, quality, and availability of the reference sequences in databases and genetic marker used (Forsman et al., 2022, Tedersoo et al., 2022). However, results are limited to some taxonomical groups.

ITS as a genetic marker

Ribosomes are essential for life due to their protein producing function. Genes encoding ribosomal activity lie in the ribosomal DNA (rDNA) and are highly conserved and present in multiple copies (Wang and Lemos, 2019, Lofgren et al., 2019). This makes the rDNA region an attractive target for organism identification, also in the case of fungi. The most popular genetic markers are located in the rDNA operon and consist of the SSU (18S) srRNA gene, the internal transcribed spacer (ITS) and the *LSU* (28s) rRNA gene. The ITS region is more variable than SSU and *LSU* and is therefore preferred for studies of lower-level phylogenetic classification, like species and genus level (Kauserud, 2023, Tedersoo et al., 2022). The ITS consists of ITS1 and ITS2 subregions separated by the 5.8S gene (figure 3). The conserved parts that flank the ITS region make it possible to use universal primers

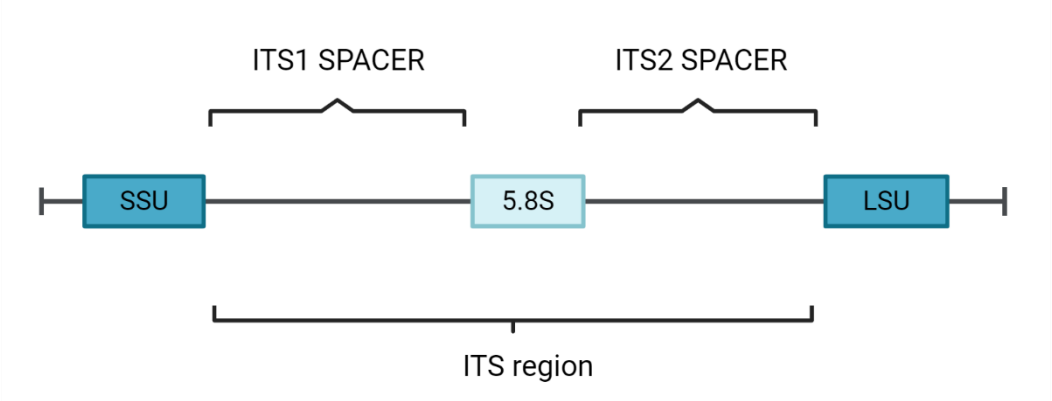

Figure 3: The schematic rDNA operon. The illustrated boxes do not corelate with the gene size. Figure was created with BioRender.com

The ITS region length can vary between fungal genera from approximately 260 bp to 1,800 bp and the average length in the kingdom fungi is approximately 517 bp (Yang et al., 2018b). Therefore, many fungal ITS regions exceed the maximum reading range for Illumina sequencing platforms that typically ranges from 150 to 300 bp (Illumina, 2023). The long length of the ITS region, hence, forces scientist that use second generation sequencing technology either of the ITS1 or ITS2 subregion in a single run (Nilsson et al., 2019a, Tedersoo et al., 2022). Even though this solution does not have the same number of suitable primers as the whole ITS region and has a lower taxonomical resolution, they offer an economically efficient way to perform metabarcoding (Amarasinghe et al., 2020, Tedersoo et al., 2022, Yang et al., 2018b). TS1 and ITS2 give similar resolution towards the fungal diversity within some groups, yet, individually they have some drawbacks (Blaalid et al., 2013, Monard et al., 2013, Yang et al., 2018b, Wang et al., 2015, Mbareche et al., 2020). For effective sequencing, amplification through polymerase chain reaction (PCR) of the target region is often performed, in order to increase the number of copies of the desired sequence.

PCR

PCR works by replicating the DNA fragments from a sample. The replication process involves several (usually 20-35) cycles of three following steps – denaturation, annealing and extending of a DNA-template. In the denaturation step the high temperature, usually 94-98 ºC cause hydrogen bonds between the DNA strands in the double helix to break, separating the DNA strands (Lorenz, 2012, McPherson and Møller, 2000). In the annealing step the temperature is lowered in order to enable oligonucleotide primers to bind to the compatible site at the DNA-template strand (McPherson and Møller, 2000). Annealing temperature is selected based on the primer melting temperature (T_m) and melting temperature of the target sequence. Primer T_m is determined by the GC-content in primer, salt content in buffer and other reactants

that have been added to the PCR solution (ThermoFisher-Scientific). The oligonucleotide primer's role in this process is to guide and create a starting point where the DNA polymerases can start the replication process. One primer is targeting the reverse strand (reverse primer), while another primer is targeting the forward strand (forward primer). In the extending stage the temperature increases to the DNA polymerase working temperature. DNA polymerases then complete the starting points in both forward and reverse strand by working in 5`to 3` direction and inserting deoxynucleotides (dNTP). The dNTPs that are compatible with the DNA-template are inserted to build a complementary DNA strand. This cycle is further repeated under pre-selected number of cycles. There are several types of DNA polymerases but the most predominantly used ones are *Taq* DNA polymerases, known for their heat-stability (McPherson and Møller, 2000). PCR is often used in metabarcoding to amplify the genetic markers found in the microorganisms to secure that no low abundant species information get lost and to highlight DNA from the intended organism (Tedersoo et al., 2022, Kelly et al., 2019). This amplification process also secures enough DNA for further analysis. Some of the negative effects of the amplification processes are that the amplification efficiency can impact the community composition results. It is therefore important to use proper primers (Kelly et al., 2019). Some of the most commonly used ITS primers are ITS1, ITS2, ITS3, ITS4 and ITS5 (figure 4). While the ITS1 and ITS2, respectively, are forward and reverse primers for the ITS1 fragment, the ITS 3 and ITS4, respectively, are forward and reverse primers for the ITS2 fragment (Bellemain et al., 2010).

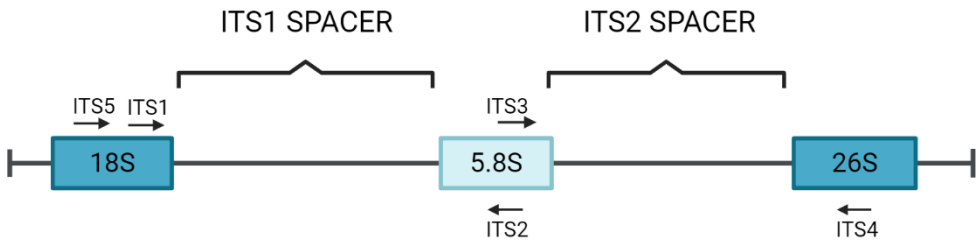

Figure 4: The schematic ITS region with primer binding areas. The figure illustrates the primers positioning and direction. The presented boxes do not correlate with the gene size. Figure was created with BioRender.com.

Sanger sequencing

For fungal taxonomic identification it is common to sequence the whole ITS region and optionally other sequences/genes if a higher resolution is needed. The first-generation sequencing, also known as Sanger sequencing, is sometimes referred to as a low throughput sequencing (Langsiri et al., 2023). This method was developed in the 1970s and is still used to sequence single longer DNA fragments up to roughly 1100bp (Sanger et al., 1977, Gupta and

Gupta, 2014).The nucleotides that are close to the primer binding sites and chain-ends tend to have a lower quality that makes these parts of the sequence impossible to basecall. This limits the reliable sequence size, often ending up at 700-800 bp or lower (GeneScript, 2021). Sanger sequencing uses fluorescent dyes for identification of nucleotides and has many of the same features as a PCR reaction. The polymerase adds dNTPs to elongate the oligonucleotide primer that is bound to the DNA template. In addition to dNTPs, dideoxynucleotides (ddNTP) are also added to the reaction. The lack of hydroxyl group that energize the polymerase causes a chain termination after adding the ddNTP. Each amino group in the ddNTP is labelled with a fluorophore to make it possible to differentiate the different ddNTPs. After many cycles of the replication processes multiple, varying in length copies of the template sequence are produced. Each of such fragments ends with a signature fluorescent termination signal (labelled ddNTP) that provides information which amino group lies at the end (Crossley et al., 2020). These fragments are then sorted by size in a capillary electrophoresis. DNA fragments travel through a conductive medium due to applied electric field. The DNA fragments travel toward the positive charged end at different speed based on their size. the fluorescent label is then detected by a CCD camera and interpreted by a base calling software to make a chromatogram (Hagemann, 2015, Karger and Guttman, 2009). A chromatogram is a visual representation of the DNA sequence, showing fluorescence for each base at each position of the sequenced DNA. One of the advantages of this sequencing platform, making it so popular, is the low cost of sequencing (GeneScript, 2021). The biggest disadvantage of this method is its time consumption (GeneScript, 2021, Slatko et al., 2018).

High throughput sequencing (HTS)

HTS, also known as next generation sequencing, refers to sequencing technologies which can perform simultaneous parallel sequencing of numerous DNA fragments (Pradhan et al., 2019). This technology is used in second-generation sequencing and third-generation sequencing.

While first generation technologies work well for single species identification, the second-generation sequencing technology can sequence millions of DNA molecules parallelly, thereby facilitating identification of many species by its multiplexing ability. Second generation include instruments like Illumina and Ion Torrent. Illumina has become a popular sequencing platform due to the relatively low cost, high yield and low error rates (Escobar-Zepeda et al., 2015). Some of the disadvantages with the Illumina sequencing platform is the low maximum read length and time consumption compared to third generation technologies (Illumina, 2023,

Escobar-Zepeda et al., 2015). The first step in Illumina sequencing is a cluster generation where each sequence is amplified through bridge amplification. From a single template up to 1,000 copies can be generated. Then the sequencing process proceeds to sequencing-by-synthesis. In one cycle, multiple fluorescent dNTPs are present to bind to the template. When a nucleotide binds, the fluorophore will emit a signal according to the nucleotide bound. The signal is then detected and subsequently recorded by a software. Base calling can then be performed based on the signal intensity (Illumina, 2010, Slatko et al., 2018).

Data processing

The data processing after HTS include quality control, sequence clustering and annotation. Quality control involves removing adaptor sequences and filtering by Q-score (Pradhan et al., 2019, Nilsson et al., 2019a). Subsequently, sequence clustering is performed through a similarity analysis within species-level operational taxonomic unit (OTUs), with a given similarity threshold, or amplicon sequence variants (ASVs). When using OTUs some grouping assumptions are made. While 85% sequence similarity corresponds to same family, 90% similarity corresponds to the same genus. A similarity at 97-98.5% or higher is considered as corresponding to the same species level. The OTU clusters can then be annotated through taxonomic annotations based on similarity with reference genomes from databases (Nilsson et al., 2019a). ASV interpret all SNP's as individual sequences before comparing sequences to reference database (Callahan et al., 2017).

There are several databases available for fungal identification. One of them is User-friendly Nordic ITS Ectomycorrhiza Database (UNITE) that is often used to identify newly generated ITS sequences by comparison (Raja et al., 2017). To classify the taxonomy, UNITE uses information from NCBI, Index Fungorum and MycoBank (Nilsson et al., 2019b). All these data processing steps can be done by pipelines like for example QIIME2 (Bolyen et al., 2019, Harbuzov et al., 2022).

Fungal cultivation

Different fungi have different preferences for environmental conditions, including temperature, nutrients, atmosphere, pH, water activity, time, and light. Therefore, it is helpful to know the fungi before cultivating them. Important environmental parameters for growth are illustrated in figure 5.

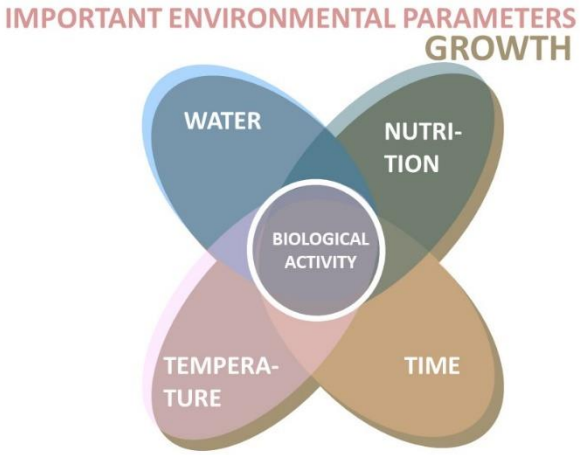

Figure 5: Important environmental parameters for fungal growth. Made by Ida Skaar.

Fungi need various nutrients for growth and reproduction. Their essential nutritional needs include carbon, nitrogen, phosphorus, sulphur and other essential metals like potassium and magnesium. They also require cofactor metals like calcium and zinc for enzyme and protein functions. Fungi have the ability to produce their own amino acids, what enables them to synthetize proteins. Fungi can also sense the nutrients in their environment to avoid energy demanding production of unnecessary enzymes. Fungi don`t need light to grow, but light can affect growth, both asexual- and sexual sporulation, circadian rhythms, phototropism, secondary metabolism, pathogenicity and nutrient uptake (Watkinson, 2016).

Fungal cellular activity is also dependent on water. While most fungi thrive at water potentials above -1 Megapascal (MPa, some can grow at water potentials as low as -69 MPa by regulating their permeability (Watkinson, 2016). When it comes to temperature, most fungi are mesophiles, which means that they can grow at temperature ranges within 10 to 35 ºC though their optimal growth temperatures can differ greatly (Ali et al., 2017). Some fungi, known as psychrophiles, can grow well in lower temperatures, while others, known as thermophiles, prefer higher temperatures. An example of psychrophiles are snow-moulds that can grow on grass beneath the snow (Watkinson, 2016). Within filamentous fungi, the growth rate can also differ greatly and be affected by factors mentioned above. For examples, *Zygomycetes* can exhibit colony formation after 24 hours of incubation, while some ascomycetes require 48 hours for the same growth result and others even longer (Meletiadis et al., 2001).

Fungi normally respire through oxygen use as a final electron acceptor, but with low oxygen concentrations, nitrate can be used as a substitute (Watkinson, 2016). Concentrations

of CO_2 above 15% can also restrict fungal growth (Magan and Lacey, 1984). The CO_2 released from respiration can dissolve into the surroundings, creating carbonic acid in presence of liquid. This leads to a decrease in pH (Valle et al., 2023). Secretion of fungal enzymes and bio reactive molecules is regulated by a pH-homeostatic system that senses the pH fluctuations in the environment. Fungi can adjust the environmental pH by secreting protons and organic acids. Even though most fungi can grow within a pH range of 3 to 8, their optimum pH in liquid media for mycelial production is approximately 5.5 and for sporulation ca. 6.5 (Deshmukh and Sabalpara, 2012, Ali et al., 2017). Since fungi lack photosynthesis, they rely on external sources of carbohydrates. The fungal carbon metabolism is usually regulated by a transcript regulator CreA. For many saprotrophic fungi, polymeric carbon structures can be broken down and utilized as carbon source, as mentioned previously (Watkinson, 2016). Fungi often prefer carbon sources that require the least amount of energy to digest, like glucose, before moving on to longer polymeric structures, which demand more energy for breakdown (Ronne, 1995).

Determination of fungal degradation of plastic.

There are many common methods than can visualize, present, describe and test different aspects of the plastic degradation results. Therefore many studies combine the results from different analytic methods in order to evaluate the degree of plastic degradation (Okal et al., 2023), what makes it unstandardised and difficult to compare results. While some methods, such as measuring plastic and fungal weight, are cost-effective and less time-consuming, other methods, such as scanning electron microscopy (SEM), are more expensive and require significantly more time. By using SEM it is possible to analyse the plastic topology and evaluate the presence of fungal adherence and tears on the plastic surface which originates from biodegradation (Shah et al., 2008).

A light microscope can magnify live objects with a resolution down to 0.2 um. To get a higher resolution electron microscopy (EM) can be used. In contrast to the light microscope, EM can only magnify dead objects, but in return it gives a resolution down to 1 nm (Evennett and Hammond, 2005). EM uses electron beams to magnify an object approximately 200 000 times at maximum. There are two different types of electron microscope, transmission electron microscope (TEM) and scanning electron microscope (SEM). While electrons from TEM microscopy are passing through the object, electrons from SEM are reflected from the object surface. To be visualized with SEM, the object needs to be dried and coated with conductive material, like for example gold or platinum, that can emit a secondary electron (SE) when hit by a primary electron (Clokie, 2018). SEs are collected by a positively charged surface detector.

The signal is then converted to a light signal that makes it possible to visualize the topography of the sample (Clokie, 2018, Kogure, 2013). The difference in intensity sent from different parts of the specimens gives the image different intensity areas. The primary electrons that change direction due to scattering can also be detected by a backscatter detector (Kogure, 2013).

The use of fungi to degrade plastic.

Many studies have demonstrated encouraging results within the field of fungal plastic degradation. Different fungi exhibit varying degrees of effectiveness in their ability to degrade such materials. The aim of this study is to investigate candidate fungi obtained from the Norwegian landscape for plastic degradation. For this purpose, the study is focusing on silage plastic wrap from agricultural land. The samples will be subjected to fungal diversity analysis conducted through metabarcoding. From here, the most promising fungi will be isolated and cultivated with pure LDPE pieces with different conditions. The effect of photodegradation will also be evaluated. Results is to be confirmed through analysing changes by observation, weight, wettability, and topography.

2. Material and methods

To reach the main goal of finding efficient Norwegian plastic-degrading fungi, the experiment workflow was divided into five sections, which are illustrated in Figure 6.

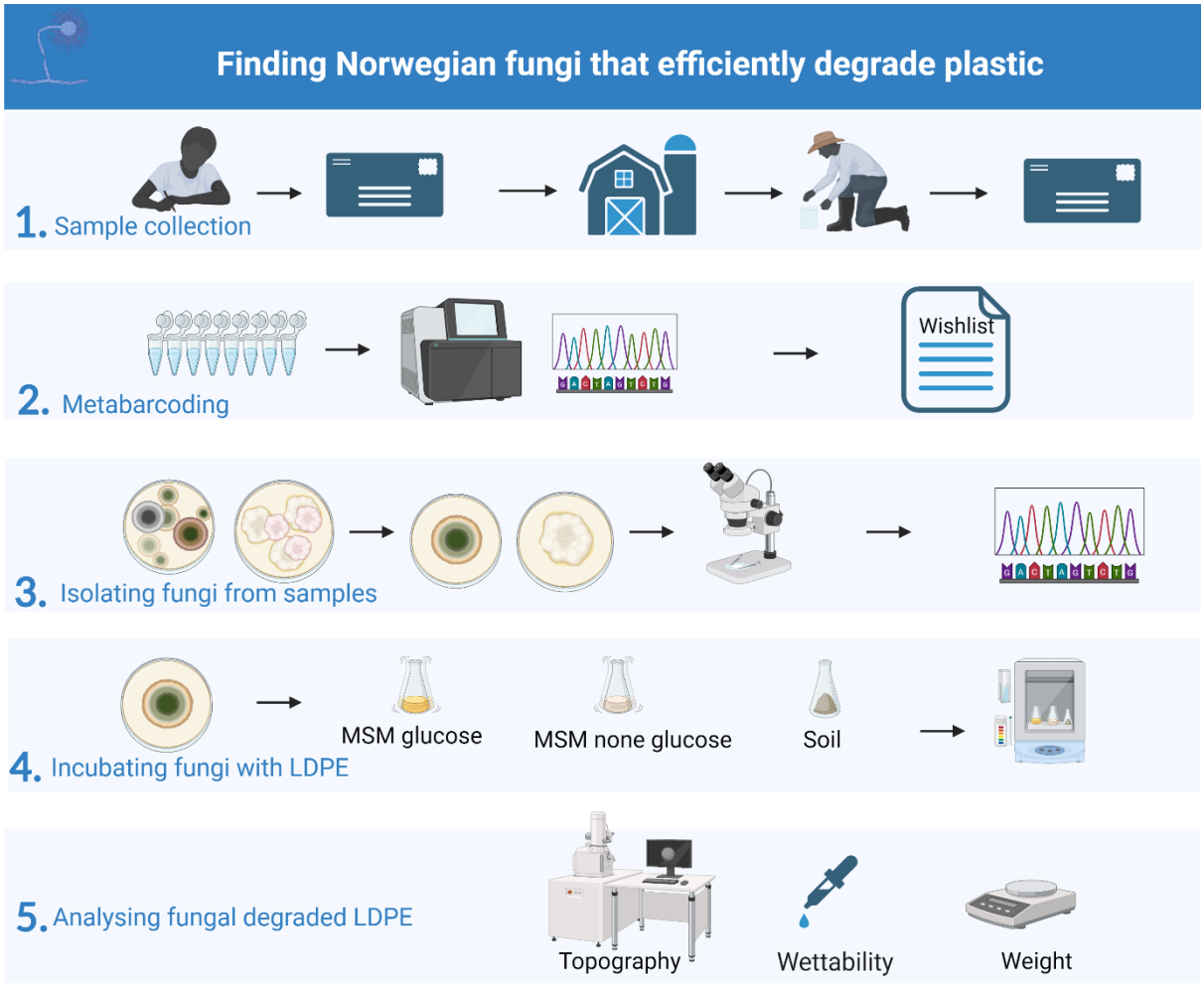

Figure 6: Project methodological workflow for finding Norwegian fungi that efficiently degrade plastic. Figure was created with BioRender.com.

2.1 Sample collection

In order to find potential plastic degrading fungi in Norway, plastic samples from various parts of the country were collected. An information about the project and request for silage ball plastic from farms was spread through interviews with news and agricultural journals (appendix 1, figure A1.1). Instructions were sent to volunteers together with a return envelope and a sampling set, consisting of two small plastic bags (appendix 1, figure A1.2). Plastic samples were collected by using one of the plastic bags as a glove. After gripping the sample wearing 'the glove' and cutting off a desired piece, the plastic bag was twisted over the sample and folded. The folded plastic bag with the sample was protected by the second plastic bag that was tied in the end. After collection, the sample was sent to the Norwegian Veterinary Institute

(NVI). Upon arrival, the envelopes with samples were stored at 4 ºC ± 1 while waiting for sample analysis.

2.2 Metabarcoding

The next step of the project was focused on collecting information about the fungal diversity present on the plastic samples. This was done by metabarcoding approach that included DNA extraction, target locus amplification, sequencing, and data processing. When performing molecular analysis, negative controls were used as a control for contamination during DNA extractions and PCR.

Sterile techniques and cultivation

Work with plastic samples and fungal cultures was performed in a laminar air flow bench in a sterile manner. The bench was washed with 70% ethanol between different samples or fungal isolates to reduce the contamination risk. The non-sterile equipment used for work was washed with 96% ethanol and burned over an open flame.

Extracting fungal DNA from plastic

Prior to fungal DNA extraction, the fungi had to be separated from the plastic. In order to explore the most efficient technique for extracting fungi and, subsequently, fungal DNA from the plastic sample, seven different extraction methods were tested on a subset of five samples (appendix 2, table A2.2).

Extraction of the DNA from the fungi was performed as illustrated in figure 7. First, approximately 0.43 g of the plastic samples were cut from the sample into a 50 ml falcon tube (appendix 2, figure A2.3). The falcon tubes were filled with milli-q water to drench the plastic samples before sonication with Bransonic 3510E-DTH Ultrasonic Cleaner (Branson, Brookfield, Connecticut, USA) for 10 minutes. The tubes were vortexed for three minutes and water from the falcon tube was filtered with EZ-Stream® Vacuum Filtration Pump (Merck Millipore, Burlington, Massachusetts, USA) using S-Pak® Membrane Filters (Merck Millipore, Burlington, Massachusetts, USA, Cat. HAWG047S6). The filters were folded and cut into small pieces before the next step.

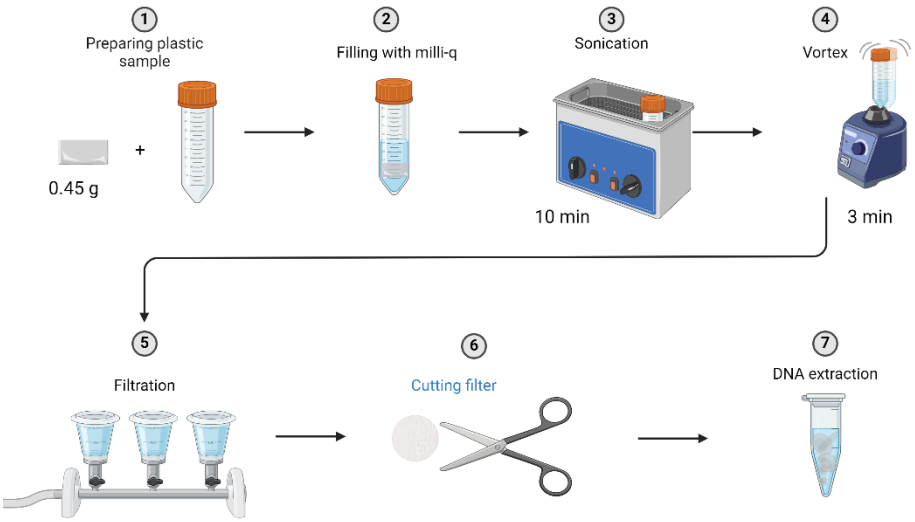

Figure 7: The process of extracting fungi from plastic. Figure was created with BioRender.com.

Fragmented filters were added to a PowerBead Pro Tube from the DNeasy® PowerSoil® Pro kit (QIAGEN, Venlo, Netherlands, Cat. 47014). DNA was extracted according to DNeasy® PowerSoil® Pro Kit Handbook (QIAGEN, 2021). Some exceptions from the protocol were made. The vortex step in the protocol (step 4) was replaced with mechanical lysis with MM 400 Mixer Mil (RETSCH, Haan, Germany) for three minutes at 30 Hz, while the elution step was extended to 5 minutes, instead of 1 minute suggested in the instruction. DNA presence after extraction was confirmed by NanoDrop™ One Microvolume UV-Vis Spectrophotometer (Thermo Scientific™, Waltham, Massachusetts, USA). NanoDrop was also used to give an estimated quality by measuring the quantity of proteins (A260/A280) and organic compounds (A260/A230) in relation to DNA present in the sample. The measurements were done by following the NanoDrop One User Guide (ThermoFisherScientific, 2016). The NanoDrop concentration measure for all samples were within the acceptance level (appendix 2, table A2.4***).***

Mock community preparation

A mock community, a mixture of known DNA concentrations of known fungal species, was prepared and used to get a PCR and sequencing bias estimation. Based on distant taxonomic positions, seven different fungal species, both from the Basidiomycetes and Ascomycetes phyla were cultivated for 4 to 10 days (appendix 2, table A2.5). Cultivation was performed at 25 ºC± 1 in dicloran glycerol agar (DG 18) media (appendix 2, table A2.1).

The initial cell lysis was preformed according to cell lysis procedure A2.6, appendix 2. DNA from each fungal isolate was first extracted with QIAcube Connect (QIAGEN, Venlo, Netherlands) according to QIAcube® Connect User Manual (QIAGEN, 2019) by using QIAamp® DNA Mini Kit (Qiagen, Vienna, Austria, Cat. 51306). The settings were as follows: DNA > QIAamp DNA Mini Kit > Tissue > Standard. Due to low DNA yield from the first DNA extraction, (appendix 2, figure A2.7), the DNA extraction was repeated through CTAB by following the protocol for CTAB extraction (Appendix 2, procedure A2.8). Qubit 4 fluorometer (Thermo Scientific™, Waltham, Massachusetts, USA, Cat. Q32850) was used for precise determining of the DNA concentrations (Appendix 2, figure A2.7), following the user guide for Qubit® dsDNA BR assay Kits (ThermoFisherScientific, 2015). DNA were extracted from plastic and controlled, while mock community was mixed proportions shown in table A2.5 appendix 2, before library preparations.

Library preparation

The most efficient annealing temperature and cycle number for ITS2 amplifications through PCR was explored through gradient PCR with different annealing temperatures and regular PCR with three different cycle numbers. The resulting amplicons from the different PCR reactions were compared in a 1.5% w/v agarose gel electrophoresis (Appendix 2, figure A2.9 and figure A2.10).

The ITS2-region was amplified in a two-step PCR reaction (figure 2.3). In the first step (PCR 1), modified by an overhang ITS3 and ITS4 primers were used to amplify the ITS region through PCR amplification. In addition, four different variants of the primers were designed by adding additional nucleotides to the 5`-end to ensure more diversity.

In the second step (PCR 2), the target sequence was extended with indexed adaptors that were designed to target the overhang sequence from the first step (Appendix 2, table A2.11). The adapter oligonucleotide is designed to bind to the Illumina flow cell oligos. Since the DNA extracted from different samples were pooled (mixed) before sequencing, they needed indexes that could show what sample the sequences originated from (Appendix 2, table A2.12). To ensure proper primer binding, reduce the probability of mismatch and get satisfactory DNA yield, the annealing temperature and the number of cycles needed optimalisation. For this purpose, eight different annealing temperatures and three different cycle numbers were tested on three samples to determine the most suitable parameters for the primers (Appendix A2, table A2.13). The ITS2 amplicon presence was confirmed in a 1.5 % w/v agarose gel after following

the procedure for agarose gel (Appendix 2, procedure A2.14 and figure A2.15). The PCR two steps are illustrated in figure 8.

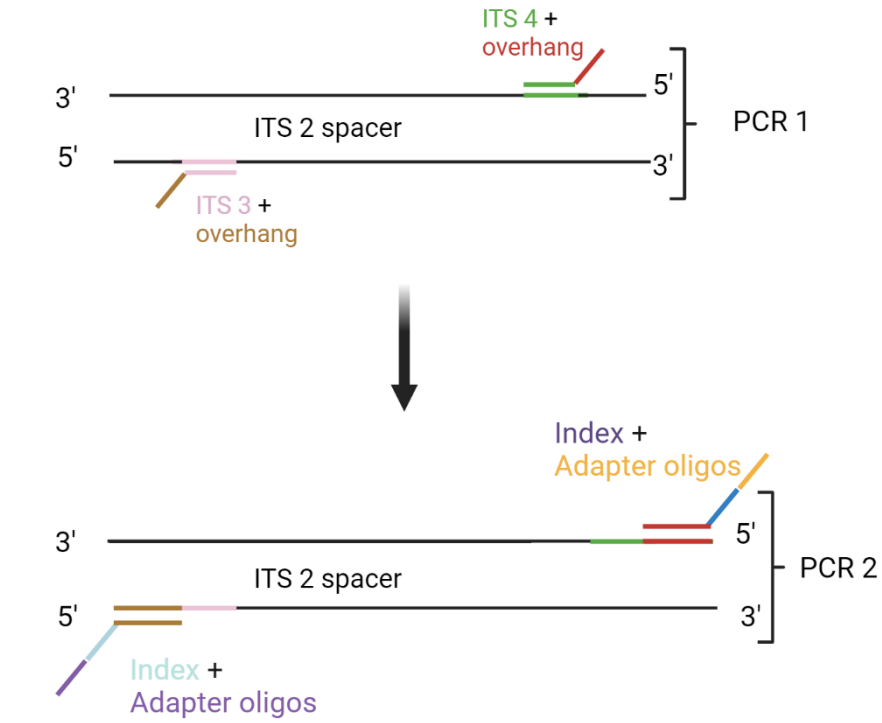

Figure 8: Two-step PCR for ITS2 library preparation. The figure was created with BioRender.com.

In both reactions the HiFi HotStart PCR kit (Kapa Biosystem, Massachusetts, United States, Cat. kk2502) was used. Reactants for the PCR amplification was mixed with the samples according to table 1. ITS 3 and ITS 4 primer variants are listed in the table 2. Cycling conditions for both PCR steps are given in the table 3.

Table 1: Reaction mixtures used in the two-step PCR.

	Volume (µL)	
Reagents	**PCR 1**	**PCR 2**
H_2O	13.8	22.5
5X KAPA HiFi Buffer	5	10
10 mM KAPA dNTP Mix	0.8	1.5
Primer (ITS3/ITS4)	5.0	
1 U/µL KAPA HiFi DNA polymerase		1
(5µM)	0.5	
Index forward		5
Index reverse		5

Template	3.0	5

Table 2: Primer sequences for ITS2 amplifications. The black coloured letters illustrate the general ITS primer sequence while the red coloured letters represent the variant sequence.

Primer	**Sequence (5´- to 3´-end)**
ITS3 v1	ACACTCTTTCCCTACACGACGCTCTTCCGATCTGCATCGATGAAGAACGCAGC
ITS3 v2	ACACTCTTTCCCTACACGACGCTCTTCCGATCTTGCATCGATGAAGAACGCAGC
ITS3 v3	ACACTCTTTCCCTACACGACGCTCTTCCGATCTCCTGTCGGCATCGATGAAGAACGCAGC
ITS3 v4	ACACTCTTTCCCTACACGACGCTCTTCCGATCTCCTGTCGGCATCGATGAAGAACGCAGC
ITS4 v1	GTGACTGGAGTTCAGACGTGTGCTCTTCCGATCTTCCTCCGCTTATTGATATGC
ITS4 v2	GTGACTGGAGTTCAGACGTGTGCTCTTCCGATCTATCCTCCGCTTATTGATATGC
ITS4 v3	GTGACTGGAGTTCAGACGTGTGCTCTTCCGATCTTGTCATCCTCCGCTTATTGATATGC
ITS4 v4	GTGACTGGAGTTCAGACGTGTGCTCTTCCGATCTGATATGTTCCTCCGCTTATTGATATGC

Table 3: PCR parameters for PCR 1 and PCR 2. The table shows the time, temperature, and number of cycles for the different the PCR reactions.

	PCR 1			**PCR 2**		
Parameters	**Time**	**Temperature** (C°)	**Cycles** (x)	**Time**	**Temperature** (C°)	**Cycles** (x)
First denaturation	3 min	95	1	3 min	95	1
Denaturation	20 sec	98		30 sec	98	
Annealing	30 sec	56	20	30 sec	55	8
Extension	30 sec	72		30 sec	72	
Final extension	10 min	72	1	5 min	72	1

Normalisation of the sample concentration was performed between both PCR1 and PCR2 to ensure equal concentration of each sample during amplification and sequencing. Samples were cleaned with AMPure XP SPRI Reagent (Beckman Coulter, Brea, California, USA) by following the PCR clean-up 2 in the procedure 16S Metagenomic sequencing Library Preparation Preparing 16S Ribosomal RNA Gene Amplicons for the Illumina MiSeq System (Illumina, 2013). The DNA concentration and fragment length was measured with TapeStation 4200 (Agilent, Santa Clara, California, USA) by following the instructions from the procedure

D1000 ScreenTape Assay for TapeStation Systems Quick guide (Agilent, 2021) (appendix 2, figure A2.16 and figure A2.17).

High throughput sequencing

The cleaned DNA amplicons with appropriate indexes and barcodes were handled by authorized personnel of the sequencing laboratory at the NVI. The sample mix was diluted to 8.5 pM and injected into the Illumina MiSeq (Illumina, San Diego, California, USA) together with 25% PhiX quality control for sequencing.

Data processing

The data were processed using QIIME 2 pipeline (v.2022/11). Sequences were imported and cut to ensure the best quality and length compromise. Sequence grouping was performed through OTUs at 95%, 97% and 99% threshold and ASV. After adding the metadata parameters, the sequences were classified by using UNITE QIIME release for Fungi 2 (Abarenkov, 2023). The flowchart for this process is illustrated in figure 9. Further statistical analysis were performed using R-studio (v. 2023.12.1). An abundance bar plot was generated to investigate the taxonomic distribution of different fungal species. Based on the results, a list (*wishlist*) with 15 potential plastic degrading fungi was created taking into account occurrence, cultivation ability, hyphae, earlier scientific findings on plastic biodegradation and growth rate. A diversity heat plot was generated in R-studio by using the package ggplot2 (v. 3.5.0). Supervised and unsupervised methods were then used to analyse the correlation between the different metadata groups in R-studio. Cluster error rate was controlled, and the parameters were tuned before the final sparse partial least squares-discriminant analysis (sPLS-DA) by using the package mixOmics (v.6.20.0).

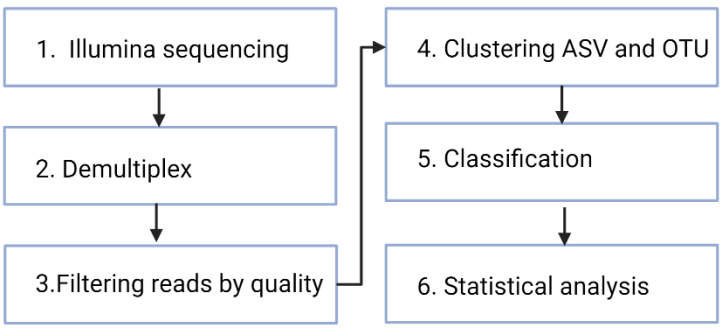

Figure 9: The QIIME2 analytical pipeline flowchart. The figure was created with BioRender.com.

2.3 Isolating fungi from samples

In the third part of the experiment, the isolation of fungal strains in the wishlist was performed. Morphological characteristics were used for isolation of the targeted fungi from the

multiculture plates. The identity of isolated fungi was confirmed morphologically and molecularly.

Cultivation

Before cultivating fungi from the plastic samples, an optimisation step was performed to find the most optimal growth conditions and extracting methods to provide the highest diversity of fungi species. Variables included growth media, dilutions, temperatures, duration times with sonication treatment and growth time. All media used were manufactured by the media production department at the NVI. After the optimisation part, DG18 in a petri dish was used as the sole media when cultivating only fungi, liquid mineral salt media (MSM) and soil were used when cultivating fungi with LDPE and malt extract agar (MEA) medium was used for contamination control. The media recipes are shown in table A2.1 in appendix 2. All incubations were performed at 25 ºC± 1.

Fungi from the plastic samples were extracted by drenching the plastic in milli-q water and using sonication and vortex as described earlier. The samples were suspended in destilled water to have the same sample weight per ml. For each sample a 10x, 100x and 1000x dilutions were made before transferring 300 µl of each dilution into separate DG18 agar plates. During the following 11 days of incubation, the culture growth was monitored. The fungi with the morphological similarity to those on the wishlist were isolated gradually by transferring the chosen colonies onto a secondary DG18 agar dish.

Morphological and molecular identification of fungal isolates.

The pure fungal isolates were examined visually on the plates and under the microscope to determine the fungal genera. Fungal slides were stained before microscopy by collecting conidia and fragments of mycelium with a tape and pasting it to a microscope slide after a dip in 70% ethanol and lactofuchsin. As morphological identification alone is not always precise, Sanger sequencing of selected loci was performed. The DNA extraction was preformed according to instructions from Quick-Start Protocol for QIAamp® DNA Mini Kit (QIAGEN, 2018) with small modifications. A ca. 1 cm^2 fragment of mycelium was transferred to a test tube containing a single 4-mm steel bead and 350 µL AL buffer, and subsequently homogenized using a MM 400 Mixer Mil (RETSCH, Haan, Germany) for 3 minutes at 30 Hz. The elution step was extended to five minutes instead of one. The targeted loci and respective primers used for molecular identification are shown in table 4.

Table 4:Primers used for fungal isolates molecular identification. LSU – Large subunit, tef1-a *– translation elongation factor 1-α,* rpb2 *– RNA polymerase II,* bt2 *– tubulin β chain,* cal *– partial calmodulin gene,* act *– partial actin gene, rpb1 – RNA polymerase I. If not specified otherwise, the primers were synthetized at Eurofins Genomics.*

Genetic marker	**Forward primer**	**Sequence**	**Reverse primer**	**Sequence**
ITS (Thermofisher scientific, Waltham, Massachusetts, USA)	ITS1 ID. UP9MD7H	GACGTTGAADCCRACRTTGTC	ITS 4 ID. UPAD4J9	TCCTCCGCTTATTGATATGC
LSU	*LSU*1Fd	GRATCAGGTAGGRATACCCG	LR5	TCCTGAGGGAAACTTCG
tef1-α (v11) (Biosearch technologies, Hoddesdon, United Kingdom)	EF1-1018F Ref. SS816121-01	GAYTTCATCAAGAACATGA	EF1-1620R Ref. SS816121-02	GACGTTGAADCCRACRTTGTC
rpb2 (v11)	b*RPB2*-6F	TGGGGYATGGTNTGYCCYGC	b*RPB2*-7.1R	CCCATRGCYTGYTTMCCCATGDC
bt2	bt2A	GGTAACCAAATCGGTGCTGCTTTC	bt2B	ACCCTCAGTGTAGTGACCCTTGGC
cal	cmd5	CCGAGTACAAGGAGGCCTTC	cmd6	CCGATAGAGGTCATAACGTGG
act	ACT-512F	ATGTGCAAGGCCGGTTTCGC	ACT-738R	TACGAGTCCTTCTGGCCCAT
tef1-α	EF1-728F	CATCGAGAAGTTCGAGAAGG	EF1-986R	TACTTGAAGGAACCCTTACC
*rpb*1	RPB1-Af	GARTGYCCDGGDCAYTTYGG	RPB1-6R1asc	ATGACCCATCATRGAYTCCTTRTG
*rpb*2	f*RPB2*-5F	GAYGAYMGWGATCAYTTYGG	f*RPB2*-7cR	CCCATRGCTTGYTTRCCCAT

To ensure precise identification, at least three different genetic markers were selected for amplification and sequencing of each isolate (Appendix 3, table A3.1). Different PCR reactions and conditions were therefore required for each genetic marker (Appendix 3, table A3.2 and table A3.3). DreamTaq DNA Polymerase (Waltham, Massachusetts, USA, Cat:

EP0701) and dNTP Mix (Waltham, Massachusetts, USA, Cat: R0192) were used for this purpose. PCR amplicon presence of the genetic marker was confirmed in a 1.5 % w / v agarose gel as described earlier. The sequencing was performed at Eurofins Genomics (Ebersberg, Germany). The raw data were processed with Geneious Prime (v.2024.0.2). Reference sequences were found in Genbank (www.ncbi.nlm.nih.gov/genbank/) A phylogenetic tree for each isolate was created by using Randomized Axelerated Maximum Likelihood Next Generation (RaxML-NG) (v.1.2.0). The most fit nucleotide substitution model (NSM) for each isolate was calculated through Molecular Evolutionary Genetics Analysis (MEGA) (v.11.0.13). Based on the results from RAxML-NG, phylogenetic trees were edited using FigTree (v.1.4.4) and Inkscape (v.1.3.2).

2.4 Incubating fungi with LDPE

In the fourth part of the experiment, the isolated and identified fungi from the collected plastic samples were cultivated together with a pure LDPE plastic piece to test degrading capabilities of fungi. Due to time and room limitations only seven of the fungal isolates from the wishlist were used further in the experiment.

Plastic pretreatment

A 1 mm thick LDPE sheet (Goodfellow, Huntingdon, UK) was sliced into small bits at approximately 0.81 cm^2. As an attempt to break the polymer structure and make the plastic carbon more available for the fungi, half of the pieces were radiated for approximately 18 days (426 hours) with an approximate distance of 2.5 cm from a UV-C disinfection fixture TMS030 1xT8 18W/TUV HFP R (Philips, Amsterdam, Nederland). The UV-C sensor RM-22 (Opsytec Dr. Gröbel, Ettlingen, Germany) was used to calculate the dosage after 10 minutes at three different points under the UV-lamp before calculating the average dosage. The average dosage was then multiplied by the exposure time.

Optical contact angle measurements were made on the LDPE surface by using a goniometer before and after the radiation to evaluate the wettability change. To recognize the UV-treated front side, the LDPE pieces were labelled with a scalpel to create a crack as a corner mark at the front side. A marker was used to label the backside.

Cultivation

The laminar flow (LAF) cabinet was radiated with UV-C for 15 minutes between the work with different fungal isolates. A spore solution containing 1000 spores/ml was prepared from each of the seven selected isolates. Spore numbers were quantified using a Bürker

counting chamber (Paul Marienfeld, Baden-Wuerttemberg, Germany). These spore solutions were used as an inoculum (150 ml ± 10 ml media, in a 300 ml Erlenmeyer flasks). The used media included mineral salt media (MSM) with and without glucose, and the soil "Sirkeljord" (Nelson Garden, Tingsryd, Sverige). Each inoculum was used for a set of three media – MSM, MSM + glucose, soil. Duplicates were made for each set to contain either UV-radiated or non-radiated LDPE pieces. The same conditions were applied to negative controls. The experimental setup is illustrated in figure 10. Sample number overview is shown in table A4.1 in appendix A4. The LDPE pieces were washed in 95% ethanol and UV-C radiated for 15 minutes at 0.251 mW/cm^2 on each side before being added into the media. While the flasks with soil were stationary, the flasks containing liquid media were incubated with stirring at 150 rpm. The starting pH was 5.5 in MSM without glucose, 4.4 in MSM with glucose and 6.5 in soil. To monitor the cultivation conditions, optical density at 600 nm (OD600) and pH were measured respectively with UV-1280 UV-VIS spectrophotometer (Shimadzu, Kyoto, Japan) and Orion VersaStar Pro (Thermo Scientific™, Waltham, Massachusetts, USA, Cat. VSTAR90), once a week. At the end of the cultivation part, 50 µl of the cultivated media were added to a Petri dish with MEA-medium as a contamination control.

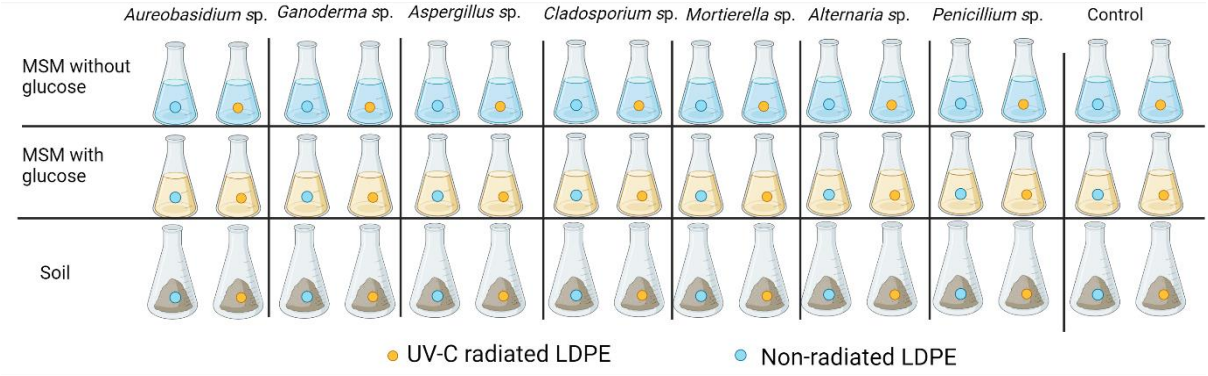

Figure 10: Cultivation experiment illustrated. The figure shows the different conditions for the seven different fungal genera in addition to a control without fungi. Figure created with BioRender.com.

Statistical analysis

All results from pH and OD measurements were recorded in a Microsoft Excel sheet for calculation. The mean values and standard deviations were calculated before identifying outliers at 95% confidence level. After removing any outliers, a two-side t-test with assumed different variations was performed to investigate if the small changes were significant. The two hypotheses consisted of H_1 and H_0. H_1 represented difference, while H_0 represented no difference.

2.5 Analysing fungal degradation of LDPE

After cultivation for 89 days, the LDPE pieces appearance, weight, wettability, and topography were analysed by visualisation, scale, goniometer, and SEM respectively. 50 µl from each sample medium were incubated in MEA-medium as a contamination control. The LDPE pieces were then extracted from the cultures and pictures were taken of each piece. Fungi and fungal spores were carefully removed with a soft tissue paper and then by sonication and vortex before weighing the LDPE pieces.

Weight

The LDPE pieces were weighed before and after the UV-treatment and biodegradation to measure any weight loss after either of the two processes, using a 5 digits scale (XPR105, Mettler Toledo, Ohio, United states).

Wettability

To analyse changes in the plastic wettability optical contact angle (Kocaoglu et al.) was measured before and after both UV-degradation and biodegradation. A droplet of 4 µl distilled water was put on the plastic surface using OCA 15EC Contact Angle Goniometer (dataphysics, Filderstadt, Germany) and a photo was taken within 15 seconds in the software SCA20 (v.4.4.1). The left and right angles on the sessile drop were calculated after adjusting baseline, adjusting area, finding contour and fitting the contour. The software used the Young-Laplace equation and other algorithms to calculate the contact angle between the water and plastic (Williams, 2022). The average of left and right angle for two parallel droplets were then calculated to decide the plastic water droplet angle for each plastic piece.

Topography

12 of the LDPE pieces were fixated by putting them in a fixation solution overnight (Appendix 5, Table A5.1). Following day LDPE pieces were dried by the dehydration procedure with stirring (Appendix 5, table A5.2) and subjected to critical point drying using a CPD 030 Critical Point Dryer (BAL-TEC, Pfäffikon, Switzerland) as described in the Operating Manual (BAL-TEC, 99). The LDPE pieces were covered with platinum by using the sputter coater EM ACE200 (LEICA, Wetzlar, Germany). The platinum covered LDPE pieces were injected into the EVO 50 SEM (ZEISS, Oberkochen, Baden-Württemberg, Germany) for topography analyses. An overview pictures at 70 x were taken for all LDPE pieces before inspecting them closer.

3. Results

3.1 Sample collection

To collect old plastic wrap residues from silage balls, a request for volunteering farmers were distributed through news media and agricultural organisations. In total, 19 people answered within two and a half months. Of these, 14 people sent in plastic wraps (figure 11).

Figure 11: Volunteer collecting silage wrap. Picture provided by volunteer.

13 samples were collected from Western Norway, 12 samples were collected from southern Norway and one sample was collected from Trøndelag. Some farmers sent plastic wraps from several sites in one area, in addition one farmer sent two plastic samples, s12a and s12b, that were not silage plastic wrap, but plastic used in berry farming. In total 27 samples were collected. The geographic distribution of the samples is shown in figure 12. The specific plastic features are described in appendix A6, figure A6.1.

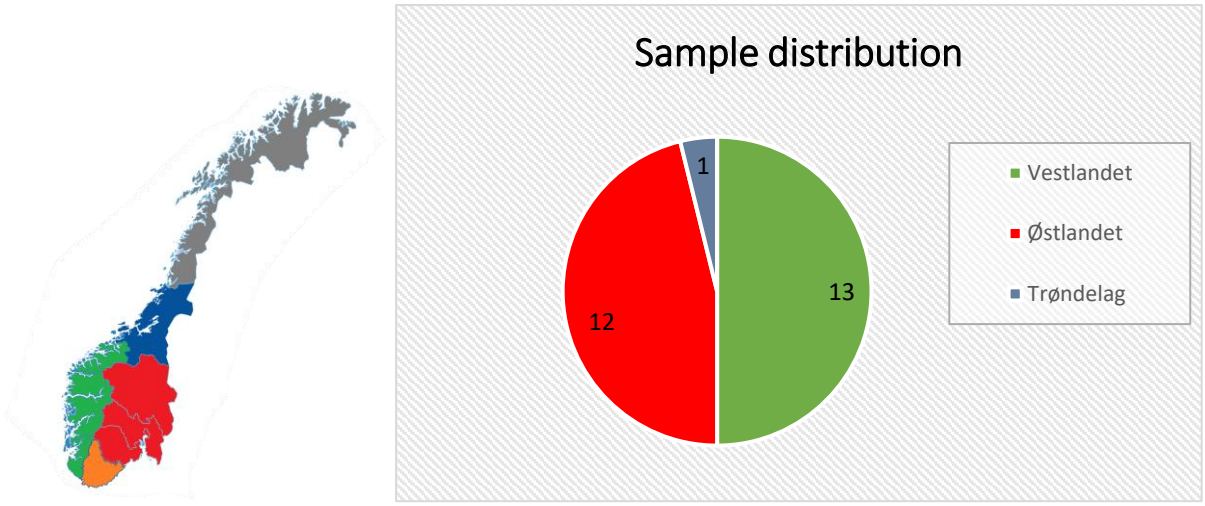

Figure 12: Distribution of sample collection sites in Norwegian country parts. The Norwegian five country parts consists of Western Norway (•), Eastern Norway (•), Southern Norway (•), Trøndelag (•) and Nord-Norge (•). The pie chart was made using Microsoft Excel

3.2 Metabarcoding

After collecting all the plastic samples, the fungal diversity on the samples was examined using the metabarcoding approach. The analysis consisted of DNA extraction, PCR amplification and Illumina sequencing.

Optimalisation

Table 5. shows the results from the optimalisation experiments testing DNA isolation techniques. Technique 4 — sonication, filtration and new kit gave the highest DNA yield and was hence selected for subsequent DNA extractions.

Table 5: Absorbance and DNA yield from various extraction techniques. The DNA yield and quality was measured through NanoDrop™ One Microvolume UV-Vis Spectrophotometer.

Experiment #	**Technique**	**Sample**	**DNA yield (ng/µl)**	**A260/A280**	**A260/A230**
1	1	S1	13.2	1.86	0.49
	1	S2	13.4	1.84	0.49
	2	S1	12.4	2.04	0.46
	2	S2	13.7	1.99	0.48
2	3	S1	65.8	1.9	1.53
	3	S2	8.6	2.29	0.52
	3	S3	5.9	2.51	0.02
	3	S4	29.7	1.93	0.15

3	4	S5a	42.6	1.87	0.42
	5	S5a	13.8	1.89	0.55
	6	S5a	28.8	1.82	0.64
	7	S5a	34.6	1.88	0.13
4	4	S1	328,90	1.89	0,64
	4	S2	84,00	1.92	0,33
	4	S3	35,30	1.95	0,21
	4	S4	39,70	1.94	0,10

The annealing temperature of 55 ºC gave fewer small fragments and an intense enough band in comparison with other temperatures tested. High abundance of ITS amplicon after 20x cycles was a reason to continue analyses with this number of cycles.

DNA extraction

In the mock community, the phylum distribution obtained by metabarcoding showed a much higher abundance of *Ascomycota* in relation to *Basidiomycota* than the actual DNA proportion mixed. While the DNA proportions mixed contained 24% *Basidiomycota*, observed proportions after sequencing were 0.057% *Basidiomycota*, see figure 13. This illustrated that *Basidiomycota* were highly underreported in metabarcoding, that needed to be accounted for when creating the wishlist.

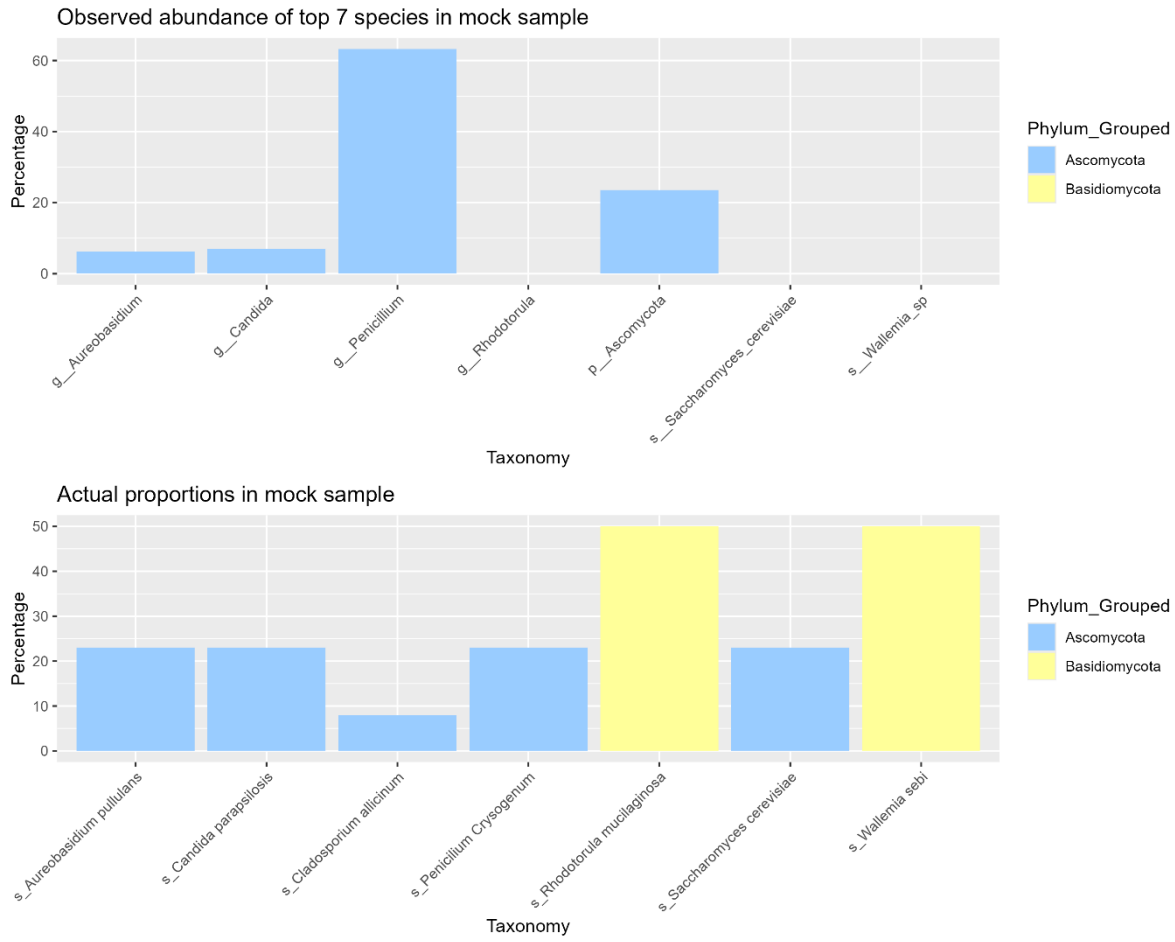

Figure 13: Observed abundance and actual abundance bar plot. The figure shows the percentage proportions identified species through illumina sequencing (A) and the DNA proportions mixed before sequencing(B). The x-axis shows the highest taxonomic resolution found

From the filtering and processing of samples in QIIME2 and R-studio, 1434 unique taxonomic classifications were found. The family *Cladosporiaceae* were identified as the most abundant (figure 14). 15 fungal species were implemented into a wishlist based on set criteria, see table 6.

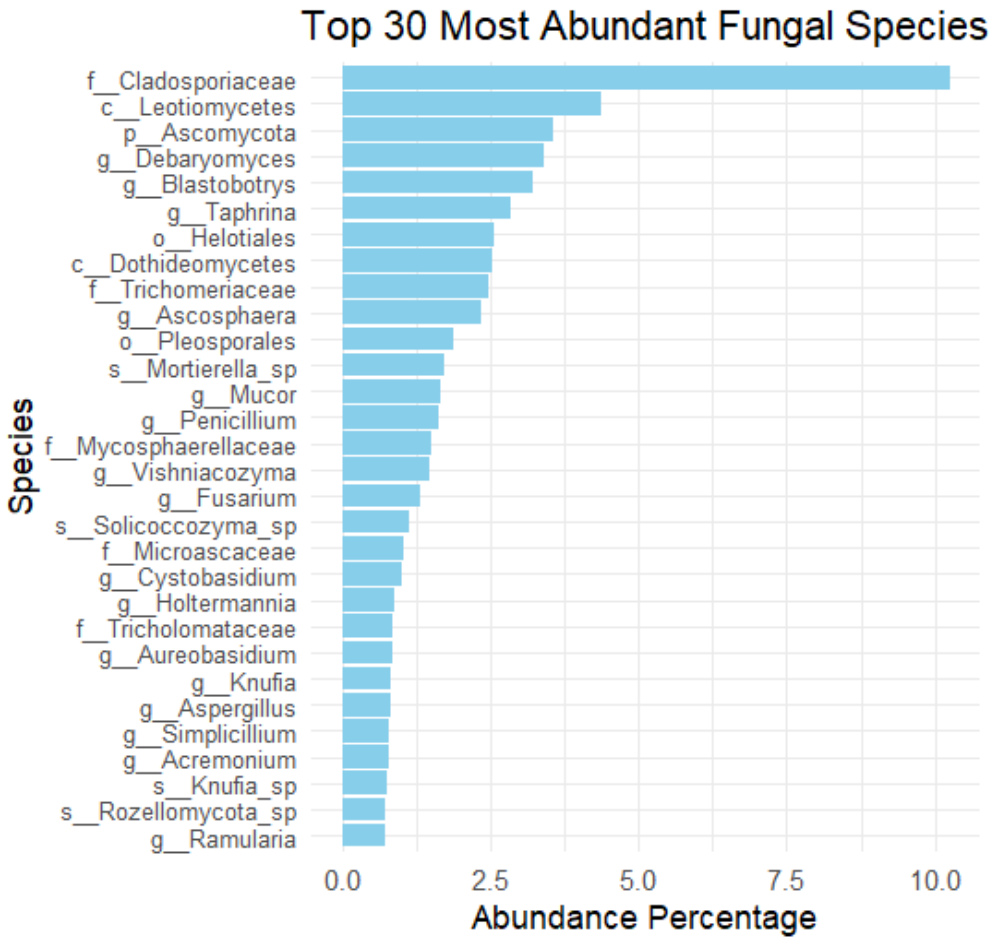

Figure 14: Abundance table. The figure shows the top 30 most abundant fungal species. The y-axis shows the highest taxonomic resolution found, either Phyla(p_), Genus(g_) or species(s_).

Table 6: Wishlist made after first view of sequencing results in QIIME2. The numeric value illustrates the order of abundance level rising from 15 to 1.

Number	**Fungal genera**
1	*Cladosporium*
2	*Mortierella*
3	*Mucor*
4	*Penicillium*
5	*Fusarium*
6	*Microascacea*
7	*Aureobasidium*
8	*Aspergillus*
9	*Simplicillium*
10	*Acremonium*

11	*Trichoderma*
12	*Alternaria alternata*
13	*Ganoderma*
14	*Colletotrichum*
15	*Trametes*

The results from the metabarcoding were further processed by using R-studio to create a heatmap with an abundance overview see figure 15. There were no signs of clustering between the different ages. An sPLS-DA plot was made to study the clustering between samples from different country parts and from different area conditions (figure 16). There was no clear clustering between features found in samples from different country parts. Samples from under roof show spreading, while samples from forest and grassland show some clustering.

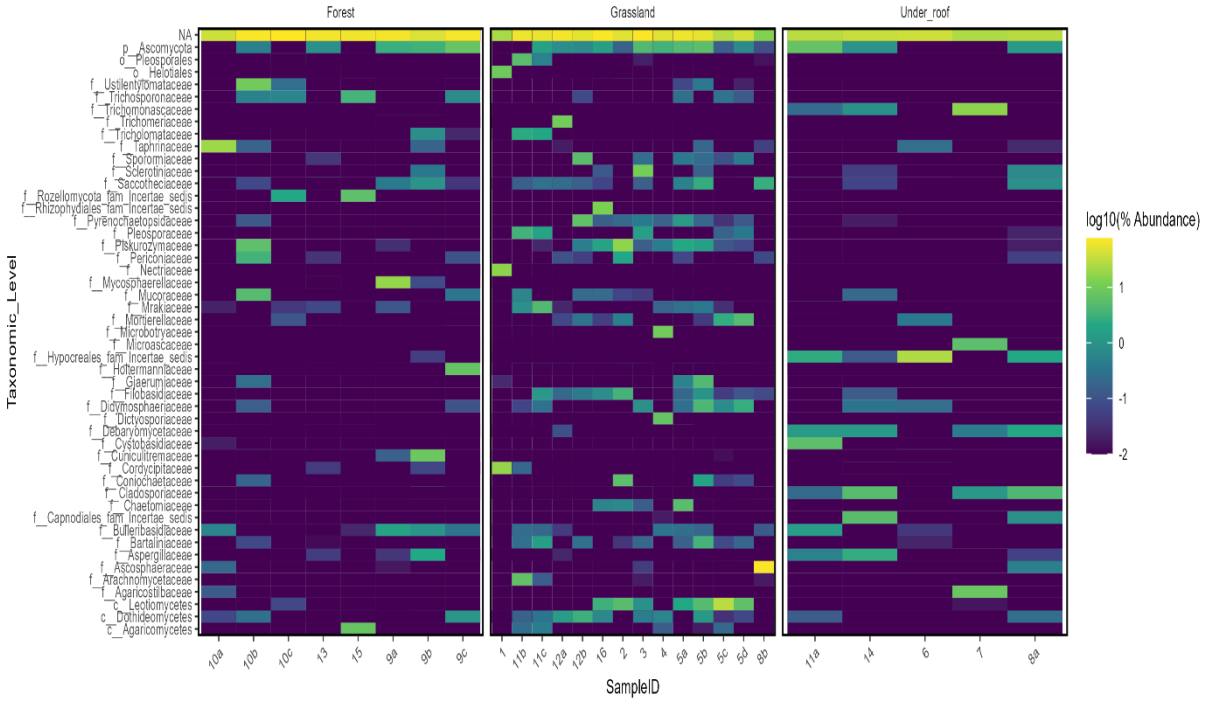

Figure 15: Fungal abundance heatmap. The heatmap shows the 100 most abundant fungi found in samples from forest, grassland and under roof. The y-axis represents the lowest taxonomic level that could be identified, while the x-axis represents the samples.

.

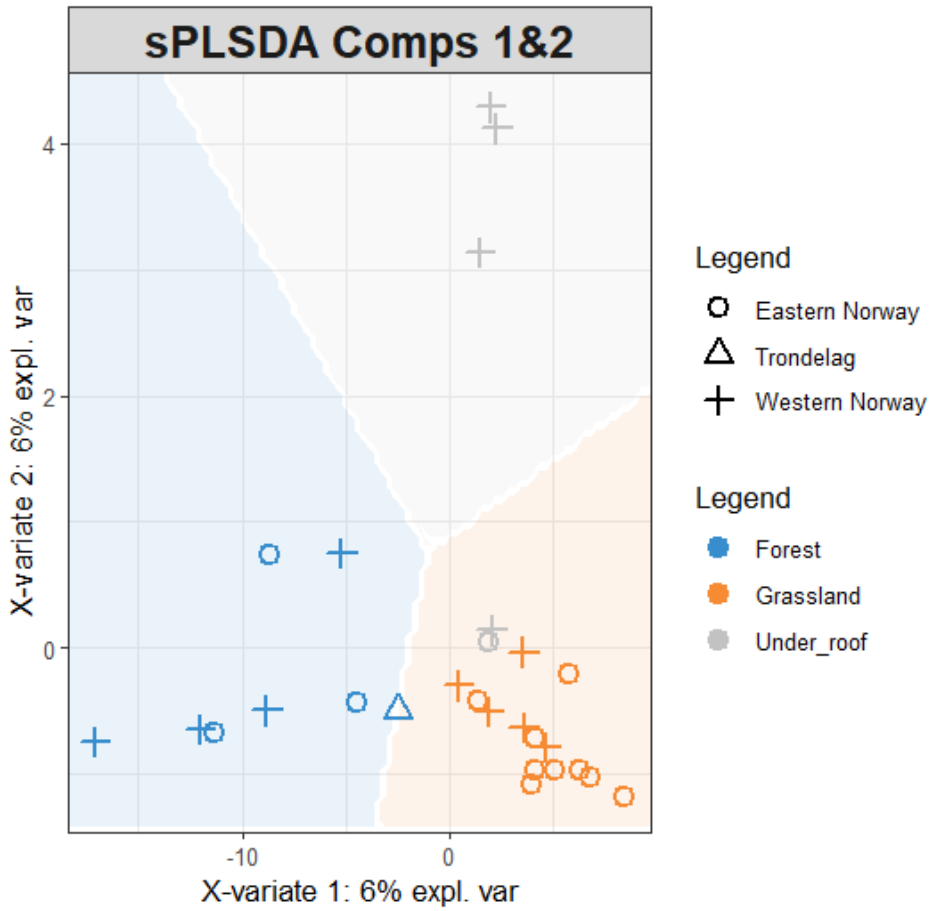

Figure 16: sPLS-DA plot of the diversity found in Norwegian country parts and area conditions. Expl. var = explained variance. Figure is made in R-studio.

3.3 Cultivating and isolation of plastic degrading fungi

The wishlist of 15 species was used as a guidance for finding potential plastic degrading fungi. First, the isolated fungi were examined visually on the agar plates and under microscope to determine the fungal genera. From the 15 species in the wishlist, seven genera were selected to be used in growth experiments (appendix 8, table A8.1). These seven genera were *Aurobasidium* sp., *Ganoderma* sp., *Aspergillus* sp., *Cladosporium sp.*, *Mortierella sp.*, *Alternaria sp.* and *Penicillium sp.*, see figure 17.

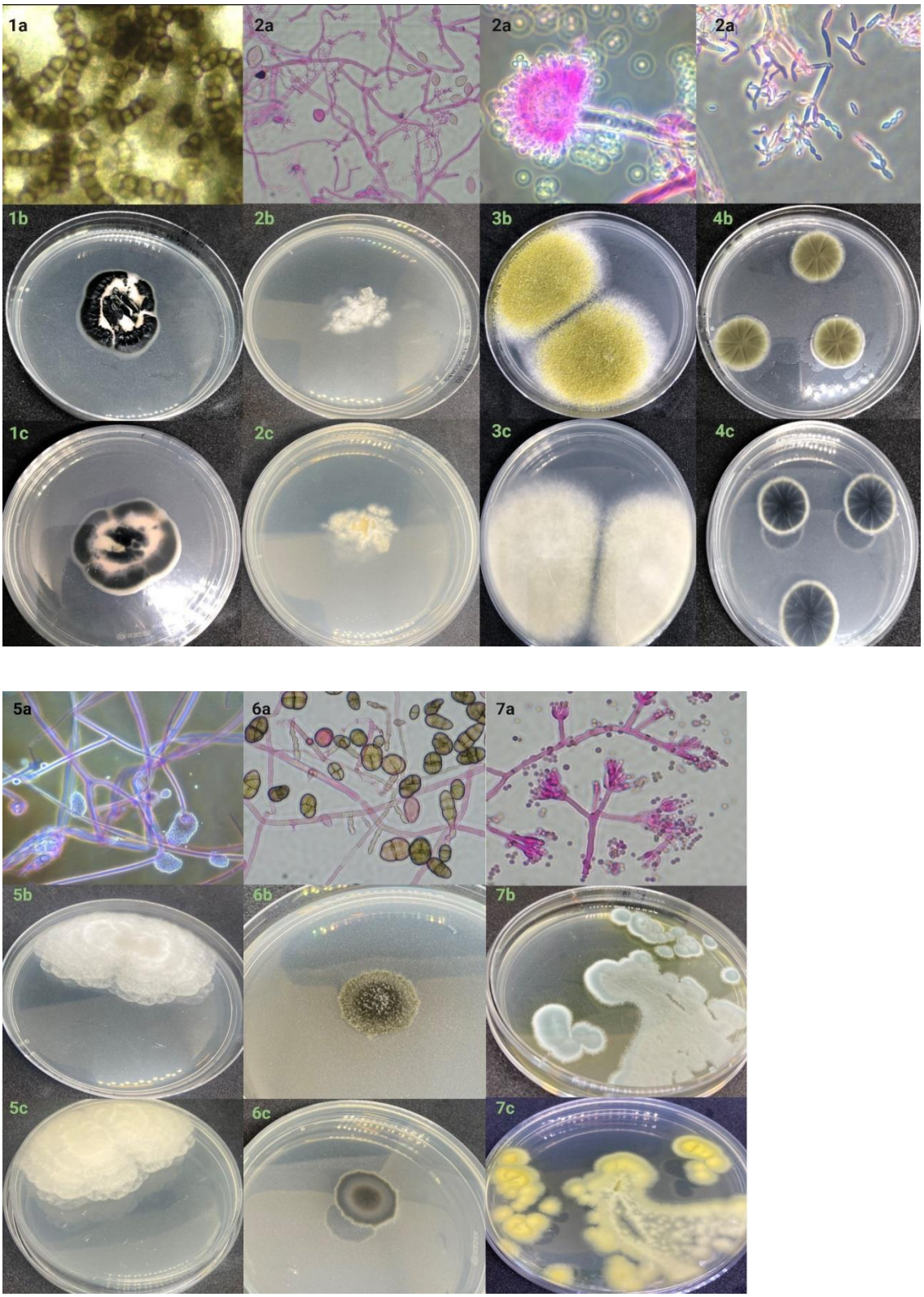

Figure 17: Morphological characteristics in isolates cultivated on DG18 from plastic samples. Isolates morphologically identified as Aurobasidium *sp. (1),* Ganoderma *sp. (2,* Aspergillus *sp. (3),* Cladosporium *sp. (4),* Mortierella *sp. (5),* Alternaria *sp. (6) and* Penicillium *sp. (7). Three figures of each isolate represent microscopy (a), front side of colony (b) and backside of colony (c).*

Ganoderma sp. was not found in the cultivated samples, but was obtained from the NVI's culture collection Mykoteket. To identify the fungal isolates at species level, Sanger sequencing was performed. The extracted DNA abundance and purity level was accepted (appendix 8, table A8.2) (appendix 8, figure A8.3). The amplicon sequencing results were analysed, trimmed and aligned through Geneious Prime and a Blast search of each sequence was performed at the NCBI GenBank database. Everything was well identified except for the isolate initially identified as *Mortierella* sp. that most likely was *Absidia* sp. MEGA11 was used to find the best NSM that were further used in to make a phylogenetic tree based on maximal likelihood (appendix 8, figure A8.4). Figtree and Inkscape were then used to make a good visualisation of the phylogenetic trees. Based on the ITS, *RPB2* and *LSU* genetic markers *Aurobasidium* sp.was identified as *Aureobasidium pullulans* with a boostrap value of 100 (figure 18). *Ganoderma* sp. isolate grouped together with *Ganoderma sessile* isolates based on ITS, TEF-1α and *rpb2* (figure 19). Based on ITS, *bt2* and *cal* sequences, *Aspergillus* sp. was found to belong to the *Flavi* sect, grouped close to *Aspergillus oryzae* and *Aspergillus flavus* with a bootstrap score of 99 (figure 20). *Cladosporium* sp. was grouped together with *Cladosporium uwebraunianum* in the phylogenetic tree based on ITS and TEF1 sequences (figure 21). Based on the ITS sequence *Absidia* sp. was places next to *Absidia coeruela* with a bootstrap value at 100 (figure 22). In the phylogenetic tree, *Alternaria* sp. was grouped in the section *Ulocladioides* based only on the ITS sequence (figure 23). Based on the genetic sequences ITS, *bt2* and *rpb2*, the *Penicillium* sp. isolate was classified as *Penicillium scabrosum* with a bootstrap support value of 100 (figure 24).

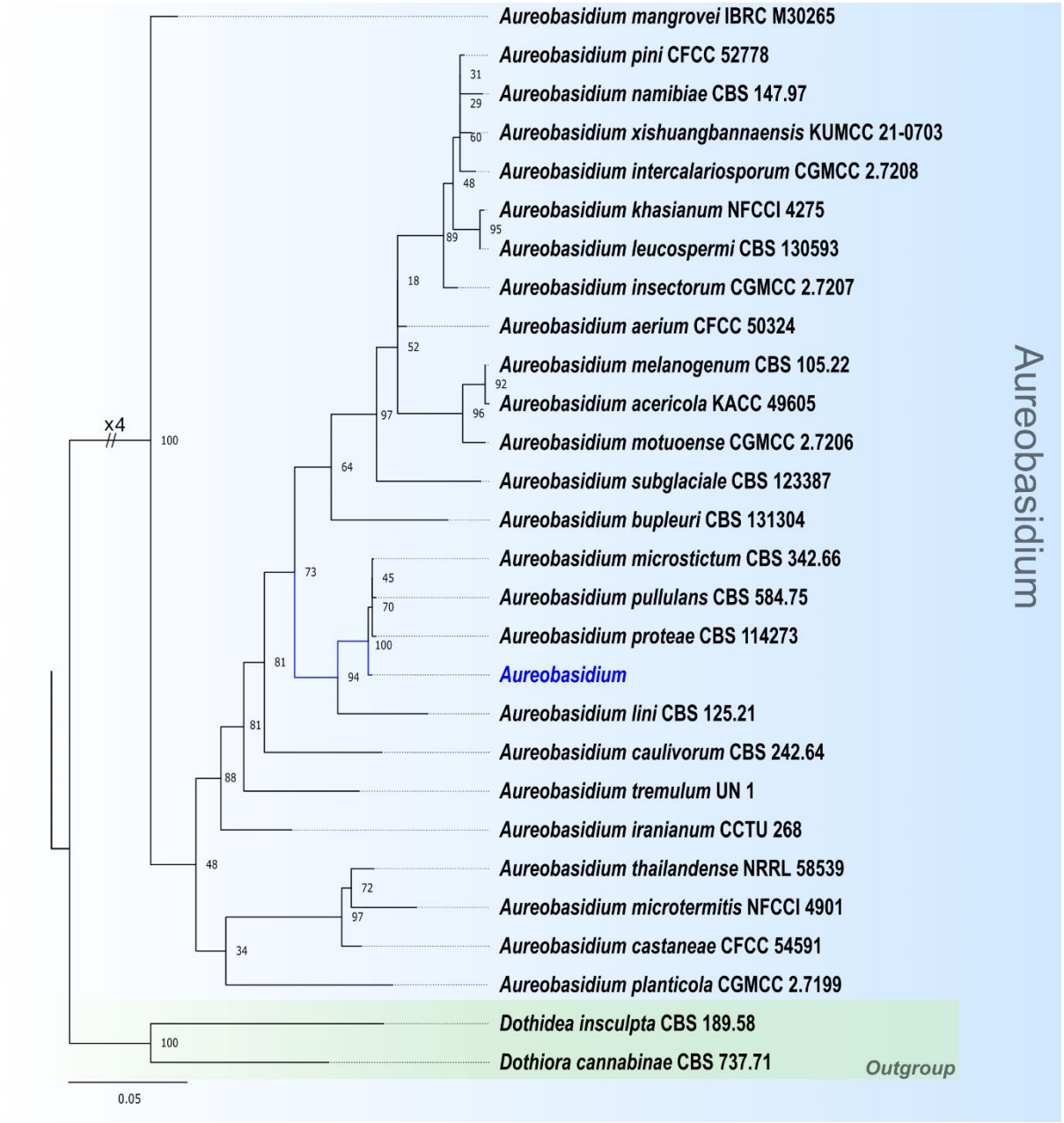

Figure 18: Aureobasidium *phylogenetic tree. The* Aureobasidium *isolate used in this study is labelled with blue colour. ITS, LSU and* rpb2 *sequences from approximately 43 species were used to create the maximal likelihood tree. The numeric values represent bootstrap scores.*

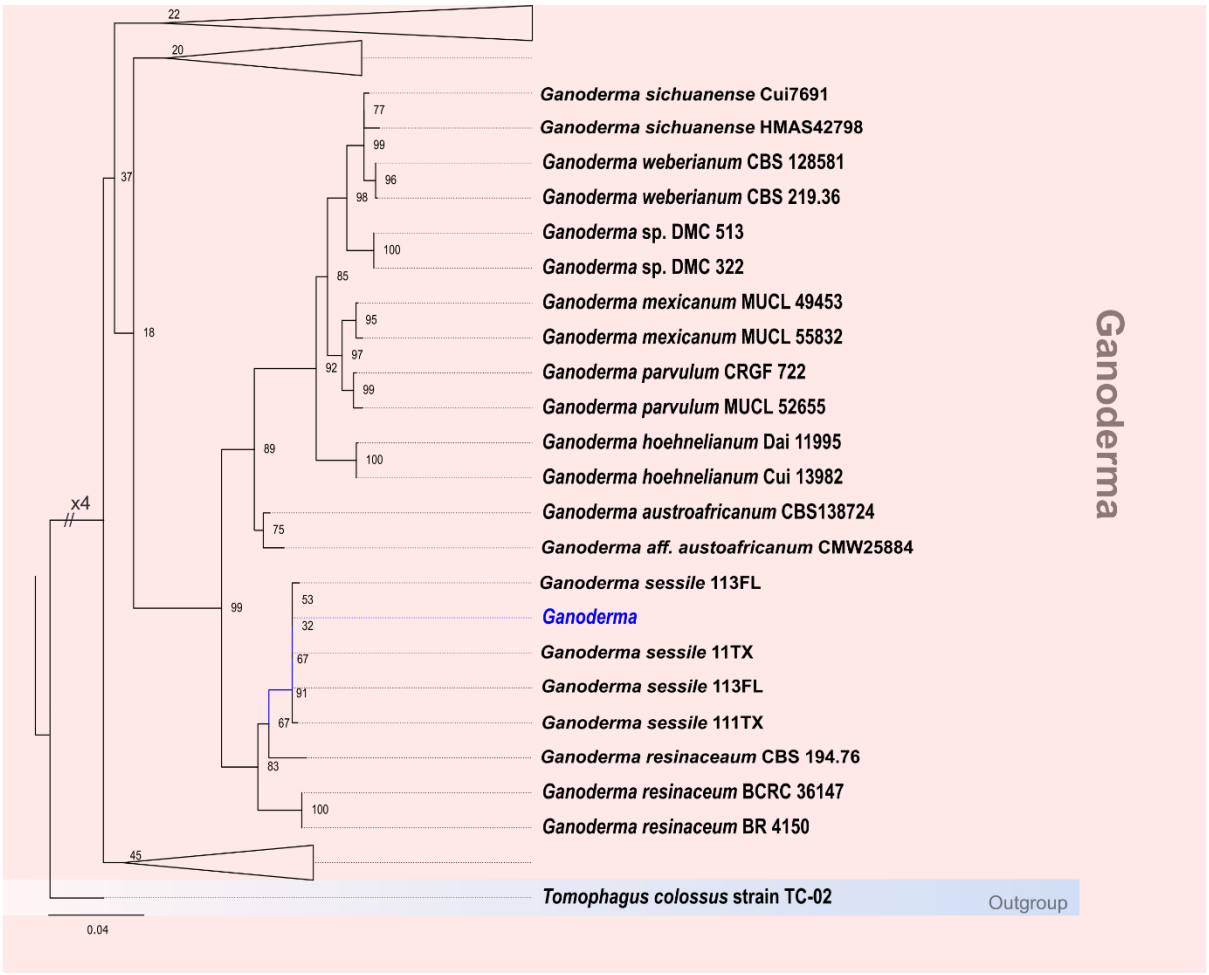

Figure 19: Ganoderma *phylogenetic tree. The* Ganoderma *isolate used in this study is labelled with blue colour. ITS,* tef1-α *and* rpb2 *sequences from approximately 117 species were used to create the maximal likelihood tree. The numeric values represent bootstrap scores.*

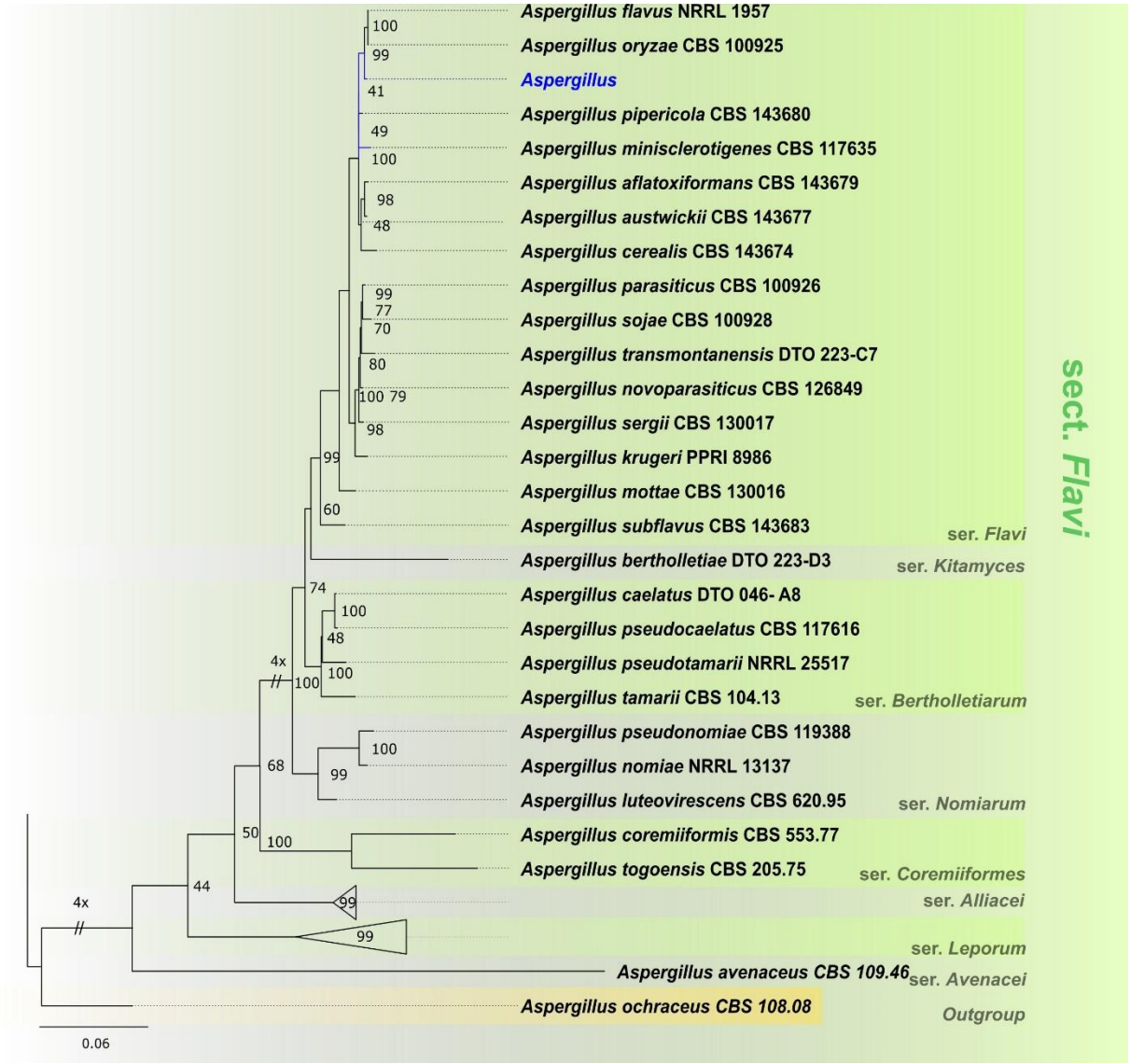

Figure 20: Aspergillus *phylogenetic tree. The* Aspergillus *isolate used in this study is labelled with blue colour. ITS,* bt2 *and* cal *sequences from approximately 36 species were used to create the maximal likelihood tree. The numeric values represent bootstrap scores.*

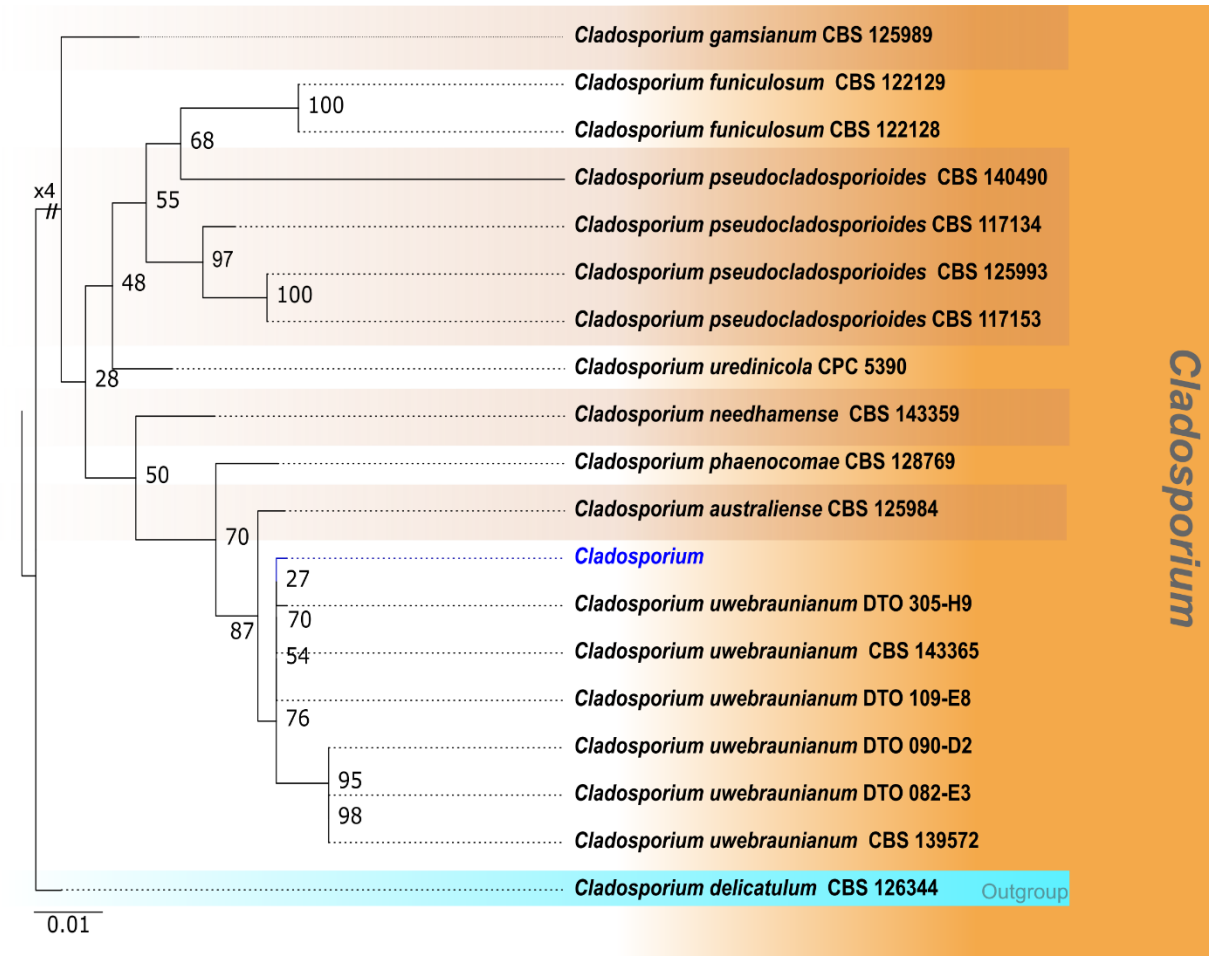

Figure 21: Cladosporium *phylogenetic tree. The* Cladosporium *isolate used in this study is labelled with blue colour. ITS and* tef1 *sequences from 19 species were used to create the maximal likelihood tree. The numeric values represent bootstrap scores.*

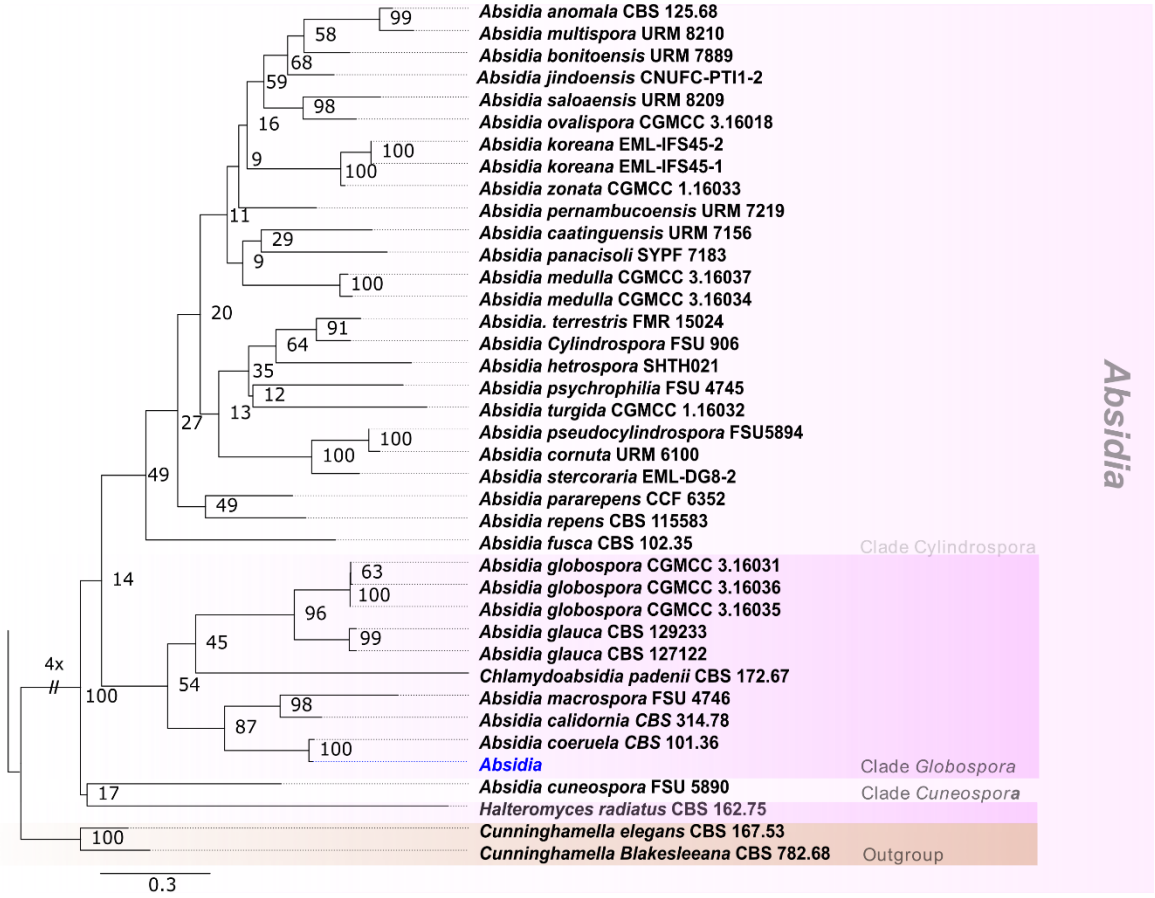

Figure 22: Absidia *phylogenetic tree. The* Absidia *isolate used in this study is labelled with blue colour. ITS sequences from 39 species were used to create the maximal likelihood tree. The numeric values represent bootstrap scores.*

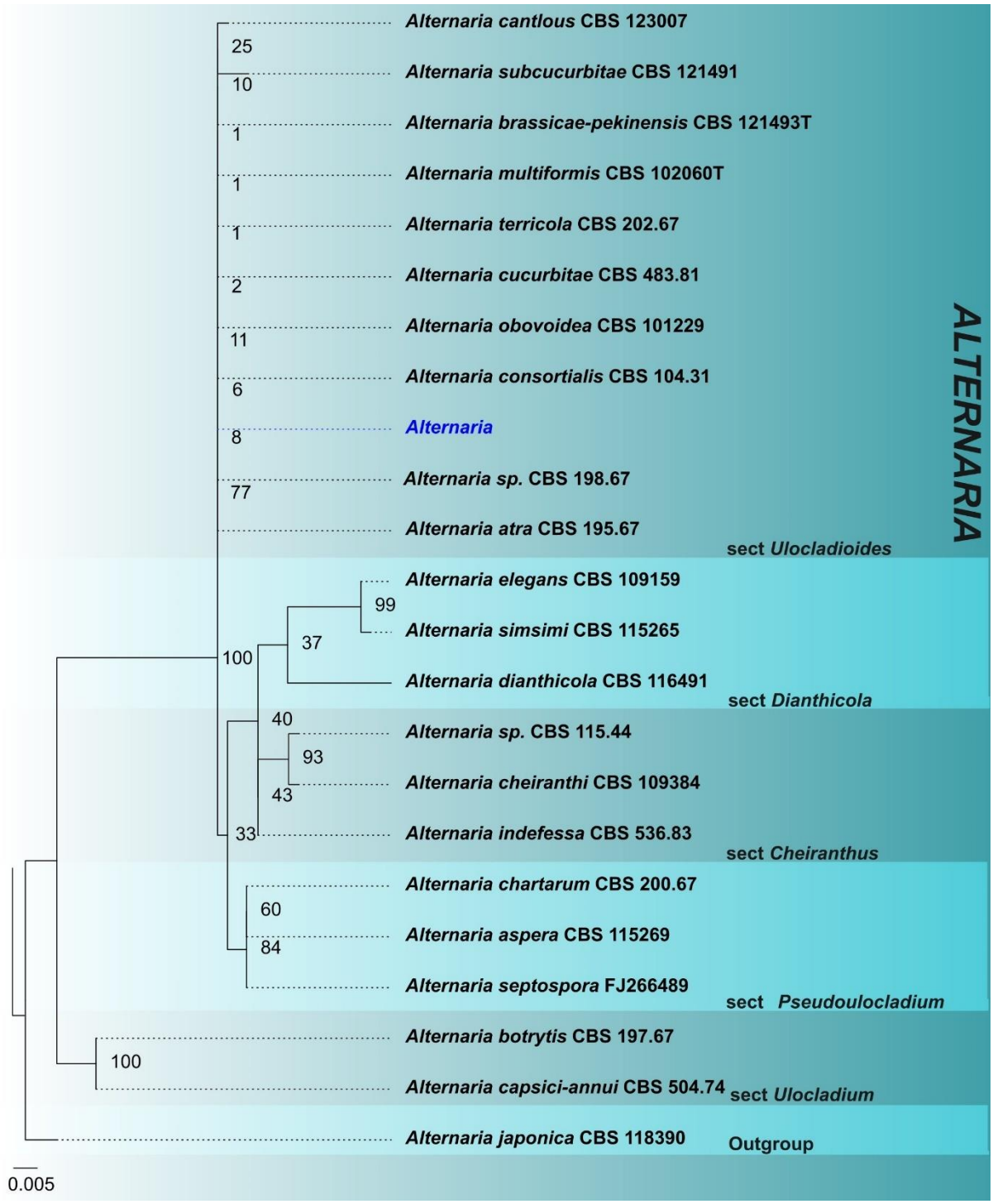

Figure 23: Alternaria *phylogenetic tree. Based on the ITS sequence. The* Alternaria *isolate used in this study is labelled with blue colour. ITS sequences from 23 species were used to create the maximal likelihood tree. The numeric values represent bootstrap scores.*

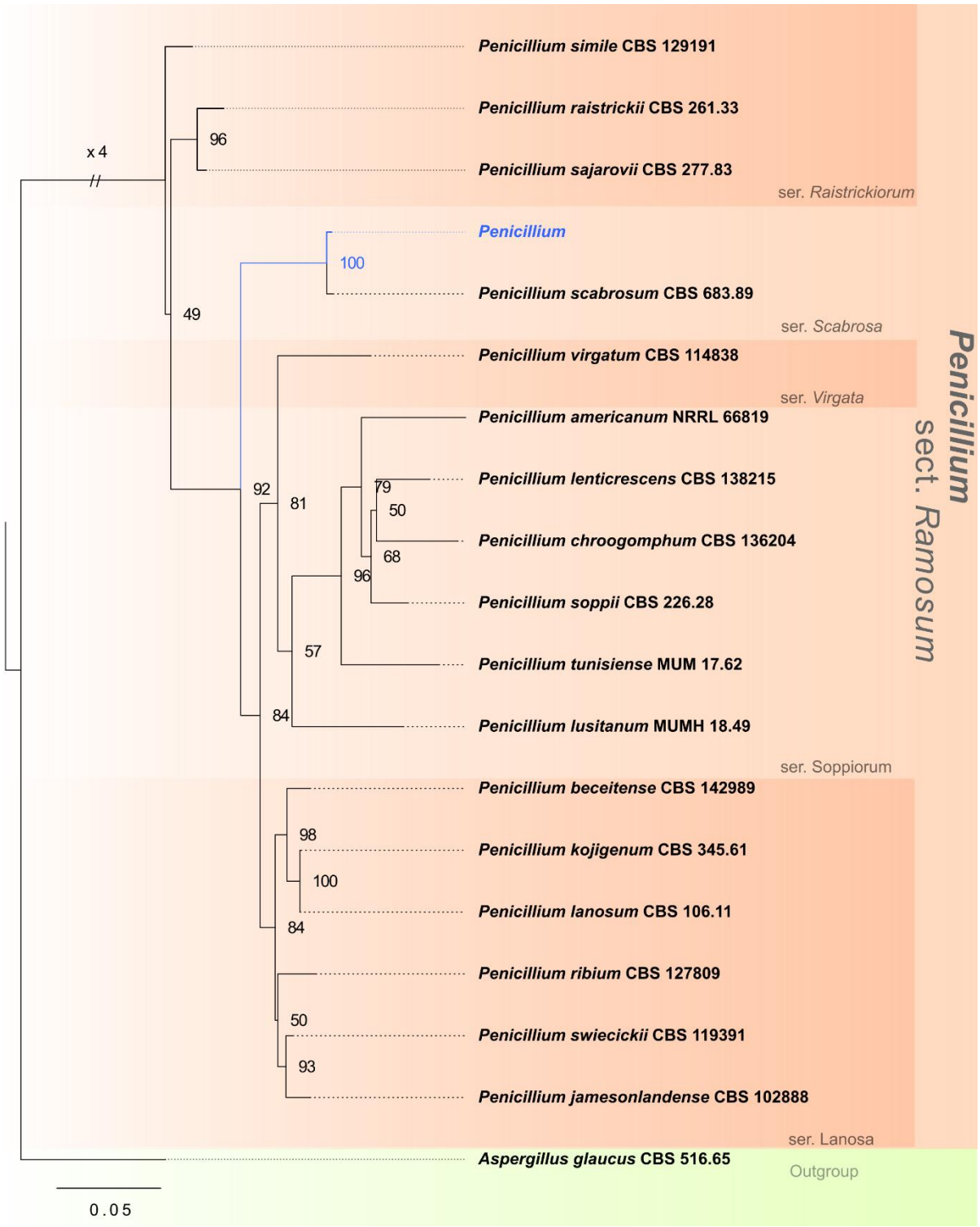

Figure 24: Penicillium *phylogenetic tree. The* Penicillium *isolate used in this study is labelled with blue colour. ITS,* bt2 *and* rpb2 *sequences from approximately 19 species were used to create the maximal likelihood tree. The numeric values represent bootstrap scores.*

3.4 Growing fungi on plastic

Plastic pretreatment

Half of the plastic pieces were radiated with UV-C arrays with a calculated dosage at 1.5 x 10^7 mJ/cm^2. Results of the LDPE-water droplet contact angle measurements before and after UV radiation showed that the optical angle on average was reduced by 23º after UV-treatment. The measured plastic droplet contact angle average values are illustrated in figure 25, while the precise measurements are listed in table A9.1 in appendix 9. The LDPE water droplet showed visible changes in shape from before and after UV-treatment (figure 26).

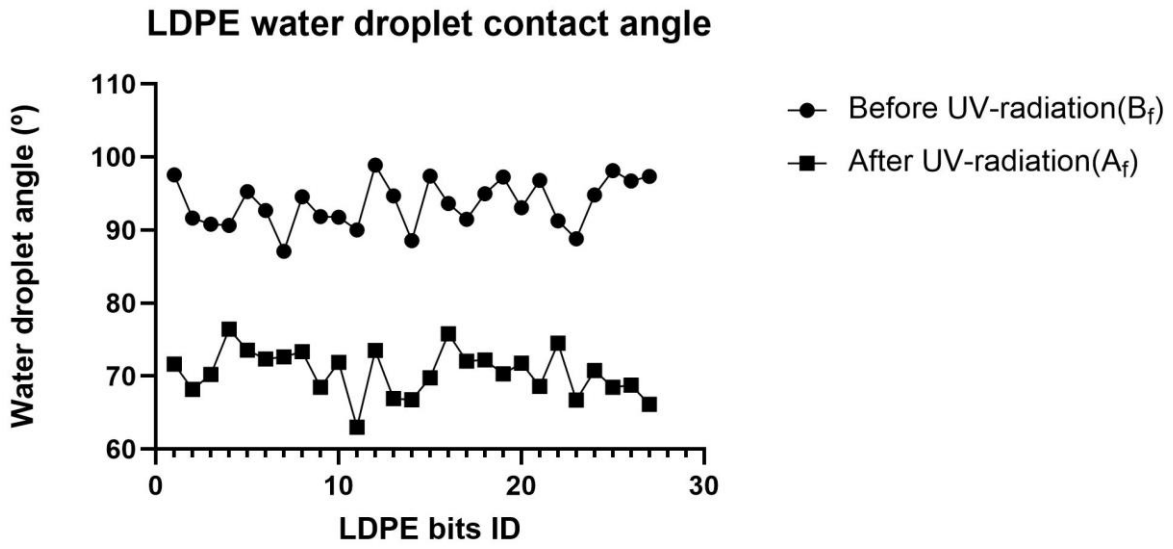

Figure 25: LDPE/water droplet contact angles. The figure shows the average measured water contact angles on the droplet that were released onto the LDPE surface before and after UV-radation. Figure is made in Graph Pad prism (v. 10.2.2).

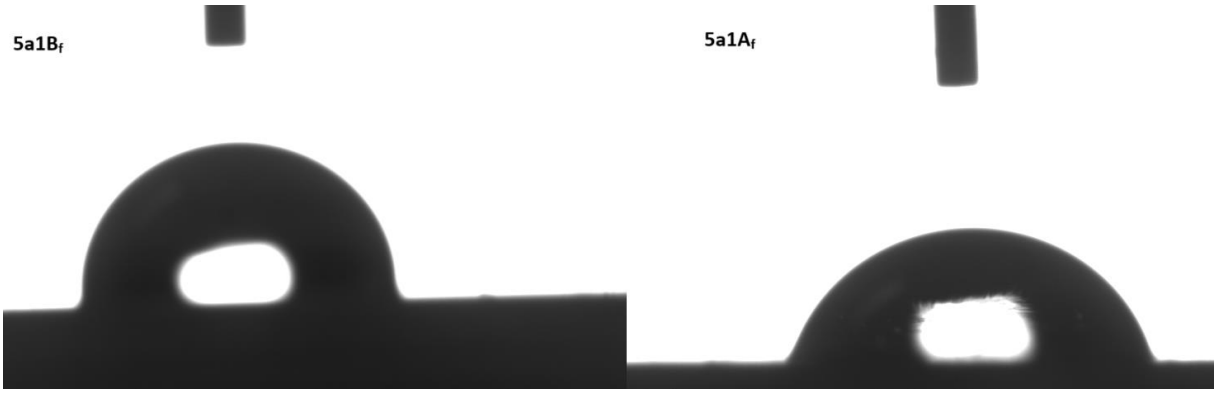

Figure 26: Plastic/water droplet contact angle. By using the OCA 15EC Contact Angle Goniometer, water droplet was released on to the plastic surface and a picture were taken after 1-10 seconds. The plastic surface belongs to plastic piece 5a parallel one before UV-treatment (5a1Bf) and after UV-treatment (5a1Af). The picture was taken at 0.7x magnification

Cultivation

OD_{600} and pH were measured weekly, with one exception, two weeks passed between the penultimate and last measurement. After removing any outliers at a 95 % confidence level,

significant change in OD, indicating fungal growth, were observed in out of 20 out of 28 samples compared to the negative controls. The measured OD can be found in table A9.2 and A9.3 in appendix 9. The highest OD-value with 95% confidence level for negative control was 0,007.

Outliers were also removed for the pH measurements. While all of cultures with glucose, except 5b, showed statistically significant differences from the negative controls, only one of the cultures without glucose, radiated LDPE cultivated with *G. Sessile* (10a), showed significant difference from the negative controls. The measured pH can be viewed in table A9.4 and A9.5 in appendix 9. Negative controls pH ranged from 4.1 to 4.384 in media with glucose, while in media without glucose the pH ranged from 5,4 to 5,623. It was observed a general more intensive growth and lower pH in samples with glucose than in samples without glucose. The contamination control performed at the end of the research showed contamination in some of the samples (appendix 6.3.4, table 6.3.4.6). Observations done at the end of cultivation are summarized in table 7.

Table 7: Observations throughout cultivation experiment summarized. Samples with no significant observation are omitted from the table. Media either consists of MSM (A) or soil (B).

Isolate	**Media**	**Glucose**	**UV**	**Observation**
A. pullulans	A	+	+	Growth. Media turned dark green
	A	+	-	Growth. Media turned dark green
G. sessile	A	+	+	Growth
	A	+	-	Growth
	A	-	+	Little growth
	A	-	-	Little growth
	B		+	Visible growth
	B		-	Visible growth along LDPE edges
Aspergillus sp.	A	+	+	Growth
	A	+	-	Growth
	A	-	+	Little growth
	A	-	-	Little growth
	B		+	Visible growth
	B		-	Visible growth
C. uwebraunianum	A	+	+	Growth. Growth covering LDPE surface
	A	+	-	Growth. Growth covering LDPE surface

	A	-	+	Little growth. Growth on plastic
	A	-	-	Little growth. Growth on plastic
A. coeruela	A	+	+	Media became less transparent
	A	-	+	Little growth. Media became less transparent
	A	-	-	Little growth
Alternaria sp.	A	+	+	Growth
	A	+	-	Growth. Media turned dark green. Not as dark as 1a and 1b
	A	-	+	Litle growth. Growth on plastic
	A	-	-	Visible growth, but not as much as the sample above
P. scabrosum	A	+	+	Growth
	A	+	-	Growth
	A	-	+	Litle growth. Media became less transparent
	A	-	-	Litle growth

The contamination control performed at the end of the research showed contamination in some of the samples (appendix 6.3.4, table 6.3.4.6).

3.5 Analysing fungal degraded plastic.

Visible growth was observed on LDPEs piece from samples inoculated with *C. uwebraunianum* and UV-radiated LDPE piece inoculated with *Alternaria* sp. in MSM without glucose (figure 27). Observations done at the end of cultivation are summarized in table 3.4.1. Discoloration of LDPE piece with *A. pullulans* grown in MSM with glucose and UV-radiated LDPE piece grown with *Alternaria* sp. in MSM with glucose were also observed.

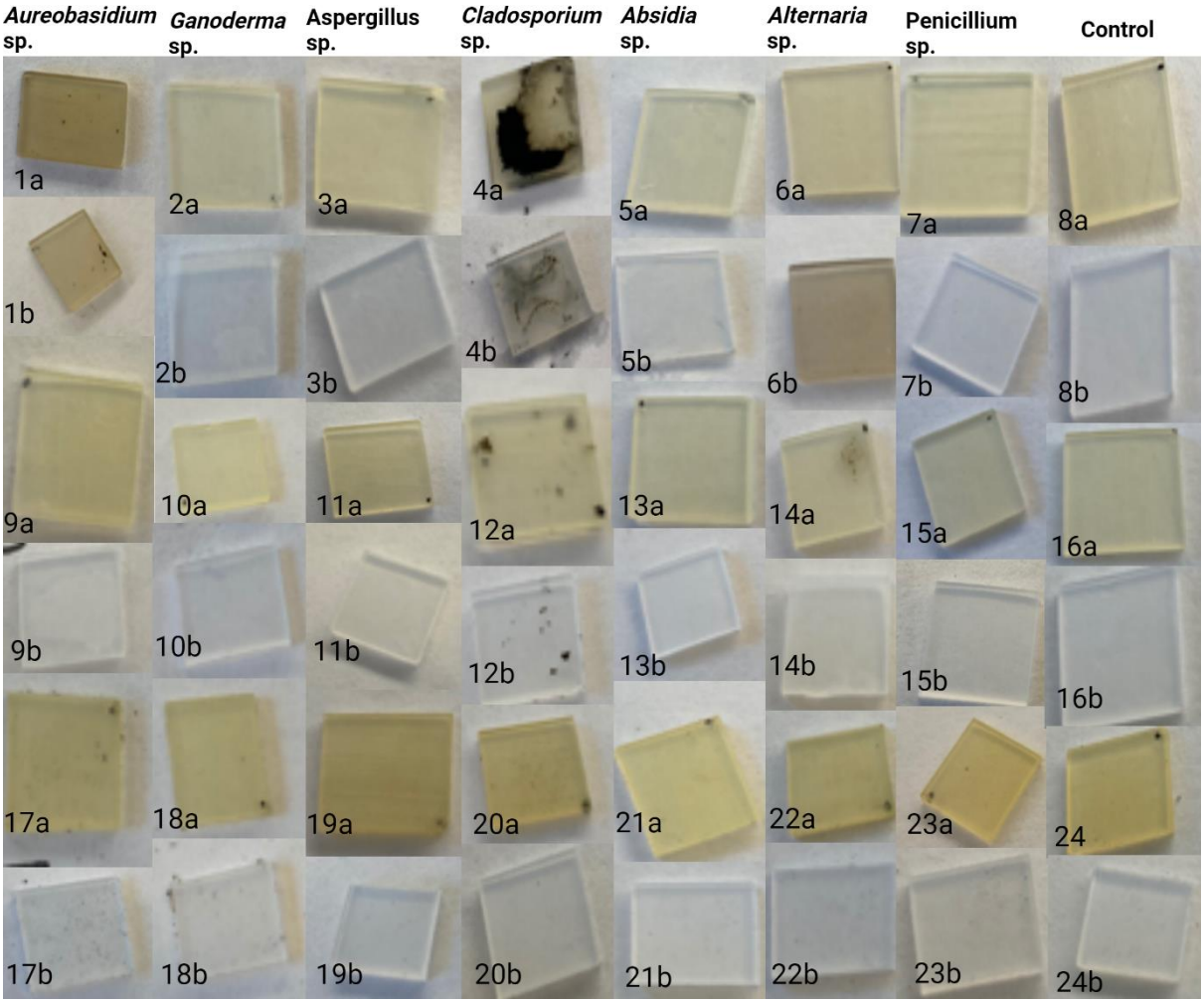

Figure 27: Plastic pieces after biodegradation experiment. The figure shows plastic pieces cultivated with (from left) A. pullulans, G. sessile, Aspergillus sp., C. uwebraunianum, A. coeruela, Alternaria sp., P. scabrosum and control. a – plastic pieces UV-radiated before experiment; b - plastic pieces without UV radiation. 1-8 – samples in MSM with glucose, 9-16 – MSM without glucose; 17-24 – soil.

Post-experimental weight and the LDPE/water angle was measured and compared to initial values. The results are shown in figure 28 and figure 29, respectively.

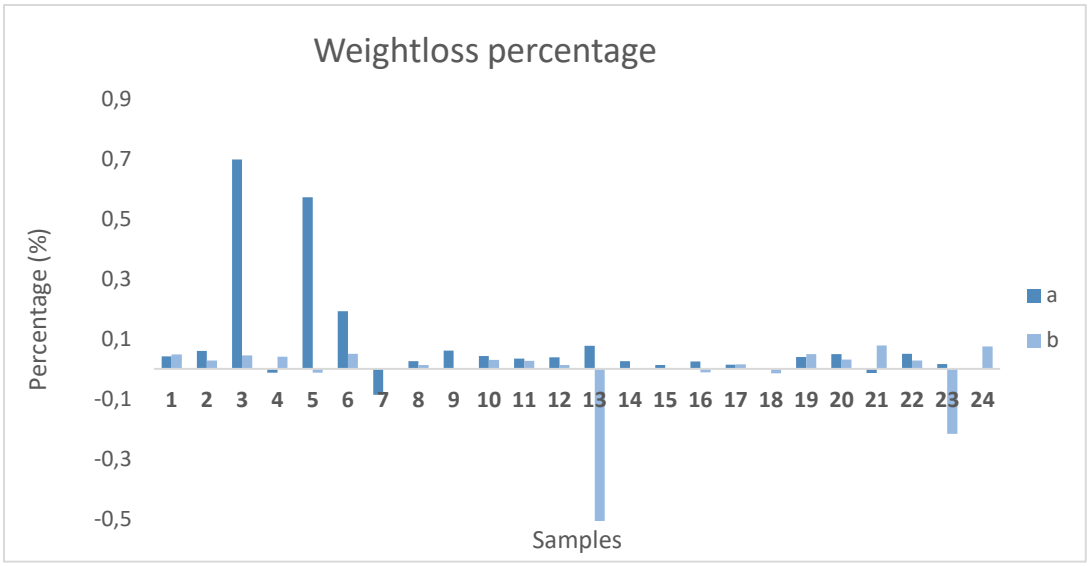

Figure 28: Weight loss measurement after biodegradation. The figure shows the percentage change in weight of each LDPE piece between before and after biodegradation. 1, 9 and 17 –A. pullulans*; 2, 10 and 18* –G. sessile*; 3,11 and 19* –Aspergillus *sp.; 4, 12 and 20* –C. uwebraunianum*; 5,13 and 21* –A. coeruela*; 6, 14 and 22* – Alternaria *sp.; 7, 15 and 23* –P. scabrosum. *a – plastic pieces UV-radiated before experiment; b - plastic pieces without UV radiation. 1-8 – samples in MSM with glucose, 9-16 –MSM without glucose; 17-24 – soil.* (,=.)

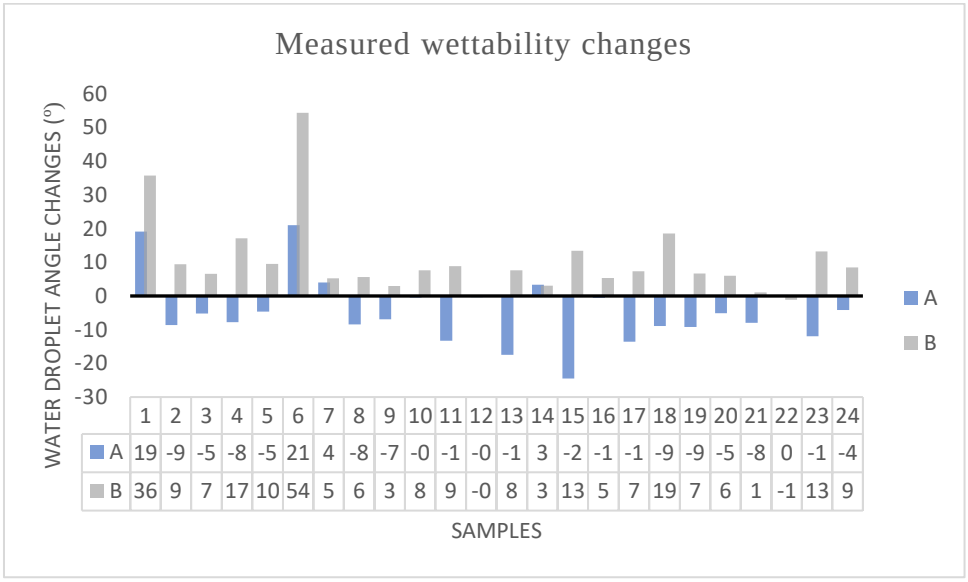

	1	2	3	4	5	6	7	8	9	10	11	12	13	14	15	16	17	18	19	20	21	22	23	24
A	19	-9	-5	-8	-5	21	4	-8	-7	-0	-1	-0	-1	3	-2	-1	-1	-9	-9	-5	-8	0	-1	-4
B	36	9	7	17	10	54	5	6	3	8	9	-0	8	3	13	5	7	19	7	6	1	-1	13	9

Figure 29: Measured LDPE wettability changes after biodegradation. Figure shows water droplet angle difference measured after 89 days with biodegradation. 1, 9 and 17 –A. pullulans*; 2, 10 and 18* –G. sessile*; 3,11 and 19* –Aspergillus *sp.; 4, 12 and 20* –C. uwebraunianum*; 5,13 and 21* –A. coeruela*; 6, 14 and 22* – Alternaria *sp.; 7, 15 and 23* –P. scabrosum. *A – plastic pieces UV-radiated before experiment; B - plastic pieces without UV radiation. 1-8 – samples in MSM with glucose, 9-16 –MSM without glucose; 17-24 – soil.*

An overview observation with SEM was performed on 15 samples to analyse the plastic topography for cracks and fungal growth that might indicate fungal degradation (figure 30). The descriptions made during microscopy are recorded in table 8. The radiated LDPE cultivated with *P. scabrosum* in MSM with glucose, showed cracks around one of the hyphae. Radiated LDPE with *C. uwebraunianum* grown with glucose and radiated LDPE with *Alternaria* sp. grown without glucose showed fungi glued to the surface in large networks (figure 31). LDPE

with *C. uwebraunianum* grown in MSM without glucose showed signs of fungal attachment to the plastic. A close up of one of the strong attachments between the fungi and the LDPE piece can be viewed in figure 32. At a higher magnification, it was observed a bright wreath were the hyphae met the plastic.

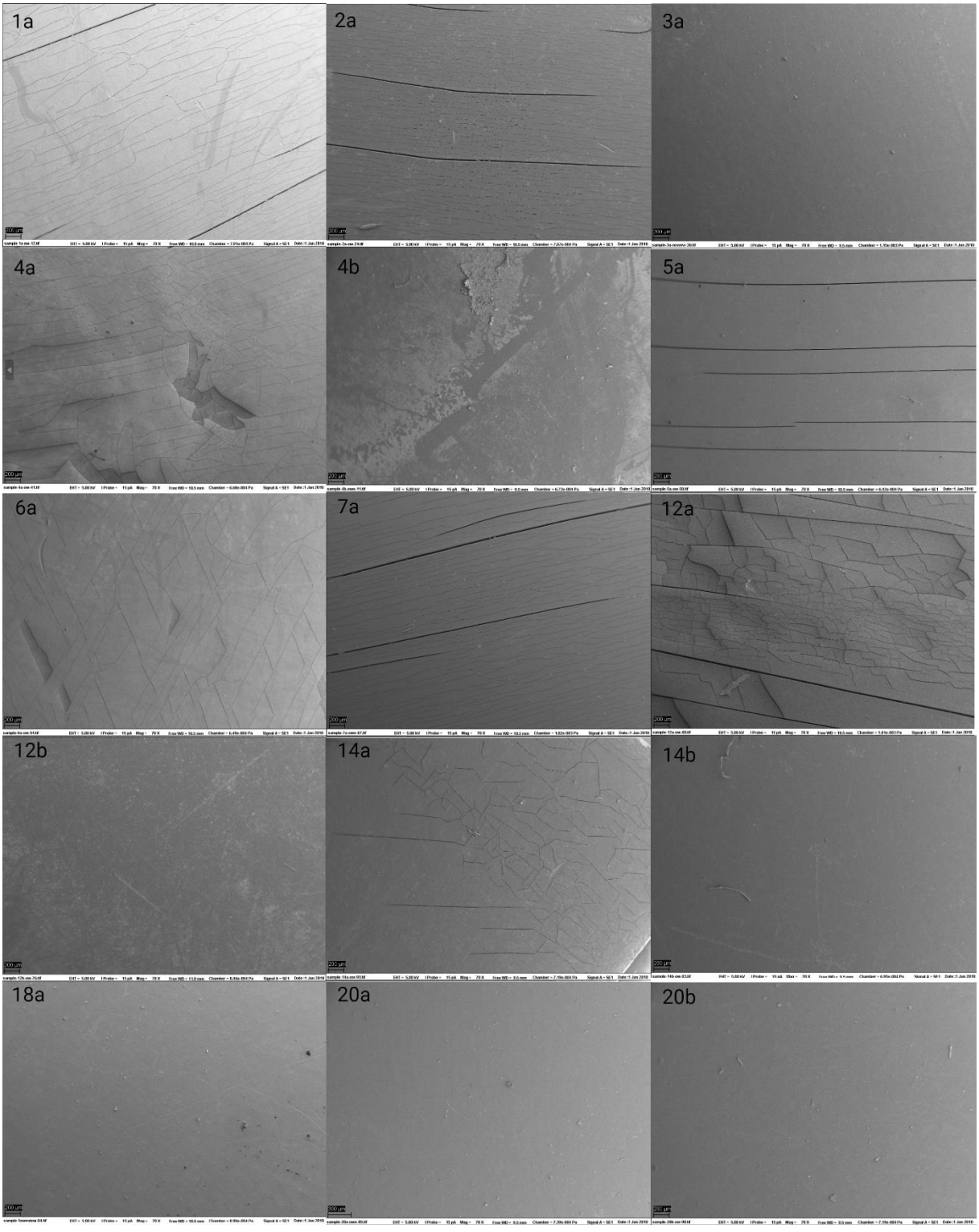

*Figure 30: SEM electron microscopy of LDPE pieces. The figure shows 15 different LDPE pieces after biodegradation. The LDPE area is enlarged 70x. 1 –*A. pullulans*; 2 and 18 –*G. sessile*; 3 –*Aspergillus sp.*; 4, 12 and 20 –*C. uwebraunianum*; 5 –* A. coeruela*; 6 and 14 –* Alternaria sp.*; 7 –*P. scabrosum*. a – plastic pieces UV-radiated before experiment; b - plastic pieces without UV radiation. 1-8 – samples in MSM with glucose, 9-16 –MSM without glucose; 17-24 – soil.*

*Table 8: SEM observations on LDPE samples cultivated with fungi. 1 –*A. pullulans*; 2 and 18 –*G. sessile*; 3 –*Aspergillus *sp.; 4, 12 and 20 –*C. uwebraunianum*; 5 –*A. coeruela*; 6 and 14 –* Alternaria *sp.; 7 –*P. scabrosum*. a – plastic pieces UV-radiated before experiment; b - plastic pieces without UV radiation. 1-8 – samples in MSM with glucose, 9-16 –MSM without glucose; 17-24 – soil.*

Sample	**Observation**
1a	Large cracks, small cracks and fungi inside the corner mark.
2a	Large cracks and small areas coated with thin layers
3a	Few small cracks
4a	Smal cracks, some indent, fungi on the surface and fungi inside corner mark
4b	Large areas with a thin coating film and fungi on the surface
5a	Large cracks
6a	Small cracks and some indent
7a	Large cracks, small cracks, bacteria and fungi in corner mark
12a	Large cracks, small cracks and indent
12b	Large areas with a thin coating film
14a	Small cracks, small areas with a thin coating film and fungi on surface
14b	Small areas with a thin coating film
18a	Small tears
20a	Few small cracks
20b	No remarks

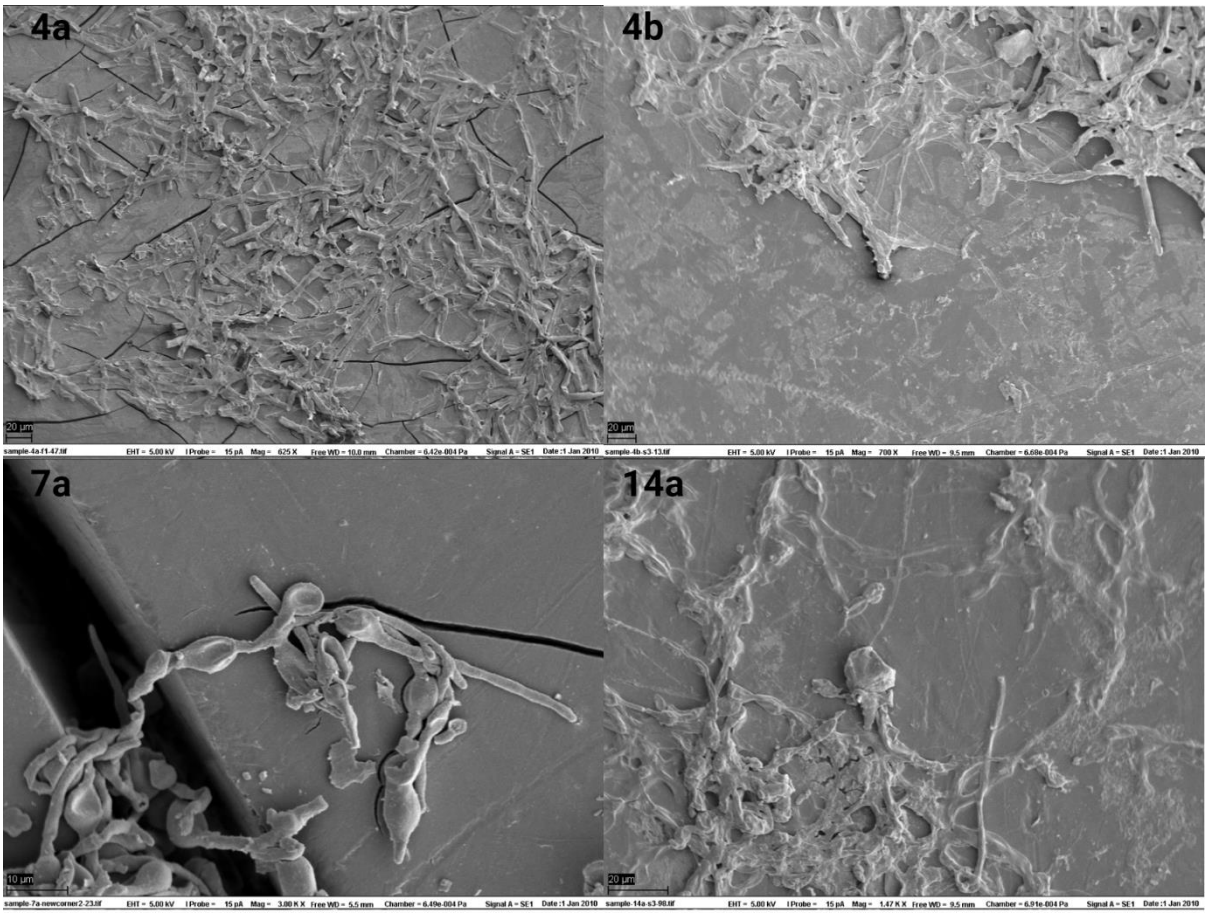

*Figure 31: SEM pictures of fungal growth on LDPE pieces. 4a is magnified by 625 X, 4b is magnified by 700 X, 7a is magnified by 3000 X and 14 a is magnified by 1470 X. 4 –*C. uwebraunianum*; 14 –* Alternaria *sp.; 7 –*P. scabrosum*. a – plastic pieces UV-radiated before experiment; b - plastic pieces without UV radiation. 1-8 – samples in MSM with glucose, 9-16 –MSM without glucose.*

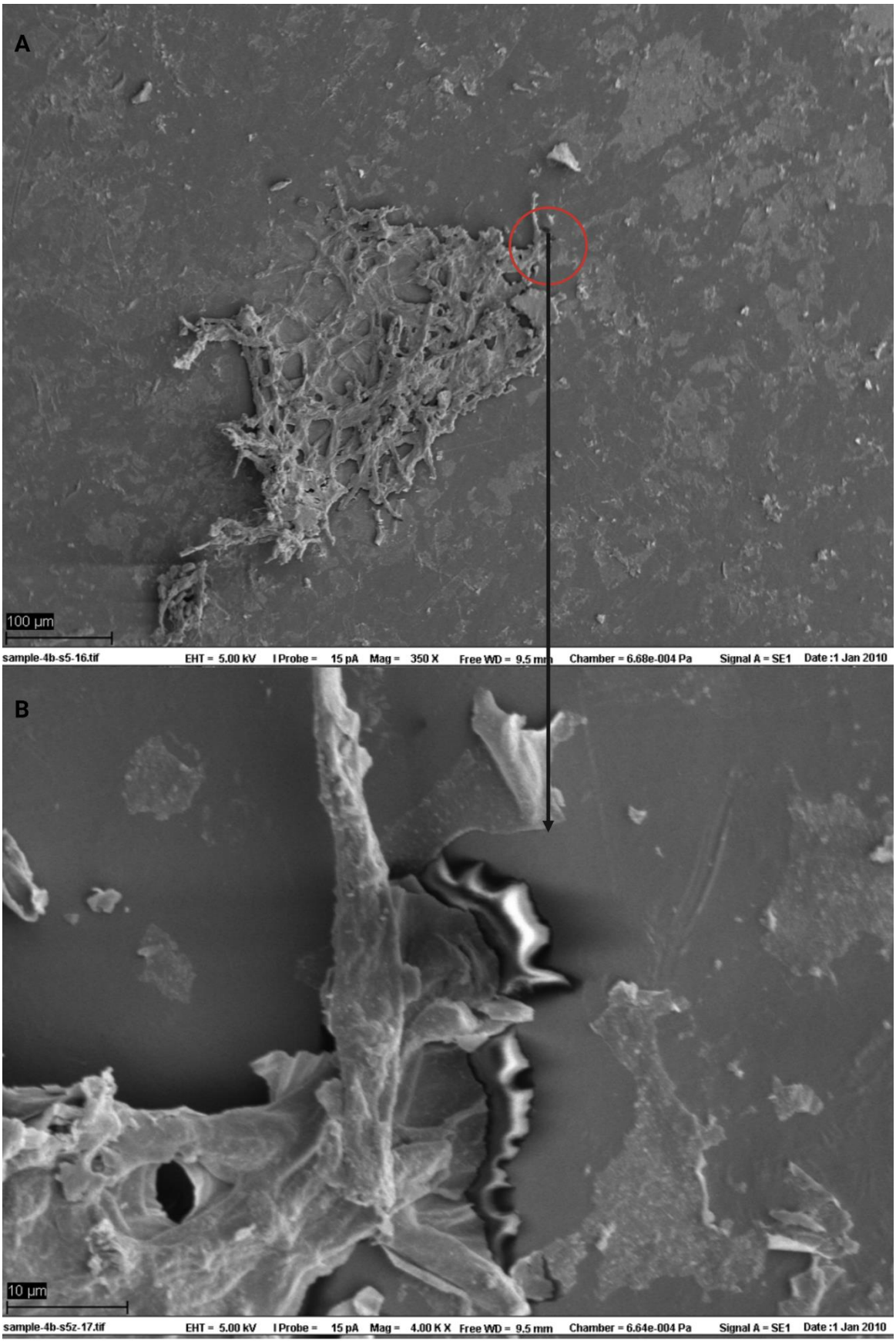

Figure 32: SEM picture of fungal attachment of non-radiated LDPE piece grown with C. uwebraunianum *in MSM with glucose. A –350 X magnification . B –4000 X magnification.*

4. Discussion

In this study *C. uwebraunianum* was found as the most promising plastic degrading fungus. From silage plastic wrap samples obtained from the Norwegian landscape, the family *Cladosporiaceae* was the most abundant, constituting 10% of all fungi found in the samples. *C. uwebraunianum* grew on the LDPE surface in liquid media showing a strong attachment with a possible anchoring/penetration. This is the first report of *C. uwebraunianum*`s plastic degrading potential.

Sample collection

In a study by NORCE, 43 rivers in the Western Norway were investigated for plastic residues. The results showed that all the rivers contained plastic and that 70% was agricultural plastic where silage plastic wrap dominated (Velle, 2020). This information suggested that a lot of potential ready-for-collecting plastic can be found around Norway. In a request for samples spread to Norwegian citizens, it was specified that the sample should be at least one year old as plastic wrapping that is older than one year is expected to be over the UV-protection limit, undergoing photodegradation, thereby losing the hydrophobic tension and creating more available carbon, allowing microbial establishment (Triowrap, 21.05.14).

19 volunteers provided 27 samples in total, from Eastern Norway, Western Norway and Trøndelag. What is noteworthy, not only farmers participated in the sample collection. The goal of collecting plastic samples from every Norwegian country part was not achieved. The uneven distribution of sampling sites can be caused by many factors. Specificity of the plastic was the most critical (and limiting) factor. Since the requested plastic type was a silage plastic wrap, the volunteer range was restricted to farmers or people living nearby agricultural lands where silage plastic wrap is used. Also, agricultural businesses that use this wrap for storing and preserving grass do not appear in the same frequency throughout the country. According to Statistisk sentral byrå in 2023, Eastern Norway had 15 356 agricultural businesses, while Western Norway 12 180, Trøndelag 5 344, Northern Norway 2 842, and Southern Norway 1 839 agricultural businesses. This could explain why most of the samples came from Eastern and Western Norway (Statistisk-sentrabyrå, 2023). Another important factor related to sample origin area was the reach of the used media channels in order to address the public. Information about the project was distributed through interviews with media that were believed to reach farmers as target audience — Norges bondelag, Bondebladet and Nynorsk presse. Nynorsk presse distributed the interviews to local newspapers that were addressing an audience living in the western part of the country. This could have contributed to the high number of volunteers

from that part of Norway. In some cases, the volunteers had limited knowledge about the plastic – silage wrap had been on the farm before ownership or some of the volunteers that collected samples were not farmers themselves. Some of the plastic samples did not look like LDPE plastic. Two samples from Western Norway were originating from berry farming, while another sample from Western Norway was produced in a time where LDPE were not the most common plastic type used for silage plastic wrap material. However, the samples were included in the study.

Metabarcoding

Optimalisation

As a result of the DNA-extraction optimalisation, the PowerSoil® DNA kit from QIAGEN with pretreatment (sonication, vortexing and filtration) was used. Although this kit gave a higher contamination according to the high absorption in 230 nm spectra measured by NanoDrop, it also gave a high DNA yield after extraction. The high absorbance at 230 nm could be a result of phenolic resins residue from the plastic which absorb wavelengths at 230 nm (Brydson, 1999). The pretreatment eliminated the need of fitting the plastic into the PowerBead Pro Tube; only a filter was required.

PCR

There are drawbacks and advantages of the use of either ITS1 or ITS2 target (Blaalid et al., 2013). One of the downsides of using ITS2 instead of ITS1 is the amplification bias that can occur with *Basidiomycota*. The ITS2 region is generally longer in *Basidiomycota* than *Ascomycota,* which can lead to lower amplicon abundance of *Basidiomycota* in relation to *Ascomycota.* ITS1 does not give this bias; however, it would enhance non-dikaya fungi amplification *(Bellemain et al., 2010)*. As the Dr. Jekyll and Mr. Hyde project is mostly interested in dikaryotic fungi ITS2 was selected as the target region.

Mock community

While the actual relationship between *Basidiomycetes* DNA and *Ascomycetes* DNA were approximately 20% and 80% respectively the DNA proportions after mixing, the sequencing results showed that the *Basidiomycetes* only accounted for 0,057% of the identified species. This is approximately 400 times less than the actual abundance. The mock community sequencing results therefore indicated that the relationship between *Basidiomycetes* and *Ascomycetes* in the sample results cannot be fully trusted, and that the actual abundance of a *Basidiomycete* could be significantly higher than shown. The reason why the *Basidiomycota*

abundance was low after sequencing could be due to the specificity of the genetic marker used, PCR reaction and database coverage. *Wallemia sebi, Rhodotorula mucilaginosa* and *Rhodotorula* sp. are classified to the genus level in the UNITE database that was used for taxonomical annotation of the results, problems with the database were therefore excluded. The fact that shorter DNA fragments are more easily amplified could explain why the *Basidiomycota* and *Ascomycota* abundance relation were skewed after sequencing. Potentially primer specificity could be an explanation for the observed bias, as both ITS3 and ITS4 primers have been found to give more mismatches with *Basidiomycota (Bellemain et al., 2010).*

Sample results

Abundance

After sequencing the sample mix with Illumina, the sequences were processed in QIIME2. The *Cladosporium* genus was the most abundant genus. This was not surprising since *Cladosporium* is a common outdoor fungus, and also among the most frequent indoor fungi (Salvatore et al., 2021). Although, instructions were sent to the participants on how to collect the sample to avoid contamination, it cannot be completely excluded that unprecise sample collection affected the results. Previous studies have also found *Cladosporium* sp. when isolating fungi from plastic (Brunner et al., 2018, Sathiyabama et al., 2024, Kim et al., 2022). This might indicate the presence of the genus on plastic is not accidental. The other abundant fungus found the samples was a *Mortierella* sp., a genus common in soil (Ozimek and Hanaka, 2021). A high abundance of fungi connected to soil habitat was expected since many of the received plastic samples contained soil residues. The abundance results are not completely accurate due to unprecise names in the reference database used. For example, one *Mortierella* sp. is called *Mortierella,* while another one is called *Mortierella* sp.. This may result in an underestimated abundance of *Mortierella*. It is possible to choose the most accurate name manually, but this requires time and caution (Nilsson et al., 2019b).

Diversity

To explore the fungal diversity between samples from different country parts and different area conditions a sPLSDA plot was produced to present a possible clustering by discriminating samples based on feature similarity. While samples from under roof were spread, clustering between samples from forest and grassland could be observed. This corresponds with findings done by other studies. In a study by Yang et al. (2020) a higher fungal diversity in soil from planted woodland than natural grass was observed (Yang et al., 2020). Another study by Zeng et al. (2020) observed a clustering within fungal diversity in soil samples from the same

vegetative ecosystems. They pointed out that *Basidiomycota* were more abundant in forest soil than grass soil (Zeng et al., 2020). If more samples exhibit these results, it could suggest significant clustering; however, this interpretation is hindered by the limited number of samples available.

Cultivation

UV treatment

In nature, plastic is exposed to both biodegradation and radiation from the sun. Usually, UV-A and UV-B, while UV-C is blocked by the atmosphere, with some exceptions due to chlorofluorocarbon pollution. UV-C is more intense, and shorter exposure time can therefore be used to simulate long time UV-A and UV-B exposures (Maverakis et al., 2010). Therefore, both – UV-C-radiated and non-UV-C-radiated LDPE pieces were used for experiment. That created a chance to validate the UV-effect on biodegradation. The article by Taghavi et al. (2001) showed that a UV dose at 7.02×10^{12} $\mu W/cm^2 \cdot s$ gave the highest surface degradation and promoted microbial viability (Taghavi et al., 2021). This effect was not possible to achieve due to low energy efficiency of the used UV-lamp, which was limited to 24 W. Therefore, the time of radiation was extended and only one side of the plastic was radiated. The approximate UV dosage was 1.5×10^{10} $\mu J/cm^2$. This dosage fits within the range of the two lowest doses, 1.051×10^8 and 1.755×10^{12} $\mu J/cm^2$, that resulted in changes in the plastic according to the mentioned research. The wettability of the plastic clearly increased, indicating chemical changes to the LDPE surface. Physical changes like large cracks were also formed in the UV-radiated plastic pieces. Since UV-radiation was supposed to create carbonyl, hydroxyl and hydroperoxide groups, this could have been investigated by measuring different carbon by-products and give an indication if there were any carboxyl groups available for β-oxidation. Before the cultivation the UV-treated LDPE pieces already showed signs off discoloration and cracks. While the UV-radiated LDPE pieces were yellow, the non-radiated LDPE pieces remained white.

Generally, UV-treated samples contained significant surface damage in form of cracks. Samples 3a (*Aspergillus* sp. in MSM medium with glucose), 18a (*G. sessile* in soil) and 20a (*C. uwebraunianum* in soil) were exceptions as these did not have any visible cracks at 70x magnification. Some minor cracks were observed at 3,000x magnification. Differences in sample positioning under the UV-lamp could be a factor, yet after analysing sample locations, this is not expected to be the cause.

Effect of glucose:

In order to test whether glucose promotes or inhibits plastic degradation, the experiment included MSM media with and without glucose. In general, glucose increases the fungal biomass, but it is not known whether the presence of additional carbon source will inhibit production of enzymes used for plastic degradation. Microorganisms tend to downregulate genes involved in the uptake of other carbon sources when in glucose presence in order to save energy (Ronne, 1995). Different studies have been testing various organisms and conditions. For example, S. J. Lodha et al. (1991) observed that the LiP production was reduced by 70% with a glucose concentration at 0.5 g/L in the bacteria *Streptomyces viridosporus* T7A (bacteria) (Lodha et al., 1991). Another study by Schneider et al. (2018) on *Marasmiellus palmivorus* VE111 (fungi) showed increased biomass, but lower laccase activity with a glucose concentration over 1.6 g/L, while a study done by R. Periasamy and Thayumanavan Palvannan (2010) on *Pleurotus ostreatus* (fungi) IMI 395545 showed that a glucose increase from 5 g/L to 20 g/L gave more than a fivefold increase of laccase activity (Schneider et al., 2018, Periasamy and Palvannan, 2010). Similar results with contradictory effects from glucose between different fungi can also be found in other important enzymes like MnP (Songulashvili et al., 2006). Project results suggest that glucose promoted fungal biomass and production of organic acids, while the biomass achieved in media without glucose was significantly lower, although the growth was not inhibited. The performed test was not capable of predicting the activity of plastic degrading enzymes. This should be done in future research. *Alternaria* sp. grew on the LDPE piece in media without glucose, while no growth was observed on the LDPE piece in media with glucose. This indicates that the glucose concentration inhibits mechanisms of interaction with LDPE in *Alternaria*. In contrast, *C. uwebraunianum* showed higher growth on the LDPE surface in media with glucose than without. This supports the mentioned previous findings, that different fungi are differently restricted by glucose.

Weight and wettability

The wettability results suggest that most of the UV-radiated LDPE pieces had a higher wettability after biodegradation. It is not possible to determine whether fungal cultivation affected the wettability or whether it was a consequence of UV radiation. None of the samples gave over 1% weight reduction. This could be due to excess humidity weight as the LDPE pieces were moist from the cultivating media, sonication and vortexing that was performed to remove excess fungi. This exposure to liquids could explain the small changes in weight (and for some samples weight gain). It was not prioritised to remove fungi with mechanical force

that could impact the plastic surface. Therefore, fungi grown on the plastic might contribute to an even higher weigh.

Growth

pH and OD measurements were performed to observe the production of organic acids as a parameter of fungal viability. The pH in both media were supposed to have a pH at 5.5. But the MSM media with glucose had a start pH at 4.7, which indicated that autoclaving was performed after adjusting the pH in the media. This pH reduction is an effect of by-product formation reaction from glucose triggered by the heat under autoclaving process (Nie et al., 2013). In most of the samples with glucose, the pH was around 3 at the end of experiment. According to pH, OD and visual measurements, no growth was observed in sample 5b, *A. coeruela* non-radiated LDPE piece in MSM with glucose. This is thought to be due to a mistake during the addition of fungal spores to the cultures since the fungi should have glucose available.

Contamination

Although some samples showed contamination at the end of the experiment, these were not considered to have a large impact since no contamination was observed during the cultivation experiment. For example, LDPE cultivated with *A. coeruela* in MSM media had a green fungus contamination. This was not observed under the cultivation experiment. The fungi observed in the contamination control had similar colony characteristics with the fungi used in the cultivation experiment, suggesting that the contamination could have occurred during sample preparations for pH and OD measurements.

Biodegradation

Biodegrading candidates

To compare the different fungi's ability to degrade LDPE through SEM, LDPE pieces had to be cultured at the same conditions. The most promising conditions were thought to be the radiated LDPE pieces grown in media with glucose, due to high growth ratio and photodegradation. Therefore, one UV-radiated LDPE piece from each isolate with this condition was included to search for any biodegrading evidence. Due to visible growth on plastic pieces in liquid media, all LDPE pieces exposed to *C. uwebraunianum* were included. *Alternaria* sp. LDPE from media without glucose and Ganoderma from soil were selected due to visible growth of fungus on or along the LDPE respectively. The LDPE negative controls were not included since the focus was directed on observations and new findings.

Absidia coeruela

Absidia sp. was initially identified as a *Mortierella* sp. The isolate showed growth in layers through the agar and showed microscopic similarity to *Mortierella* sp. This resemblance is a result of their taxonomic affinity to the order *Mucorales* within the phylum *Zygomycota* (Ozimek and Hanaka, 2021, Zhao et al., 2022). ITS was used as the only genetic marker for inferring the phylogenetic tree. The strain was identified as *A. coeruela* with a bootstrap value of 100. Due to MnP activity, fungi from the *Absidia* genera have the potential to degrade plastic (Al-Dossary, 2021). Some earlier findings also show high occurrence of *Absidia* in plastic polluted soil (Jeszeová et al., 2018). This did not correlate with our findings, as the *Absidia* genera was not among the top 100 most abundant fungi and *A. coeruela* were not showing indications of plastic degradation.

Ganoderma sessile

The mock community sequencing results demonstrated that the *Basidiomycota* abundance most likely was underestimated in relation to *Ascomycota* abundance. Due to the skewed distribution of these fungal phyla in the mock community, it was assumed that the Basidiomycota was more abundant than the bioinformatic results showed. It was therefore important to include one of the highly abundant *Basidiomycota*. For that reason, *G. sessile* was implemented into the wishlist. *Ganoderma* sp. is a white rot fungi, that has been reported to degrade plastics, including LDPE (Bautista-Zamudio et al., 2023). White rot fungi cultivation is demanding in regard to slow growth rate and lack of distinctive morphological characteristics at the early cultivation stage, hence a *G. sessile* isolate was obtained from NVI's culture collection. The LDPE samples in soil were hard to observe during the cultivation experiment, however some plastic samples were laying right next to the glass making it possible to observe fungal development. It was noticed that *G. sessile* grew alongside the plastic edges.

Aspergillus sp.

The *Aspergillus* sp. genus was identified based on its morphology – green/yellow powdery colony, vesicle, and flask shaped phialides structures observed under the microscope. This genus was also on the 25th position on the abundance list. Based on literature data, many species within the *Aspergillus* genus, including *Aspergillus flavus* and *Aspergillus oryzae,* can degrade plastics like LDPE (Ndahebwa Muhonja et al., 2018, Ibrahim et al., 2011, Spina et al., 2021, Verma and Gupta, 2019). This indicated that the isolate is a good candidate for LDPE degradation.

Aureobasidium pullulans and *Penicillium chrysogenum*

Aureobasidium sp. was the 23rd most abundant fungal genera found in the collected samples. Initially it was identified by morphology – colour changing colony, slimy exudate, and yeast-like structures observed under the microscope. The phylogenetic analysis confirmed morphological diagnosis and identified the strain as *A. pullulans* with a bootstrap value of 100. For isolation of the fungi belonging to the *Penicillium* genera, the green colony with white shades, brush like conidia with metula and phialides were useful characteristics. One of the reasons why *Penicillium* genera was interesting for the project was its high abundance – it was the 14th most abundant fungi found in the samples. Phylogenetic analysis of isolated strain has identified it as *Penicillium scabrosum*, with a 100-bootstrap value. *A. pullulans* has been found to degrade other types of plastic than LDPE in other studies (Darby and Kaplan, 1968, Fields et al., 1974). No significant weight loss was observed in this study; however LDPE weight loss related to *A. pullulans* has been observed in some studies (Nowak et al., 2012). Additionally, earlier studies have found that *P. chrysogenum* and *P. oxalicum* can degrade LDPE (Ojha et al., 2017). Upon writing this thesis, no papers about *P. scabrosum*s ability to degrade plastic were found.

Radiated LDPE with *A. pullulans* (1a) and *P. scabrosum* (7a), both grown in MSM with glucose, had fungal establishment in the corner mark crack. This crack was larger than the cracks that were developed after UV-treatment. It is likely that more - or bigger, cracks would provide a better housing condition for fungi, helping with establishing culture. Even though the constant movement of the rinsed medium made attachment to the LDPE surface hard, the fungal drive to grow inside the cracks is noteworthy. Sample 7a also showed crack development under the *P. scabrosum* fungus. Could it be that the fungi are secreting some enzymes that makes the surface crack? Or could there be something helping the fungi adhere to the surface?

The UV-radiated and non-radiated LDPE pieces with *A. pullulans* (1a and 1b), and the non-radiated bits with *Alternaria* sp. (6b) had a darker colour after cultivation in glucose supplemented media than before. The colour of the media also turned from transparent to dark green under cultivation. Melanin pigment production can be responsible for discolouration that affected both – the media and the LDPE pieces (Zheng et al., 2008, Fernandes et al., 2023).

Alternaria sp.

The next of the isolated strains was preliminarily classified as an *Alternaria* sp. based on the greyish culture, and pigmented cylindrical conidia that formed in chains. It was in the top 60 fungi at the abundance table. It was problematic to identify *Alternaria* down to species

level. The isolated *Alternaria* sp. strain was grouped in the section *Ulocladioides*. Only one genetic marker, ITS, was used to identify the fungus, what explains the low taxonomic resolution. Though three genetic markers had been selected for use when sequencing *Alternaria*, the calmodulin amplification was unsuccessful despite several attempts, while *BT2* sequencing resulted in a low sequence quality. Low primer specificity and genetic variations are the most likely explanation for the lack of success.

Alternaria grown in MSM media without glucose with a UV-radiated LDPE (14a) had visibly/significantly more growth compared to the same media with non-radiated LDPE (14b). This growth could be due to exploratory growth that occurs under glucose depletion. In this process fungi can undergo macroautophagy as a desperate attempt to use all the remaining energy and nutrients on foraging (Nitsche et al., 2012, Jones et al., 2017). But since the *Alternaria* sp. growth difference between with UV-radiated and non-radiated LDPE was visually high and the UV-treated plastic showed fungal growth on the plastic, this could indicate that the fungus is obtaining its carbon from the UV-treated plastic piece. Although no direct growth was observed on the LDPE, *Alternaria* sp. radiated LDPE grown in glucose (6a) showed a indent area in the plastic. Earlier findings suggests that the *Alternaria alternata* species can degrade polyethylene (Gao et al., 2022). Although, to this date, not much about plastic degradation abilities within the *Ulocladioides* section is investigated.

C. *uwebraunianum*

The *C. uwebraunianum* was recognized as a *Cladosporium* genera by its dark brown/green colonies with a darker reverse side and chained conidia that fragmented. Based on the phylogenetic analysis the *Cladosporium* sp. isolate was identified as *C. uwebraunianum.* Due to the high abundance of the *Cladosporiaceae* family in samples, it was important to investigate whether *C. uwebraunianum* could interact with plastic. *Cladosporium* sp. had also been found to degrade LDPE in previous studies (Gong et al., 2023). Yet, to this date, no studies about *C. uwebraunianum* ability to degrade plastic has been found.

Radiated LDPE with *C. uwebraunianum* grown with and without glucose indent area in the plastic. This could be an indication of biodegradation since *C. uwebraunianum* showed signs of adhering to the surface under both conditions. Some samples had a thin film coating on the surface. This was particularly observed in *C. uwebraunianum* grown on non-radiated LDPE in media without glucose, and even more in *C. uwebraunianum* grown on non-radiated LDPE in media with glucose. It is not sure what this film is but if it were a residue from the

liquid media, it would have been observed in all the samples with liquid media. It could be EPS residues that were produced by fungi (as an attempt to establish on the plastic surface). It could also be new organic compounds that is formed from the plastic, due to fungal and plastic interactions.

In the closeup SEM-images of this sample it looked like the hyphae went into the plastic, and a bright wreath was observed. The change of electron intensity indicates that this wreath neither had the same charge as the fungi or the plastic which is observed in the brightness. It would be interesting to examine whether this wreath could be due to chemical interactions between the fungi and plastic. This LDPE piece was non-radiated and thereby more hydrophobic. To attach to hydrophobic surfaces, fungi use hydrophobins. This might be the case for *C. uwebraunianum* (Wu et al., 2023). It would have been interesting to observe SEM results after longer incubations with this condition and fungus combination. It's important to notice that the continuous movement of the LDPE due to stirring under cultivation could make it difficult for fungi to adhere to the surface.

Important findings

The surfaces of LDPE pieces inoculated with *C. uwebraunianum* in media with and without glucose and radiated LDPE pieces inoculated with *Alternaria* sp. in medium containing glucose stood out from the other samples in different ways. *C. uwebraunianum* grown on radiated LDPE with and without glucose and *Alternaria* sp. radiated LDPE with glucose showed an indent in the plastic. This could be an indication of biodegradation since both *C. uwebraunianum* and *Alternaria* sp. had shown signs of adhering to the surface. Some samples had a thin film coating on the surface. This was observed in *C. uwebraunianum* on non-radiated LDPE grown in media without glucose, and at an even higher degree in *C. uwebraunianum* on non-radiated LDPE grown in media with glucose.

Finally, the sample containing *C. uwebraunianum* on radiated and non-radiated LDPE grown in media with glucose and *Alternaria* sp. on radiated LDPE grown in media without glucose (4a, 4b and 14a respectively), were the only samples that showed strong attachment to the plastic surface. This might be even stronger evidence of possible biodegradation than other previous factors that have been discussed. Of these, the strongest indication of LDPE degradation was seen on sample *C. uwebraunianum* non-radiated LDPE grown in glucose. Strong attachment, that looked like some kind of anchoring between the non-radiated LDPE and *C. uwebraunianum* in glucose indicated that there would be some damage done to the plastic. It would have been interesting to remove the fungus to view if any damage has occurred.

It seems that both *Cladosporium* and *Alternaria* produce adhesives that they use to adhere to the LDPE surface. The adhesive properties in *Cladosporium* and *Alternaria* have also been observed by other studies (Gong et al., 2023, Epstein and Nicholson, 2016, Khatua et al., 2024). This makes them both good candidates for plastic degradation, but *C. uwebraunianum* might be considered as the best candidate due to higher abundance and growth rate on the plastic surfaces in all LDPE pieces grown in liquid media.

For future prospects

In this study the bioinformatic data was restricted by the low number of samples. Again, the low sample number was restricted by time and plastic specificity. For future research it is recommended to expand the collection time and reduce the plastic specificity to increase the number of samples thereby giving more statistically significant findings when it comes to diversity and abundance.

When using changes in mass and wettability as a parameter for measuring the biodegradation, more parallels should be included. This would make it easier to make a normal distribution curve and determine whether the results are significant or not. The weight results would also be more accurate if samples were desiccated to remove excess water. This should be done before and after biodegradation to get comparable results. It is not recommended to use wettability as a measure for biodegradation in further research as the results after growth experiment seems to be linked to earlier UV-radiation.

In this study it was difficult to understand why some radiated LDPE pieces had cracks, while some did not. Potential surface damage should be noted before cultivating fungi with LDPE, to establish whether the crack formation is due to UV-radiation or biodegradation.

When cultivating fungi with LDPE plastic without glucose, a parallel without LDPE could be used as a comparison to determine if the growth is the result of an exploratory growth due to carbon starvation or due to available carbon from the LDPE piece due to plastic degradation.

There are some recommendations for the future s that have become clearer after this master project. First, measuring pH and OD at the rate of once a week is time consuming and increases the possibility for contamination in the samples. Based on the results, the OD-measurement did not correlate with fungal growth. The pH only had a large decrease in samples with glucose at the start, therefore it would not have been necessary to measure that often. Also, the contamination risk must be carefully assessed against the remaining results. Secondly, other

analyses like Attenuated Total Reflection Fourier Transform Infrared (ATR-FTIR) could be useful to investigate the LDPE piece for degradation products. This method has been used in other plastic biodegradation studies to determine chemical changes that could indicate biodegradation byproducts(Porter et al., 2023, Paço et al., 2017).

C. uwebraunium showed a potential for plastic degradation, and for further studies, it is recommended keep studying this fungus by looking at the proteins transcribed. An enzymatic assay could be added to determine the abundance of specific LDPE degrading enzymes like, MnP, LiP and laccase. By sequencing of the *C. uwebraunium* genome and implementing transcriptomics it could be possible to investigate existing metabolic pathways and EPS production.

Conclusion

In this study, the main goal was to find and identify Norwegian LDPE degrading fungi. There have been found promising candidates for LDPE degradation like *A. pullulans, Alternaria* sp and *P. scabrosum*, but *C. uwebraunium* was the most promising. There were observed three strong indications that *Cladosporium* is a good Norwegian LDPE-degrading candidate fungus. The first indication is the high abundance of *Cladosporium* found in the samples collected. The second indication is the high visible growth on the LDPE plastic surface under cultivation both with and without glucose. The third indication is the strong attachment between the fungi and LDPE surface that were discovered on SEM. More evidence is needed, yet these results are good indicators that *C. uwebraunium* can utilize LDPE as a carbon source.

5. Sources

Landsdeler i Norge. Store Norske leksikon: licens: CC BY NC SA 3.0.

AB MAJID, A. H., ZAHRAN, Z., ABD RAHIM, A. H., ISMAIL, N. A., ABDUL RAHMAN, W., MOHAMMAD ZUBAIRI, K. S., DIENG, H. & SATHO, T. 2015. Morphological and molecular characterization of fungus isolated from tropical bed bugs in Northern Peninsular Malaysia, Cimex hemipterus (Hemiptera: Cimicidae). *Asian Pacific Journal of Tropical Biomedicine,* 5**,** 707-713.

ABARENKOV, K. Z., ALLAN; PIIRMANN,TIMO; PÖHÖNEN, RAIVO; IVANOV, FILIPP; NILSSON, R. HENRIK; KÕLJALG, URMAS 2023. UNITE QIIME release for Fungi 2. 2023-07-18 ed.: UNITE Community.

ABDEL-HAMID, A. M., SOLBIATI, J. O. & CANN, I. K. O. 2013. Chapter One - Insights into Lignin Degradation and its Potential Industrial Applications. *In:* SARIASLANI, S. & GADD, G. M. (eds.) *Advances in Applied Microbiology.* Academic Press.

AGILENT 2021. D1000 ScreenTape Assay for TapeStation Systems

Quick Guide.

AL-DOSSARY, M. S. A. A. M. A.-A. 2021. Evaluation of the enzymatic activity of some fungi isolated from the plastic contaminated soils and their LDPE biodegradation ability. *MARSH BULLETIN*.

ALBERTSSON, A.-C., ANDERSSON, S. O. & KARLSSON, S. 1987. The mechanism of biodegradation of polyethylene. *Polymer Degradation and Stability,* 18**,** 73-87.

ALI, S., FRADI, A. & AL-ARAJI, A. 2017. Effect of some physical factors on growth of five fungal species. *European Academic Research,* V**,** 1069-1078.

AMARASINGHE, S. L., SU, S., DONG, X., ZAPPIA, L., RITCHIE, M. E. & GOUIL, Q. 2020. Opportunities and challenges in long-read sequencing data analysis. *Genome Biology,* 21**,** 30.

BAL-TEC 99. Operating Manual CPD 030 Critical Point Dryer and coating rate measuring device.

BATTULGA, B., ATARASHI-ANDOH, M., NAKANISHI, T. & KOARASHI, J. 2022. A new approach to extracting biofilm from environmental plastics using ultrasound-assisted syringe treatment for isotopic analyses. *Science of The Total Environment,* 849**,** 157758.

BAUTISTA-ZAMUDIO, P. A., FLÓREZ-RESTREPO, M. A., LÓPEZ-LEGARDA, X., MONROY-GIRALDO, L. C. & SEGURA-SÁNCHEZ, F. 2023. Biodegradation of plastics by white-rot fungi: A review. *Science of The Total Environment,* 901**,** 165950.

BELLEMAIN, E., CARLSEN, T., BROCHMANN, C., COISSAC, E., TABERLET, P. & KAUSERUD, H. 2010. ITS as an environmental DNA barcode for fungi: an in silico approach reveals potential PCR biases. *BMC Microbiology,* 10**,** 189.

BLAALID, R., KUMAR, S., NILSSON, R. H., ABARENKOV, K., KIRK, P. M. & KAUSERUD, H. 2013. ITS1 versus ITS2 as DNA metabarcodes for fungi. *Mol Ecol Resour,* 13**,** 218-24.

BOLYEN, E., RIDEOUT, J. R., DILLON, M. R., BOKULICH, N. A., ABNET, C. C., AL-GHALITH, G. A., ALEXANDER, H., ALM, E. J., ARUMUGAM, M., ASNICAR, F., BAI, Y., BISANZ, J. E., BITTINGER, K., BREJNROD, A., BRISLAWN, C. J., BROWN, C. T., CALLAHAN, B. J., CARABALLO-RODRÍGUEZ, A. M., CHASE, J., COPE, E. K., DA SILVA, R., DIENER, C., DORRESTEIN, P. C., DOUGLAS, G. M., DURALL, D. M., DUVALLET, C., EDWARDSON, C. F., ERNST, M., ESTAKI, M., FOUQUIER, J., GAUGLITZ, J. M., GIBBONS, S. M., GIBSON, D. L., GONZALEZ, A., GORLICK, K., GUO, J., HILLMANN, B., HOLMES, S., HOLSTE, H., HUTTENHOWER, C., HUTTLEY, G. A., JANSSEN, S., JARMUSCH, A. K., JIANG, L., KAEHLER, B. D., KANG, K. B., KEEFE, C. R., KEIM, P., KELLEY, S. T., KNIGHTS, D., KOESTER, I., KOSCIOLEK, T., KREPS, J., LANGILLE, M. G. I., LEE, J., LEY, R., LIU, Y. X., LOFTFIELD, E., LOZUPONE, C., MAHER, M., MAROTZ, C., MARTIN, B. D., MCDONALD, D., MCIVER, L. J., MELNIK, A. V., METCALF, J. L., MORGAN, S. C., MORTON, J. T., NAIMEY, A. T., NAVAS-MOLINA, J. A., NOTHIAS, L. F., ORCHANIAN, S. B., PEARSON, T., PEOPLES, S. L., PETRAS, D., PREUSS, M. L., PRUESSE, E., RASMUSSEN, L. B., RIVERS, A., ROBESON, M. S., 2ND, ROSENTHAL, P., SEGATA, N., SHAFFER, M., SHIFFER, A., SINHA, R., SONG, S. J., SPEAR, J. R., SWAFFORD, A. D., THOMPSON, L. R., TORRES, P. J., TRINH, P., TRIPATHI, A., TURNBAUGH, P. J., UL-HASAN, S., VAN DER HOOFT, J. J. J., VARGAS, F., VÁZQUEZ-BAEZA, Y., VOGTMANN, E., VON HIPPEL, M., WALTERS, W., et al. 2019. Reproducible, interactive, scalable and extensible microbiome data science using QIIME 2. *Nat Biotechnol,* 37**,** 852-857.

BOŻENA, N., JOLANTA, P. & JAGNA, K. 2012. Biodegradation of Pre-Aged Modified Polyethylene Films. *In:* VIACHESLAV, K. (ed.) *Scanning Electron Microscopy.* Rijeka: IntechOpen.

BREITENBACH, R., GERRITS, R., DEMENTYEVA, P., KNABE, N., SCHUMACHER, J., FELDMANN, I., RADNIK, J., RYO, M. & GORBUSHINA, A. A. 2022. The role of extracellular polymeric substances of fungal biofilms in mineral attachment and weathering. *npj Materials Degradation,* 6**,** 42.

BRUNNER, I., FISCHER, M., RÜTHI, J., STIERLI, B. & FREY, B. 2018. Ability of fungi isolated from plastic debris floating in the shoreline of a lake to degrade plastics. *PLoS One,* 13**,** e0202047.

BRYDSON, J. A. 1999. 23 - Phenolic Resins. *In:* BRYDSON, J. A. (ed.) *Plastics Materials (Seventh Edition).* Oxford: Butterworth-Heinemann.

CALLAHAN, B. J., MCMURDIE, P. J. & HOLMES, S. P. 2017. Exact sequence variants should replace operational taxonomic units in marker-gene data analysis. *The ISME Journal,* 11**,** 2639-2643.

CHAMAS, A., MOON, H., ZHENG, J., QIU, Y., TABASSUM, T., JANG, J. H., ABU-OMAR, M., SCOTT, S. L. & SUH, S. 2020. Degradation Rates of Plastics in the Environment. *ACS Sustainable Chemistry & Engineering,* 8**,** 3494-3511.

CHEN, C. C., DAI, L., MA, L. & GUO, R. T. 2020. Enzymatic degradation of plant biomass and synthetic polymers. *Nat Rev Chem,* 4**,** 114-126.

CHOLEWIŃSKA, P., MONIUSZKO, H., WOJNAROWSKI, K., POKORNY, P., SZELIGOWSKA, N., DOBICKI, W., POLECHOŃSKI, R. & GÓRNIAK, W. 2022. The Occurrence of Microplastics and the Formation of Biofilms by Pathogenic and Opportunistic Bacteria as Threats in Aquaculture. *Int J Environ Res Public Health,* 19.

CLOKIE, A. H. A. S. 2018. *Wilson and Walker's Principles and Techniques of Biochemistry and Molecular Biology,* Cambridge, Cambridge University Press.

CROSSLEY, B. M., BAI, J., GLASER, A., MAES, R., PORTER, E., KILLIAN, M. L., CLEMENT, T. & TOOHEY-KURTH, K. 2020. Guidelines for Sanger sequencing and molecular assay monitoring. *Journal of Veterinary Diagnostic Investigation,* 32**,** 767-775.

DARBY, R. T. & KAPLAN, A. M. 1968. Fungal Susceptibility of Polyurethanes. *Applied Microbiology,* 16**,** 900-905.

DESHMUKH, A. J. & SABALPARA, A. N. In vitro effect of various nitrogen , carbon sources and pH regimes on the growth and sporulation of Colletotrichum gloeosporioides Penz . and Sacc causing anthracnose of Indian bean. 2012.

DI MARTINO, P. 2018. Extracellular polymeric substances, a key element in understanding biofilm phenotype. *AIMS Microbiol,* 4**,** 274-288.

DSOUZA, G. C., SHERIFF, R. S., ULLANAT, V., SHRIKRISHNA, A., JOSHI, A. V., HIREMATH, L. & ENTOORI, K. 2021. Fungal biodegradation of low-density polyethylene using consortium of Aspergillus species under controlled conditions. *Heliyon,* 7**,** e07008.

EKANAYAKA, A. H., TIBPROMMA, S., DAI, D., XU, R., SUWANNARACH, N., STEPHENSON, S. L., DAO, C. & KARUNARATHNA, S. C. 2022. A Review of the Fungi That Degrade Plastic. *J Fungi (Basel),* 8.

EPSTEIN, L. & NICHOLSON, R. 2016. Adhesion and Adhesives of Fungi and Oomycetes. *In:* SMITH, A. M. (ed.) *Biological Adhesives.* Cham: Springer International Publishing.

ESCLAPEZ, M. D., GARCÍA-PÉREZ, J. V., MULET, A. & CÁRCEL, J. A. 2011. Ultrasound-Assisted Extraction of Natural Products. *Food Engineering Reviews,* 3**,** 108-120.

ESCOBAR-ZEPEDA, A., VERA-PONCE DE LEÓN, A. & SANCHEZ-FLORES, A. 2015. The Road to Metagenomics: From Microbiology to DNA Sequencing Technologies and Bioinformatics. *Front Genet,* 6**,** 348.

EVENNETT, P. J. & HAMMOND, C. 2005. MICROSCOPY | Overview. *In:* WORSFOLD, P., TOWNSHEND, A. & POOLE, C. (eds.) *Encyclopedia of Analytical Science (Second Edition).* Oxford: Elsevier.

FAIRBROTHER, A., HSUEH, H.-C., KIM, J. H., JACOBS, D., PERRY, L., GOODWIN, D., WHITE, C., WATSON, S. & SUNG, L.-P. 2019. Temperature and light intensity effects on

photodegradation of high-density polyethylene. *Polymer Degradation and Stability,* 165**,** 153-160.

FANNING, S. & MITCHELL, A. P. 2012. Fungal biofilms. *PLoS Pathog,* 8**,** e1002585.

FERNANDES, C., CASADEVALL, A. & GONÇALVES, T. 2023. Mechanisms of Alternaria pathogenesis in animals and plants. *FEMS Microbiology Reviews,* 47.

FIELDS, R. D., RODRÍGUEZ, F. & FINN, R. K. 1974. Microbial degradation of polyesters: Polycaprolactone degraded by P. pullulans†. *Journal of Applied Polymer Science,* 18**,** 3571-3579.

FORSMAN, A. M., SAVAGE, A. E., HOENIG, B. D. & GAITHER, M. R. 2022. DNA Metabarcoding Across Disciplines: Sequencing Our Way to Greater Understanding Across Scales of Biological Organization. *Integr Comp Biol,* 62**,** 191-198.

GANESAN, S., RUENDEE, T., KIMURA, S. Y., CHAWENGKIJWANICH, C. & JANJAROEN, D. 2022. Effect of biofilm formation on different types of plastic shopping bags: Structural and physicochemical properties. *Environmental Research,* 206**,** 112542.

GAO, R., LIU, R. & SUN, C. 2022. A marine fungus Alternaria alternata FB1 efficiently degrades polyethylene. *Journal of Hazardous Materials,* 431**,** 128617.

GENESCRIPT. 2021. *Sanger Sequencing vs. Next-Generation Sequencing (NGS)* [Online]. Molecular Biology News. Available: https://www.genscript.com/gene-news/sanger-sequencing-vs-next-generation-sequencing.html [Accessed].

GEYER, R. 2020. A Brief History of Plastics. *In:* STREIT-BIANCHI, M., CIMADEVILA, M. & TRETTNAK, W. (eds.) *Mare Plasticum - The Plastic Sea: Combatting Plastic Pollution Through Science and Art.* Cham: Springer International Publishing.

GEYER, R., JAMBECK, J. R. & LAW, K. L. 2017. Production, use, and fate of all plastics ever made. *Science Advances,* 3**,** e1700782.

GONG, Z., JIN, L., YU, X., WANG, B., HU, S., RUAN, H., SUNG, Y.-J., LEE, H.-G. & JIN, F. 2023. Biodegradation of Low Density Polyethylene by the Fungus Cladosporium sp. Recovered from a Landfill Site. *Journal of Fungi,* 9**,** 605.

GRØNT-PUNKT-NORGE. 2022. *Fakta og tall fra 2022, Landbruksplast* [Online]. Grontpunkt.no. Available: https://www.grontpunkt.no/resirkulering/fakta-og-tall#2022 [Accessed 12.09 2023].

GUPTA, A. K. & GUPTA, U. D. 2014. Chapter 19 - Next Generation Sequencing and Its Applications. *In:* VERMA, A. S. & SINGH, A. (eds.) *Animal Biotechnology.* San Diego: Academic Press.

HAGEMANN, I. S. 2015. Chapter 1 - Overview of Technical Aspects and Chemistries of Next-Generation Sequencing. *In:* KULKARNI, S. & PFEIFER, J. (eds.) *Clinical Genomics.* Boston: Academic Press.

HARBUZOV, Z., FARBEROVA, V., TOM, M., PALLAVICINI, A., STANKOVIĆ, D., LOTAN, T. & LUBINEVSKY, H. 2022. Amplicon sequence variant-based meiofaunal community

composition revealed by DADA2 tool is compatible with species composition. *Marine Genomics,* 65**,** 100980.

HODZIC, A. 2004. 12 - Re-use, recycling and degradation of composites. *In:* BAILLIE, C. (ed.) *Green Composites.* Woodhead Publishing.

IBRAHIM, I. N., MARAQA, A. D., HAMEED, K. M., SAADOUN, I. & MASWADEH, H. 2011. Assessment of potential plastic-degrading fungi in Jordanian habitats. *Turkish Journal of Biology,* 35**,** 551-557.

ILLUMINA. 2010. *Illumina Sequencing Technology* [Online]. Available: https://www.illumina.com/documents/products/techspotlights/techspotlight_sequencing.pdf [Accessed 29.10 2023].

ILLUMINA 2013. 16S Metagenomic Sequencing Library

Preparation.

ILLUMINA. 2023. *Illumina sequencing platforms* [Online]. Available: https://www.illumina.com/systems/sequencing-platforms.html [Accessed].

JAMBECK, J. R., GEYER, R., WILCOX, C., SIEGLER, T. R., PERRYMAN, M., ANDRADY, A., NARAYAN, R. & LAW, K. L. 2015. Plastic waste inputs from land into the ocean. *Science,* 347**,** 768-771.

JESZEOVÁ, L., PUŠKÁROVÁ, A., BUČKOVÁ, M., KRAKOVÁ, L., GRIVALSKÝ, T., DANKO, M., MOSNÁČKOVÁ, K., CHMELA, Š. & PANGALLO, D. 2018. Microbial communities responsible for the degradation of poly(lactic acid)/poly(3-hydroxybutyrate) blend mulches in soil burial respirometric tests. *World Journal of Microbiology and Biotechnology,* 34.

JONES, S. E., HO, L., REES, C. A., HILL, J. E., NODWELL, J. R. & ELLIOT, M. A. 2017. Streptomyces exploration is triggered by fungal interactions and volatile signals. *Elife,* 6.

KARGER, B. L. & GUTTMAN, A. 2009. DNA sequencing by CE. *Electrophoresis,* 30 Suppl 1**,** S196-202.

KAUSERUD, H. 2023. ITS alchemy: On the use of ITS as a DNA marker in fungal ecology. *Fungal Ecology,* 65**,** 101274.

KELLY, R. P., SHELTON, A. O. & GALLEGO, R. 2019. Understanding PCR Processes to Draw Meaningful Conclusions from Environmental DNA Studies. *Scientific Reports,* 9**,** 12133.

KHAN, S., NADIR, S., SHAH, Z. U., SHAH, A. A., KARUNARATHNA, S. C., XU, J., KHAN, A., MUNIR, S. & HASAN, F. 2017. Biodegradation of polyester polyurethane by Aspergillus tubingensis. *Environmental Pollution,* 225**,** 469-480.

KHATUA, S., SIMAL-GANDARA, J. & ACHARYA, K. 2024. Myco-remediation of plastic pollution: current knowledge and future prospects. *Biodegradation,* 35**,** 249-279.

KIM, J. S., KIM, S. H., LEE, W., SEO, C. W., LEE, J. W., PARK, K. H. & LIM, Y. W. 2022. Five Previously Unrecorded Fungal Species Isolated from Marine Plastic Wastes in South Korea. *Mycobiology,* 50**,** 420-428.

KOCAOGLU, O., TSUI, H.-C. T., WINKLER, M. E. & CARLSON, E. E. 2015. Profiling of β-Lactam Selectivity for Penicillin-Binding Proteins in Streptococcus pneumoniae D39. *Antimicrobial Agents and Chemotherapy,* 59**,** 3548-3555.

KOGURE, T. 2013. Chapter 2.9 - Electron Microscopy. *In:* BERGAYA, F. & LAGALY, G. (eds.) *Developments in Clay Science.* Elsevier.

KOROL, J., HEJNA, A., WYPIÓR, K., MIJALSKI, K. & CHMIELNICKA, E. 2021. Wastes from Agricultural Silage Film Recycling Line as a Potential Polymer Materials. *Polymers (Basel),* 13.

KRUEGER, M. C., HARMS, H. & SCHLOSSER, D. 2015. Prospects for microbiological solutions to environmental pollution with plastics. *Applied Microbiology and Biotechnology,* 99**,** 8857-8874.

LANDMARKS., A. C. S. N. H. C. 1993. *Bakelite: The World's First Synthetic* [Online]. Available: Plastic. http://www.acs.org/content/acs/en/education/whatischemistry/landmarks/bakelite.html [Accessed].

LANGSIRI, N., WORASILCHAI, N., IRINYI, L., JENJAROENPUN, P., WONGSURAWAT, T., LUANGSA-ARD, J. J., MEYER, W. & CHINDAMPORN, A. 2023. Targeted sequencing analysis pipeline for species identification of human pathogenic fungi using long-read nanopore sequencing. *IMA Fungus,* 14**,** 18.

LEE, Q. Y. & LI, H. 2021. Photocatalytic Degradation of Plastic Waste: A Mini Review. *Micromachines (Basel),* 12.

LI, D.-W., YANG, C. S. & HARRINGTON, F. 2007. Microscopic Analytical Methods for Fungi. *Sampling and Analysis of Indoor Microorganisms.*

LI, P., WANG, X., SU, M., ZOU, X., DUAN, L. & ZHANG, H. 2021. Characteristics of Plastic Pollution in the Environment: A Review. *Bulletin of Environmental Contamination and Toxicology,* 107**,** 577-584.

LODHA, S. J., KORUS, R. A. & CRAWFORD, D. L. 1991. Synthesis and properties of lignin peroxidase fromstreptomyces viridosporus T7A. *Applied Biochemistry and Biotechnology,* 28**,** 411-420.

LOFGREN, L. A., UEHLING, J. K., BRANCO, S., BRUNS, T. D., MARTIN, F. & KENNEDY, P. G. 2019. Genome-based estimates of fungal rDNA copy number variation across phylogenetic scales and ecological lifestyles. *Mol Ecol,* 28**,** 721-730.

LÓPEZ, D., VLAMAKIS, H. & KOLTER, R. 2010. Biofilms. *Cold Spring Harb Perspect Biol,* 2**,** a000398.

LORENZ, T. C. 2012. Polymerase chain reaction: basic protocol plus troubleshooting and optimization strategies. *J Vis Exp***,** e3998.

MAGAN, N. & LACEY, J. 1984. Effects of gas composition and water activity on growth of field and storage fungi and their interactions. *Transactions of the British Mycological Society,* 82**,** 305-314.

MAVERAKIS, E., MIYAMURA, Y., BOWEN, M. P., CORREA, G., ONO, Y. & GOODARZI, H. 2010. Light, including ultraviolet. *J Autoimmun,* 34**,** J247-57.

MBARECHE, H., VEILLETTE, M., BILODEAU, G. & DUCHAINE, C. 2020. Comparison of the performance of ITS1 and ITS2 as barcodes in amplicon-based sequencing of bioaerosols. *PeerJ,* 8**,** e8523.

MCPHERSON, M. & MØLLER, S. 2000. *PCR*, Taylor & Francis.

MELETIADIS, J., MEIS, J. F. G. M., MOUTON, J. W. & VERWEIJ, P. E. 2001. Analysis of Growth Characteristics of Filamentous Fungi in Different Nutrient Media. *Journal of Clinical Microbiology,* 39**,** 478-484.

MO BIO LABORATORIES, I. 2016. PowerSoil® DNA Isolation Kit instruction manual. QIAGEN.

MONARD, C., GANTNER, S. & STENLID, J. 2013. Utilizing ITS1 and ITS2 to study environmental fungal diversity using pyrosequencing. *FEMS Microbiol Ecol,* 84**,** 165-75.

MORRIS, J. 1996. Recycling versus incineration: an energy conservation analysis. *Journal of Hazardous Materials,* 47**,** 277-293.

MUKHERJEE, S. & KUNDU, P. P. 2014. Alkaline fungal degradation of oxidized polyethylene in black liquor: Studies on the effect of lignin peroxidases and manganese peroxidases. *Journal of Applied Polymer Science,* 131.

NDAHEBWA MUHONJA, C., MAGOMA, G., IMBUGA, M. & MAKONDE, H. M. 2018. Molecular Characterization of Low-Density Polyethene (LDPE) Degrading Bacteria and Fungi from Dandora Dumpsite, Nairobi, Kenya. *Int J Microbiol,* 2018**,** 4167845.

NIE, S., HUANG, J., HU, J., ZHANG, Y., WANG, S., LI, C., MARCONE, M. & XIE, M. 2013. Effect of pH, temperature and heating time on the formation of furan in sugar–glycine model systems. *Food Science and Human Wellness,* 2**,** 87-92.

NILSSON, R. H., ANSLAN, S., BAHRAM, M., WURZBACHER, C., BALDRIAN, P. & TEDERSOO, L. 2019a. Mycobiome diversity: high-throughput sequencing and identification of fungi. *Nature Reviews Microbiology,* 17**,** 95-109.

NILSSON, R. H., LARSSON, K. H., TAYLOR, A. F. S., BENGTSSON-PALME, J., JEPPESEN, T. S., SCHIGEL, D., KENNEDY, P., PICARD, K., GLÖCKNER, F. O., TEDERSOO, L., SAAR, I., KÕLJALG, U. & ABARENKOV, K. 2019b. The UNITE database for molecular identification of fungi: handling dark taxa and parallel taxonomic classifications. *Nucleic Acids Res,* 47**,** D259-d264.

NITSCHE, B. M., JØRGENSEN, T. R., AKEROYD, M., MEYER, V. & RAM, A. F. 2012. The carbon starvation response of Aspergillus niger during submerged cultivation: insights from the transcriptome and secretome. *BMC Genomics,* 13**,** 380.

OJHA, N., PRADHAN, N., SINGH, S., BARLA, A., SHRIVASTAVA, A., KHATUA, P., RAI, V. & BOSE, S. 2017. Evaluation of HDPE and LDPE degradation by fungus, implemented by statistical optimization. *Scientific Reports,* 7**,** 39515.

OKAL, E. J., HENG, G., MAGIGE, E. A., KHAN, S., WU, S., GE, Z., ZHANG, T., MORTIMER, P. E. & XU, J. 2023. Insights into the mechanisms involved in the fungal degradation of plastics. *Ecotoxicology and Environmental Safety,* 262**,** 115202.

OZIMEK, E. & HANAKA, A. 2021. Mortierella Species as the Plant Growth-Promoting Fungi Present in the Agricultural Soils. *Agriculture,* 11**,** 7.

PAÇO, A., DUARTE, K., DA COSTA, J. P., SANTOS, P. S. M., PEREIRA, R., PEREIRA, M. E., FREITAS, A. C., DUARTE, A. C. & ROCHA-SANTOS, T. A. P. 2017. Biodegradation of polyethylene microplastics by the marine fungus Zalerion maritimum. *Science of The Total Environment,* 586**,** 10-15.

PERIASAMY, R. & PALVANNAN, T. 2010. Optimization of laccase production by Pleurotus ostreatus IMI 395545 using the Taguchi DOE methodology. *J Basic Microbiol,* 50**,** 548-56.

PORTER, R., ČERNOŠA, A., FERNÁNDEZ-SANMARTÍN, P., CORTIZAS, A. M., ARANDA, E., LUO, Y., ZALAR, P., PODLOGAR, M., GUNDE-CIMERMAN, N. & GOSTINČAR, C. 2023. Degradation of polypropylene by fungi Coniochaeta hoffmannii and Pleurostoma richardsiae. *Microbiological Research,* 277**,** 127507.

PRADHAN, D., KUMAR, A., SINGH, H. & AGRAWAL, U. 2019. Chapter 4 - High-throughput sequencing. *In:* MISRA, G. (ed.) *Data Processing Handbook for Complex Biological Data Sources*. Academic Press.

PROMEGA. 2023. *Protocols for transfection and information on optimization* [Online]. Available: https://no.promega.com/resources/guides/cell-biology/transfection/ [Accessed 17.04 2023].

QIAGEN 2018. Quick-Start Protocol: QIAamp® DNA Mini Kit.

QIAGEN. 2019. *QIAcube®Connect User Manual* [Online]. portalimages. Available: https://portalimages.blob.core.windows.net/products/pdfs/s3evwadj_HB-2594-002_UM_QIAcubeConnect_0919_WW.pdf [Accessed 17.01 2024].

QIAGEN. 2021. *DNeasy® PowerSoil® Pro Kit Handbook* [Online]. Available: https://www.qiagen.com/fi/resources/resourcedetail?id=9bb59b74-e493-4aeb-b6c1-f660852e8d97&lang=en [Accessed 25.04 2023].

QIN, X., SUN, X., HUANG, H., BAI, Y., WANG, Y., LUO, H., YAO, B., ZHANG, X. & SU, X. 2017. Oxidation of a non-phenolic lignin model compound by two Irpex lacteus manganese peroxidases: evidence for implication of carboxylate and radicals. *Biotechnology for Biofuels,* 10**,** 103.

RAJA, H. A., MILLER, A. N., PEARCE, C. J. & OBERLIES, N. H. 2017. Fungal Identification Using Molecular Tools: A Primer for the Natural Products Research Community. *Journal of Natural Products,* 80**,** 756-770.

RONNE, H. 1995. Glucose repression in fungi. *Trends in Genetics,* 11**,** 12-17.

SALVATORE, M. M., ANDOLFI, A. & NICOLETTI, R. 2021. The Genus Cladosporium: A Rich Source of Diverse and Bioactive Natural Compounds. *Molecules,* 26.

SANGER, F., AIR, G. M., BARRELL, B. G., BROWN, N. L., COULSON, A. R., FIDDES, J. C., HUTCHISON, C. A., SLOCOMBE, P. M. & SMITH, M. 1977. Nucleotide sequence of bacteriophage φX174 DNA. *Nature,* 265**,** 687-695.

SANTACRUZ-JUÁREZ, E., BUENDIA-CORONA, R. E., RAMÍREZ, R. E. & SÁNCHEZ, C. 2021. Fungal enzymes for the degradation of polyethylene: Molecular docking simulation and biodegradation pathway proposal. *Journal of Hazardous Materials,* 411**,** 125118.

SATHIYABAMA, M., BOOMIJA, R. V., SATHIYAMOORTHY, T., MATHIVANAN, N. & BALAJI, R. 2024. Mycodegradation of low-density polyethylene by Cladosporium sphaerospermum, isolated from platisphere. *Scientific Reports,* 14**,** 8351.

SCHNEIDER, W. D. H., FONTANA, R. C., MENDONÇA, S., DE SIQUEIRA, F. G., DILLON, A. J. P. & CAMASSOLA, M. 2018. High level production of laccases and peroxidases from the newly isolated white-rot basidiomycete Marasmiellus palmivorus VE111 in a stirred-tank bioreactor in response to different carbon and nitrogen sources. *Process Biochemistry,* 69**,** 1-11.

SCHULZ, H. 2013. Fatty Acid Oxidation. *In:* LENNARZ, W. J. & LANE, M. D. (eds.) *Encyclopedia of Biological Chemistry (Second Edition).* Waltham: Academic Press.

SECCHI, E. & ZARZUR, S. 1999. Plastic debris ingested by a Blainville's beaked whale, Mesoplodon densirostris, washed ashore in Brazil. *Aquatic Mammals,* 25**,** 21-24.

SHAH, A. A., HASAN, F., HAMEED, A. & AHMED, S. 2008. Biological degradation of plastics: A comprehensive review. *Biotechnology Advances,* 26**,** 246-265.

SLATKO, B. E., GARDNER, A. F. & AUSUBEL, F. M. 2018. Overview of Next-Generation Sequencing Technologies. *Curr Protoc Mol Biol,* 122**,** e59.

SONGULASHVILI, G., ELISASHVILI, V., WASSER, S., NEVO, E. & HADAR, Y. 2006. Laccase and manganese peroxidase activities of Phellinus robustus and Ganoderma adspersum grown on food industry wastes in submerged fermentation. *Biotechnol Lett,* 28**,** 1425-9.

SPINA, F., TUMMINO, M. L., POLI, A., PRIGIONE, V., ILIEVA, V., COCCONCELLI, P., PUGLISI, E., BRACCO, P., ZANETTI, M. & VARESE, G. C. 2021. Low density polyethylene degradation by filamentous fungi. *Environmental Pollution,* 274**,** 116548.

STATISTISK-SENTRABYRÅ. 2023. *Statistikkbanken: Gardsbruk, Jordbruksareal og husdyr* [Online]. ssb. Available: https://www.ssb.no/statbank/table/05988 [Accessed 28.03 2024].

STATISTISK-SENTRALBYRÅ. 2020. *Jordbruk og miljø 2019* [Online]. SBB.no. Available: https://www.ssb.no/natur-og-miljo/artikler-og-publikasjoner/_attachment/410151?_ts=16fc1fc8730 [Accessed].

TAGHAVI, N., ZHUANG, W.-Q. & BAROUTIAN, S. 2021. Enhanced biodegradation of non-biodegradable plastics by UV radiation: Part 1. *Journal of Environmental Chemical Engineering,* 9**,** 106464.

TEDERSOO, L., BAHRAM, M., ZINGER, L., NILSSON, R. H., KENNEDY, P. G., YANG, T., ANSLAN, S. & MIKRYUKOV, V. 2022. Best practices in metabarcoding of fungi: From experimental design to results. *Molecular Ecology,* 31**,** 2769-2795.

TEMPORITI, M. E. E., NICOLA, L., NIELSEN, E. & TOSI, S. 2022. Fungal Enzymes Involved in Plastics Biodegradation. *Microorganisms,* 10.

THERMOFISHER-SCIENTIFIC. *PCR Cycling Parameters–Six Key Considerations for Success* [Online]. Available: https://www.thermofisher.com/no/en/home/life-science/cloning/cloning-learning-center/invitrogen-school-of-molecular-biology/pcr-education/pcr-reagents-enzymes/pcr-cycling-considerations.html [Accessed].

THERMOFISHERSCIENTIFIC 2015. User guide: Qubit® dsDNA BR assay Kits.

THERMOFISHERSCIENTIFIC 2016. NanoDrop One User Guide.

THOMPSON, R. C., OLSEN, Y., MITCHELL, R. P., DAVIS, A., ROWLAND, S. J., JOHN, A. W. G., MCGONIGLE, D. & RUSSELL, A. E. 2004. Lost at Sea: Where Is All the Plastic? *Science,* 304**,** 838-838.

TRIOWRAP. 21.05.14. *Instructions* [Online]. Felleskjøpet. Available: https://www.felleskjopet.no/planteproduksjon/grovfor/strekkfilm-og-rundballenett/triowrap-500x25x1800-hvit-50011216/ [Accessed 28.03 2024].

TUVO, B., SCARPACI, M., BRACALONI, S., ESPOSITO, E., COSTA, A. L., IOPPOLO, M. & CASINI, B. 2023. Microplastics and Antibiotic Resistance: The Magnitude of the Problem and the Emerging Role of Hospital Wastewater. *Int J Environ Res Public Health,* 20.

V11, U. *Quality (Phred) scores* [Online]. Drive5. Available: https://www.drive5.com/usearch/manual/quality_score.html [Accessed 23.04 2023].

VALLE, M., NGUYEN VAN LONG, N., JANY, J.-L., KOULLEN, L., COUVERT, O., HUCHET, V. & COROLLER, L. 2023. Impact of carbon dioxide on the radial growth of fungi isolated from dairy environment. *Food Microbiology,* 115**,** 104324.

VASILE, C. & PASCU, M. 2005. *Practical Guide to Polyethylene*, RAPRA Technology.

VELLE, G. B., BJØRN TORGEIR; ESPEDAL, ESPEN OLSEN; HAAVE, MARTE; LANDRO, YNGVE; NORMANN, EIRIK; POSTLER, CHRISTOPH; SKOGLUND, HELGE; STRANZL, SEBASTIAN; STÖGER, ELISABETH; WIERS, TORE 2020. Plast i elver på Vestlandet. *NORCE Miljø*.

VERMA, N. & GUPTA, S. 2019. Assessment of LDPE degrading potential Aspergillus species isolated from municipal landfill sites of Agra. *SN Applied Sciences,* 1**,** 701.

VOSS, R., LEE, R. P. & FRÖHLING, M. 2022. Chemical Recycling of Plastic Waste: Comparative Evaluation of Environmental and Economic Performances of Gasification- and Incineration-

based Treatment for Lightweight Packaging Waste. *Circular Economy and Sustainability,* 2**,** 1369-1398.

WANG, M. & LEMOS, B. 2019. Ribosomal DNA harbors an evolutionarily conserved clock of biological aging. *Genome Res,* 29**,** 325-333.

WANG, X. C., LIU, C., HUANG, L., BENGTSSON-PALME, J., CHEN, H., ZHANG, J. H., CAI, D. & LI, J. Q. 2015. ITS1: a DNA barcode better than ITS2 in eukaryotes? *Mol Ecol Resour,* 15**,** 573-86.

WATKINSON, S. C. 2016. Chapter 5 - Physiology and Adaptation. *In:* WATKINSON, S. C., BODDY, L. & MONEY, N. P. (eds.) *The Fungi (Third Edition).* Boston: Academic Press.

WILKES, R. A. & ARISTILDE, L. 2017. Degradation and metabolism of synthetic plastics and associated products by Pseudomonas sp.: capabilities and challenges. *J Appl Microbiol,* 123**,** 582-593.

WILLIAMS, A. 2022. Standard Operating Procedures of OCA 15EC Contact Angle Goniometer. NED3.

WRIGHT, S. L., ROWE, D., THOMPSON, R. C. & GALLOWAY, T. S. 2013. Microplastic ingestion decreases energy reserves in marine worms. *Current Biology,* 23**,** R1031-R1033.

WU, F., GUO, Z., CUI, K., DONG, D., YANG, X., LI, J., WU, Z., LI, L., DAI, Y. & PAN, T. 2023. Insights into characteristics of white rot fungus during environmental plastics adhesion and degradation mechanism of plastics. *Journal of Hazardous Materials,* 448**,** 130878.

YAMADA-ONODERA, K., MUKUMOTO, H., KATSUYAYA, Y., SAIGANJI, A. & TANI, Y. 2001. Degradation of polyethylene by a fungus, Penicillium simplicissimum YK. *Polymer Degradation and Stability,* 72**,** 323-327.

YANG, F., DING, F., CHEN, H., HE, M., ZHU, S., MA, X., JIANG, L. & LI, H. 2018a. DNA Barcoding for the Identification and Authentication of Animal Species in Traditional Medicine. *Evid Based Complement Alternat Med,* 2018**,** 5160254.

YANG, R. H., SU, J. H., SHANG, J. J., WU, Y. Y., LI, Y., BAO, D. P. & YAO, Y. J. 2018b. Evaluation of the ribosomal DNA internal transcribed spacer (ITS), specifically ITS1 and ITS2, for the analysis of fungal diversity by deep sequencing. *PLoS One,* 13**,** e0206428.

YANG, Y., CHENG, H., LIU, L., DOU, Y. & AN, S. 2020. Comparison of soil microbial community between planted woodland and natural grass vegetation on the Loess Plateau. *Forest Ecology and Management,* 460**,** 117817.

YAO, C., XIA, W., DOU, M., DU, Y. & WU, J. 2022. Oxidative degradation of UV-irradiated polyethylene by laccase-mediator system. *Journal of Hazardous Materials,* 440**,** 129709.

YOUSIF, E. & HADDAD, R. 2013. Photodegradation and photostabilization of polymers, especially polystyrene: review. *Springerplus,* 2**,** 398.

YUAN, J., MA, J., SUN, Y., ZHOU, T., ZHAO, Y. & YU, F. 2020. Microbial degradation and other environmental aspects of microplastics/plastics. *Science of The Total Environment,* 715**,** 136968.

YUE, B. 2014. Biology of the extracellular matrix: an overview. *J Glaucoma,* 23**,** S20-3.

ZENG, Q., LIU, Y., XIAO, L. & AN, S. 2020. Climate and soil properties regulate soil fungal communities on the Loess Plateau. *Pedobiologia,* 81-82**,** 150668.

ZHAO, H., NIE, Y., ZONG, T. K., WANG, Y. J., WANG, M., DAI, Y. C. & LIU, X. Y. 2022. Species Diversity and Ecological Habitat of Absidia (Cunninghamellaceae, Mucorales) with Emphasis on Five New Species from Forest and Grassland Soil in China. *J Fungi (Basel),* 8.

ZHENG, W., CAMPBELL, B. S., MCDOUGALL, B. M. & SEVIOUR, R. J. 2008. Effects of melanin on the accumulation of exopolysaccharides by Aureobasidium pullulans grown on nitrate. *Bioresour Technol,* 99**,** 7480-6.

ZINK, T. & GEYER, R. 2019. Material Recycling and the Myth of Landfill Diversion. *Journal of Industrial Ecology,* 23**,** 541-548.

6. Appendix

Appendix methodology

Appendix 1: Sample collection

Figure A1.1: *Paper interviews. Interviews were conducted to encourage volunteers to participation in the project. Two different interviews were published in at least six different media platforms: Bondebladet, Norges Bondelag, Nationen, Firda, Firda Tidend og Sogn Avis.*

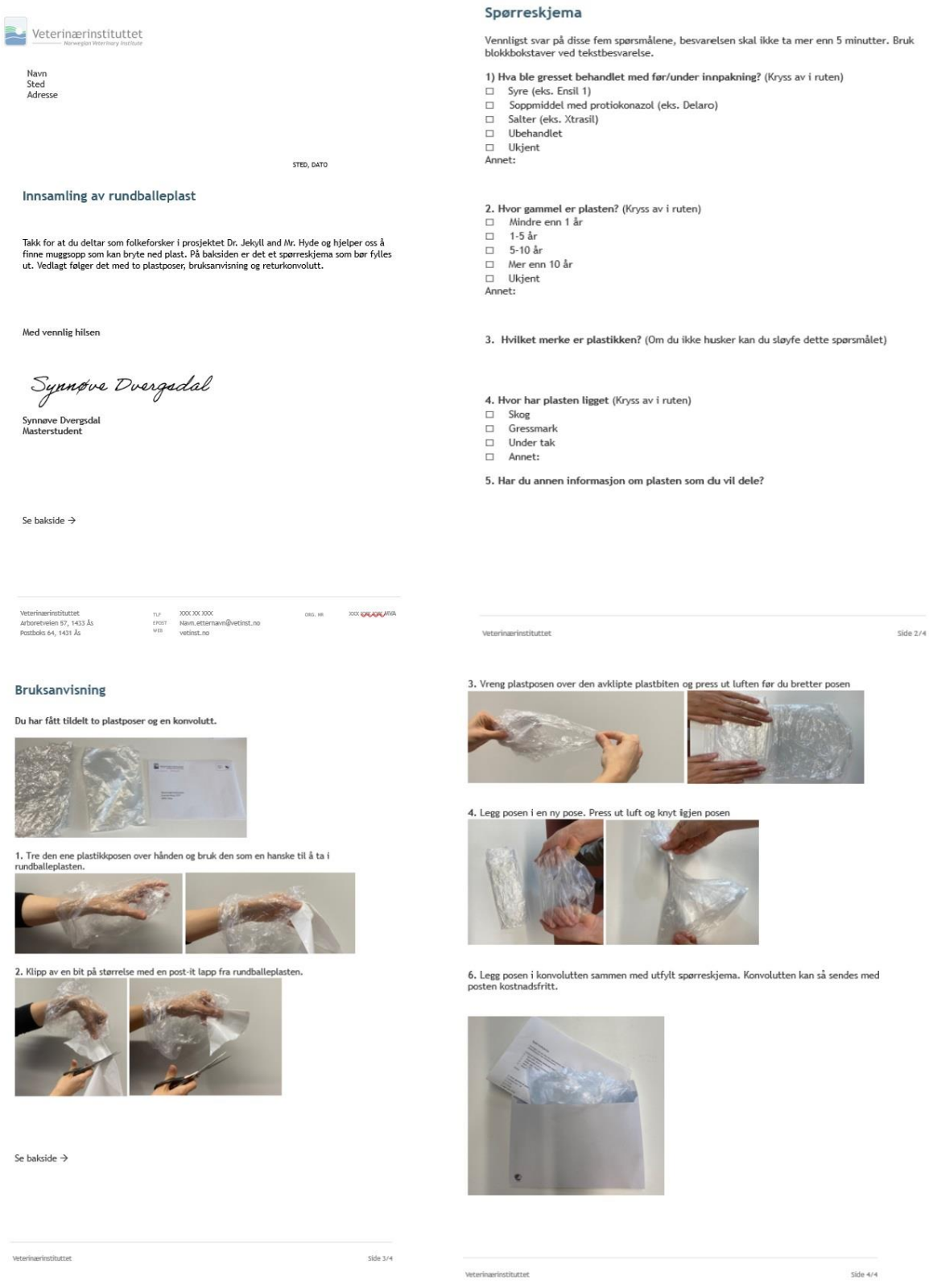

Veterinærinstituttet
Norwegian Veterinary Institute

Navn
Sted
Adresse

STED, DATO

Innsamling av rundballeplast

Takk for at du deltar som folkeforsker i prosjektet Dr. Jekyll and Mr. Hyde og hjelper oss å finne muggsopp som kan bryte ned plast. På baksiden er det et spørreskjema som bør fylles ut. Vedlagt følger det med to plastposer, bruksanvisning og returkonvolutt.

Med vennlig hilsen

Synnøve Dvergsdal

Synnøve Dvergsdal
Masterstudent

Se bakside →

Veterinærinstituttet
Arboretveien 57, 1433 Ås
Postboks 64, 1431 Ås

TLF XXX XX XXX
EPOST Navn.etternavn@vetinst.no
WEB vetinst.no

ORG. NR XXX XXX XXX MVA

Spørreskjema

Vennligst svar på disse fem spørsmålene, besvarelsen skal ikke ta mer enn 5 minutter. Bruk blokkbokstaver ved tekstbesvarelse.

1) Hva ble gresset behandlet med før/under innpakning? (Kryss av i ruten)
- ☐ Syre (eks. Ensil 1)
- ☐ Soppmiddel med protiokonazol (eks. Delaro)
- ☐ Salter (eks. Xtrasil)
- ☐ Ubehandlet
- ☐ Ukjent

Annet:

2. Hvor gammel er plasten? (Kryss av i ruten)
- ☐ Mindre enn 1 år
- ☐ 1-5 år
- ☐ 5-10 år
- ☐ Mer enn 10 år
- ☐ Ukjent

Annet:

3. Hvilket merke er plastikken? (Om du ikke husker kan du sløyfe dette spørsmålet)

4. Hvor har plasten ligget (Kryss av i ruten)
- ☐ Skog
- ☐ Gressmark
- ☐ Under tak
- ☐ Annet:

5. Har du annen informasjon om plasten som du vil dele?

Veterinærinstituttet Side 2/4

Bruksanvisning

Du har fått tildelt to plastposer og en konvolutt.

1. Tre den ene plastikkposen over hånden og bruk den som en hanske til å ta i rundballeplasten.

2. Klipp av en bit på størrelse med en post-it lapp fra rundballeplasten.

Se bakside →

Veterinærinstituttet Side 3/4

3. Vreng plastposen over den avklipte plastbiten og press ut luften før du bretter posen

4. Legg posen i en ny pose. Press ut luft og knyt igjen posen

6. Legg posen i konvolutten sammen med utfylt spørreskjema. Konvolutten kan så sendes med posten kostnadsfritt.

Veterinærinstituttet Side 4/4

Figure A1.2: *Sampling instruction sent to participants. The figures show four different pages from the instructions sent to the participants. In the top left corner, the front page is shown. The front page presented the tasks and thanked the participants for participating in the project. The second page is shown in the top right corner showing*

the information about the sample that were requested. The Third and fourth page is shown in the bottom left and right corner respectively. They show an illustration of how to pick up a plastic sample from the environment.

Appendix 2: DNA Metabarcoding

Table A2.1: *Descriptions of media used in the study. Table shows recipes used for preparation of 1 L of MEA, D18 and MSM media. The media and ingredient list were produced by the NVI media production department. *Added only to the MSM media that were described to contain glucose.*

DG18

Ingredients	**Producer/Product number**	**Amount(g/l)**
Dichloran-Glycerol Agar Base	Oxoid CM729	31.5 g
Glycerol 85%	Merck 1.04094	220 g
Distilled/RO-water		1.0 L
Trace metal solution for CZID and others	NVI, medieproduksjon. KA_K 0009	1.0 ml
Chloramphenicol (50 mg/ml)	NVI, medieproduksjon. KA_K 0007	1.0 ml
Chlortetracycline (5 mg/ml)	NVI, medieproduksjon. KA_K 0010	10.0 ml

MSM with glucose

Ingredients	**Producer/Product number**	**Amount(g/l)**
KH_2PO_4	Merck 1.04873	0,04
K_2HPO_4	Merck 1.05104	0,5
$(NH_4)_2SO_4$	Merck 1.01217	0,2
$MgSO_4 \cdot 7H_2O$	Merck 1.05886	0,02
$CaCl_2 \cdot 2H_2O$	Merck 1.02382	0,002
NaCl	Merck 1.06404	0,1
$FeSO_4$	Merck 1.03965	0,001
Glucose*	Merck 1.08337	20
Distilled/RO-water		

MEA-medium

Ingredients	**Producer/Product number**	**Amount(g/l)**

Malt extract	Oxoid LP0039	20.0 g
Bacto Peptone	Difco 211677	1.0 g
Glucose	Merck	20.0 g
Distilled/RO-water 1.0 L		1.0 L
Agar, Bacteriological grade	Oxoid LP0011	20.0 g

Methods	1	2	3	4		6	7
Pretreatment	Yes	No	No	Yes	Yes	No	No
Beads	None	None	None	None	None	3 x 1 mm	1 x 4 mm
Extraction method	PowerSoil® DNA Isolation Kit	PowerSoil® DNA Isolation Kit	DNeasy® PowerSoil® Pro kit	DNeasy® PowerSoil® Pro kit	PowerSoil® DNA Isolation Kit	DNeasy® PowerSoil® Pro kit	DNeasy® PowerSoil® Pro kit

Table A2.2: Optimalisation of DNA extraction methods. Eight different techniques for DNA extractions were compared to find the most efficient technique that gave the highest DNA yield. Sample 1, 2, 3 4 and 5a were used as test object due to sample abundance. Pretreatment consisted of sonication, vortex, and filtration as described in material and methods. Two of the techniques used different number of beads in different sizes. For extraction, PowerSoil® DNA Isolation (MO BIO, Carlsbad California, USA, Cat: 12888-100) (no longer in sale), and the DNeasy® PowerSoil® Pro kit from QIAGEN was used. PoweSoil® DNA Isolation procedure can be found in PowerSoil® DNA Isolation Kit instruction manual (MO BIO Laboratories, 2016).

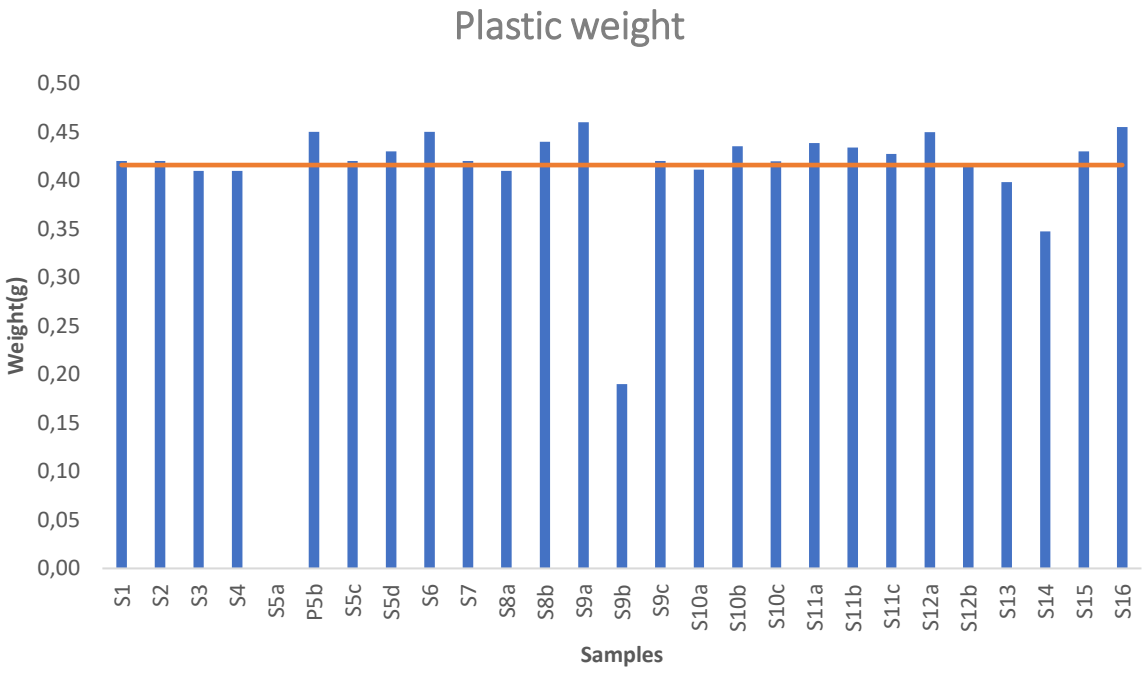

***Figure A2.3**: Extracted plastic samples weight. The figure shows a bar chart over the measured plastic piece weight in grams, that were extracted from each sample to be used in molecular analysis. The orange line illustrates the average. Sample 5a was not weighted (,=.).*

***Table A2.4:** NanoDrop measurement of extracted DNA from plastic samples. From left, column one shows what sample that has been measured while column two shows the measured DNA concentration based on wavelength absorbance. The third column show the absorbance relationship between DNA and proteins, while the fourth column shows the absorbance relationship between DNA and organic compounds. *The same results as shown in table 3.1a.*

Samples	**Concentration (ng/µl)**	**A260/A280**	**A260/A230**
*S1	328.90	1.89	0.64
*S2	84.00	1.92	0.33
*S3	35.30	1.95	0.21
*S4	39.70	1.94	0.10
S5a	42.60	1.87	0.42
S5b	16.10	1.92	0.34
S5c	46.40	1.93	0.31
S5d	79.50	1.90	1.18
S6	16.70	1.91	0.83

S7	4.80	2.27	0.05
S8a	17.80	1.64	0.24
S8b	10.50	2.09	0.04
S9a	13.10	2.06	0.22
S9b	60.60	1.69	0.29
S9c	136.70	1.79	0.90
S10a	16.20	1.67	0.13
S10b	29.70	1.94	0.42
S10c	148.80	1.89	0.76
S11a	9.7	1.84	0.11
S11b	116.40	1.7	0.98
S11c	49.80	1.92	0.32
S12a	74.20	1.9	0.41
S12b	26.60	1.91	0.95
S13	42.3	1.89	0.59
S14	31.00	1.60	0.45
S15	160.40	1.88	0.30
S16	61.70	1.89	1.19

Table A2.5*: Mock community composition. The chosen species originated from Mykeoteket at NVI with exception of Aureobasidium pullulans that was obtained during the project. DNA concentration was determined by Qubit 4 fluorometer.*

Phyllum	**Species**	**Library ID at NVI**	**Proportions (%)**	**DNA concentration (ng/µl)**
Ascomycota	*Penicilium chrysogenum*	VI 06902	17.5	2.51975127
	Saccharomyces cerevisiae	VI 06460	17.5	2.51975127
	Cladosporium allicinum	VI 07060	6	0.86391472
	Candida parapsilosis	VI 07003	17.5	2.51975127

	Aureobasidium pullulans		17.5	2.51975127
Basidiomycota	*Rhodotorula mucilaginosa*	VI 06758	12	1.72782944
	Wallemia sebi	VI 96828	12	1.72782944

Procedure A2.6: *Cell lysis procedure.*

Step	Description
1	Cut 1x1 cm of the fungal colony with a scalpel and transfer to a 2-mL test tube.
2	Add a 4mm sterile steel bead
3	Add 350µl AL-buffer (QIAGEN, Venlo, Netherlands, Cat. 19157)
4	Disrupt the sample by using MM 400 Mixer Mil (RETSCH, Haan, Germany) for 3 minutes at 30 Hz
5	Spin down sample to remove liquid residue from lid
6	Add 10 µl of 20mg/ml Proteinase K (Venlo, Netherlands)
7	Vortex for 5 seconds and spin down the sample
8	Place the tube on a heating block at 56°C with shaking at 550rpm for 30 minutes.
9	Centrifuge the tubes for 5 minutes at 12 000X G
10	Add 200 µl of the supernatant to a new 2-ml test tube.

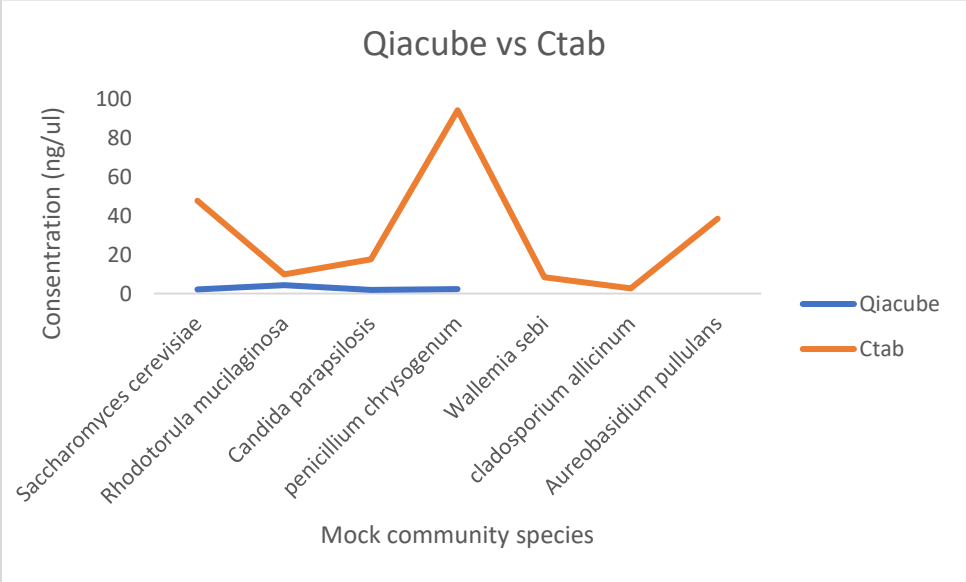

Figure A2.7: *The DNA abundance after Qiacube were meshured with NanoDrop, while the DNA abundance after CTAB were meshured with qubit.*

Procedure A2.8: *CTAB procedure.*

Step	Description
1	Cut 1x1 cm of the fungal colony with a scalpel and transfer to a 2 mL Eppendorf tube
2	Transfer three sterile steel beads into the same tube before freezing the samples for -80 °C in five minutes.
3	Homogenize samples with MM 400 Mixer Mil (RETSCH, Haan, Germany) for 1.5 minutes at 30 Hz
4	Add 500 µl CTAB buffer (TRIS 0,1M m/CTAB 2%, NaCl 1.4M, EDTA 20mM, Ph8.0).
5	Repeat step 3
6	Add 10 µl of 20mg/ml Proteinase K (QIAGEN, Venlo, Netherlands, Cat. 19157)
7	Incubate samples for 15 minutes at 56°C
8	Add 500 µl kloroform.
9	Vortex for 5-10 seconds before shaking on 550rpm for 5 minutes.
10	Centrifuge the samples for 5 minutes at 12 000 x g.
11	Pipet the supernatant to a new 1.5ml Eppendorf tube (approximately 400 uL). Avoid the chloroform.
12	Add 2. volumes (2 x 400 uL). 70% EtOH (-20 °C) and carefully mix by inverting the tube to dissolve the chromatin.
13	Incubate samples in minimum 30 minutes (-20 °C).
14	Centrifuge samples at 14 000 x rpm for 5 minutes.
15	Throw alcohol manually by dynamic inversion.
16	Wash pellet with 500 70% EtOH (-20 °C).
17	Throw alcohol away by using a pipette
18	Let pellet dry
19	Solve the DNA pellet in 75-100 µl TrisHCl buffer, pH 8,0

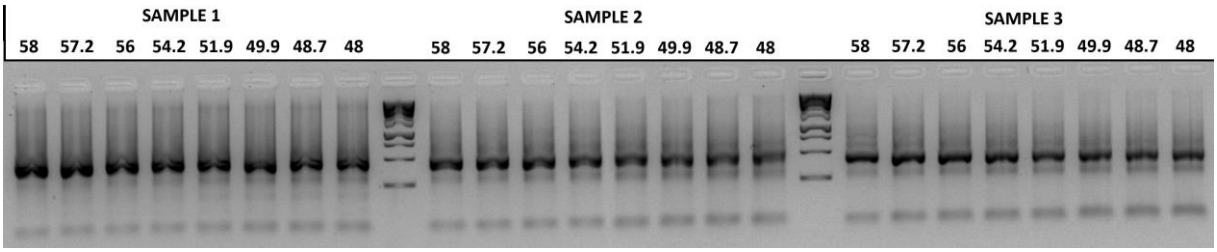

Figure A2.9: Agarose gel electrophoresis results from different annealing temperatures in PCR with 30 x cycles. The figure shows sample one, two and three after PCR 1 amplification with primers for ITS2. The numbers show the different temperatures for the annealing process. Between the samples there is a 1 kB ladder where the second line from the bottom illustrates 500pb. The Samples show clear bands at approximately 410 bp. The ladder intensity does not represent the concentration. Picture was taken with Azure c150 Gel Imaging System (Azure Biosystems, Dublin, California, United States). Figure made by Magdalena MonikaOwczarek-Koscielniak.

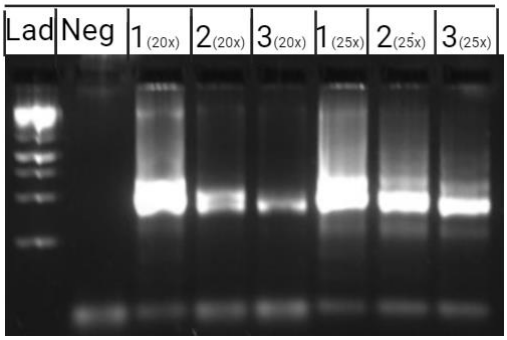

Figure A2.10: *Agarose gel electrophoresis results from different numbers of cycles in PCR. The figure shows sample one, two and three after PCR 1 amplification with primers for ITS2. The numbers show sample under and in parenthesis it is shown the cycle number. Lad stands for 1 kB ladder where the second line from the bottom illustrates 500pb. Neg stand for negative control. The Samples show clear bands at approximately 410 bp. The ladder intensity does not represent the concentration. Picture was taken with Azure c150 Gel Imaging System (Azure Biosystems, Dublin, California, United States).*

Table A2.11: Additional sequences for PCR 2. The table shows the reverse and forward nucleotide sequence that were added to the ITS2 amplicon through PCR 2 together with indexes. The overhand sequence functioned as a binding link between the new sequences and

ITS2 amplicons while Adapter oligos functioned as a binding link between ITS2 amplicons and the Illumina flow cell.

Description	**Overhang sequence**	**Adapter oligo sequence**
Forward sequence	ACACTCTTTCCCTACACGAC	AATGATACGGCGACCACCGAGATCTACAC
Reverse sequence	GTGACTGGAGTTCAGACGTG	CAAGCAGAAGACGGCATACGAGAT

Table A2.12*: Index sequences. The table shows the index sequences used for sample identification. All sequences go from 5`- to 3`- end. The six nucleotides in front of the hyphen illustrates the forward index sequence, while the six nucleotides after the hyphen illustrates the reverse index sequence.*

Sample	**Index**	**Sample**	**Index**
1	TAGTTG-AGGAAT	10c	ATCGTG-ATCAGT
2	TAGTTG-GCTCAT	11a	CGCCTG-AGGAAT
3	TAGTTG-ATCAGT	11b	ATCGTG-CCACTC
4	TAGTTG-GCTACC	11c	ATCGTG-CGTACG
5a	TAGTTG-CCACTC	12a	ATCGTG-CGAAAC
5b	TAGTTG-CGTACG	12b	TGAGTG-CTTTTG
5c	TAGTTG-CGAAAC	13	TGAGTG-AGGAAT
5d	CCGGTG-CTTTTG	14	TGAGTG-GCTCAT
6	CCGGTG-AGGAAT	15	TGAGTG-ATCAGT
7	CCGGTG-ATCAGT	16	TGAGTG-GCTACC
8a	CCGGTG-GCTACC	MOCK	TGAGTG-CGTACG
8b	CCGGTG-CCACTC	Negative from filtration	TGAGTG-CCACTC
9a	CCGGTG-CGTACG	PCR1 negativ from PCR 1 (v11)	TAGTTG-CTTTTG
9b	CCGGTG-CGAAAC	Negative from PCR 1 (Bolyen et al.)	CCGGTG-GCTCAT
9c	ATCGTG-CTTTTG	Negative from PCR 1 (3)	TGAGTG-CGAAAC
10a	ATCGTG-AGGAAT	Negative from PCR 2	CGCCTG-CTTTTG
10b	ATCGTG-GCTCAT		

Table A2.13*: PCR optimalization parameters. The table shows the tested number of cycles and the tested temperatures for PCR amplifications of ITS2 in three samples.*

Optimized PCR processes	**Cycles**	**Temperatures(°C)2.**
Annealing temperature optimalization	30	58, 57.2, 56, 54.2, 49.9, 48.7 and 48
Cycle optimalization	25	56
	20	56

Procedure A2.14: *Agarose gel electrophoresis procedure 1.5% agarose.*

Step	**Description**
1	Weigh up 1.5 g Agarose I™ powder (VWR, Radnor, Pennsylvania, USA, Cas. 9012-36-6)
2	Measure 100mL Tris-borate-EDTA (TBE) buffer into an 100mL Erlendmeyer flask
3	Mix the agarose powder and TBE buffer and boil in microwave until they are mixed
4	Add 7 µl (10 000X GelRed® Nuclei Acid Stain (MERCK Millipore, Burlington, Massachusetts, USA, Cat. SCT123)c to the solution
5	Add the solution to the GelTray and add the combs
6	Transfere the gel to a prefilled system with TBE buffer
7	Mix 5 µl sample with 1µl Loading Dye (ThermoFisher, Waltham, Massachusetts, USA, Cat. R1161) before adding the mixture to a well in the agarose gel
8	Add 3 µl 1 kb GeneRuler Ready-to-use (ThermoFisher, Waltham, Massachusetts, USA, Cat. SM0313) to the left end well. The GeneRuler does not represent the real concentration with this volume
9	Run the gel for approximately 45 minutes on 80 V

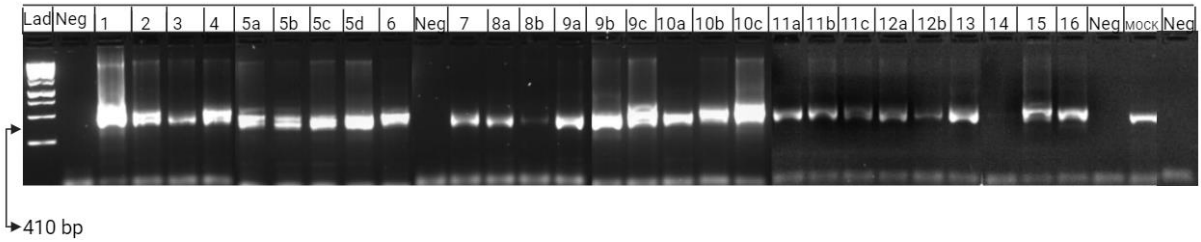

Figure A2.15: Agarose gel electrophoresis of all samples. The figure shows Agarose gel electrophoresis results after PCR 1 amplification with primers for ITS2. Lad stands for 1 kB ladder where the second line from the bottom illustrates 500pb. The ladder intensity does not represent the concentration. Picture was taken with Azure c150 Gel Imaging System (Azure Biosystems, Dublin, California, United States).

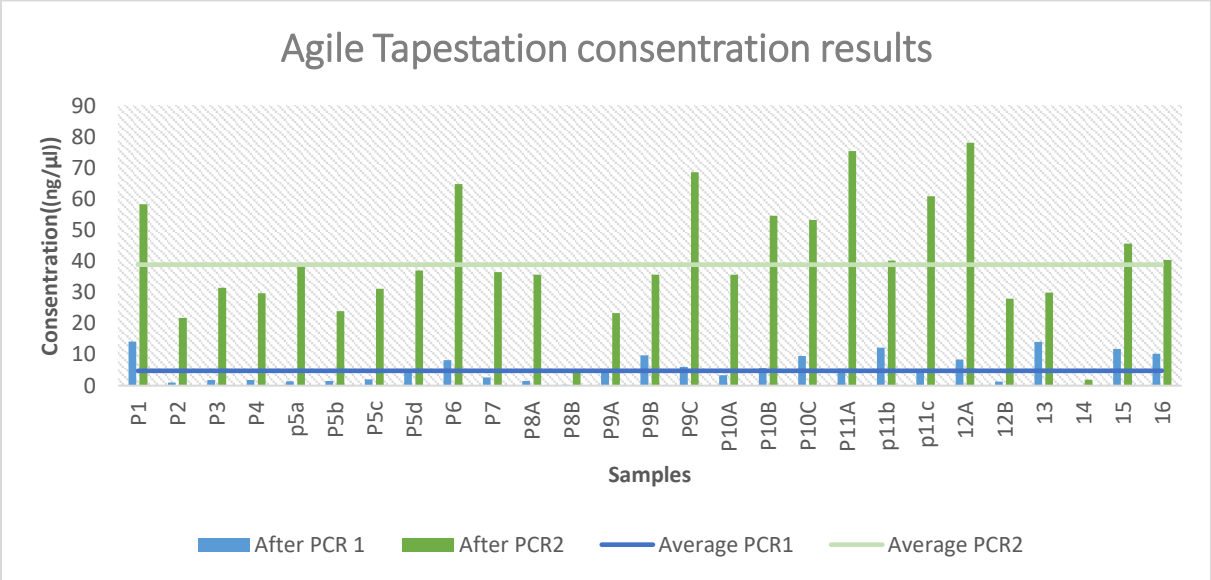

***Figure A2.16**: Agilent tape station measured concentration. The figure shows sample 1 to sample 16 and their respective DNA concentration after both PCR1 and PCR2. The measurement with agile tape station were preformed after PCR and ampure cleaning.*

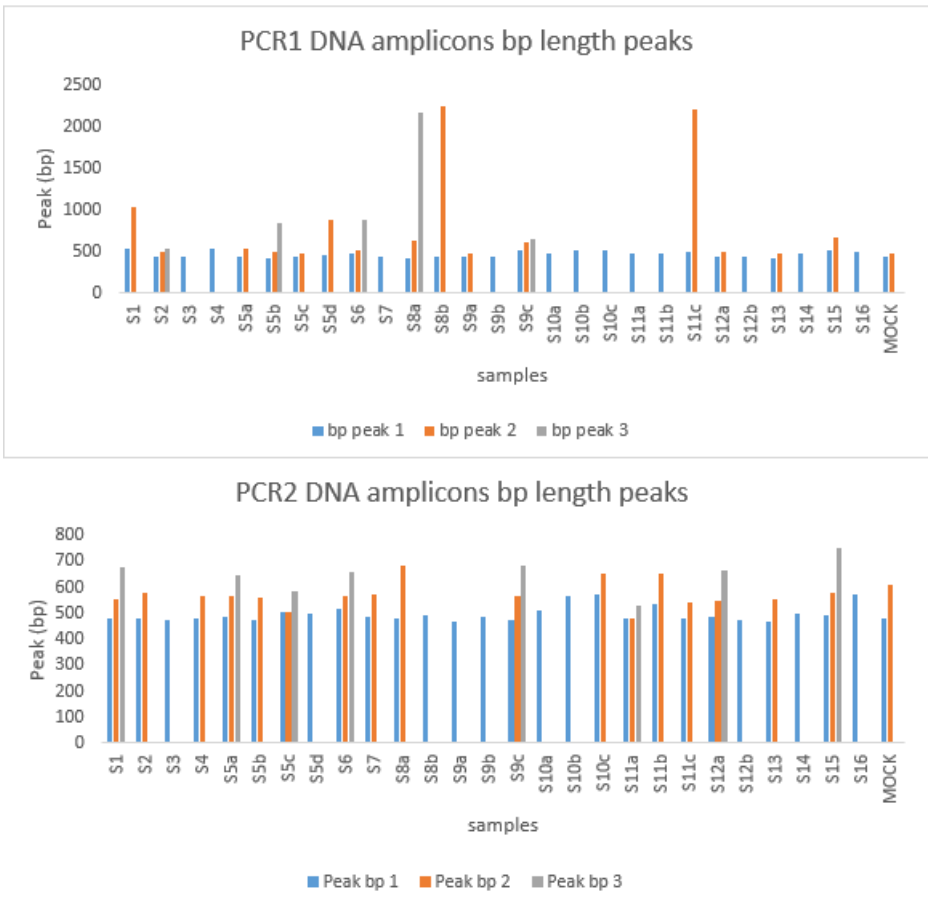

***Figure A2.17**: PCR DNA amplicon bp length peaks results. The table shows the bp peaks measured with agile tape station for each sample. For the figure representing PCR2 amplicon, peaks with a concentration at 1 ng/µl or lower were excluded from the results.*

Appendix 3: Cultivation and isolation of plastic degrading fungi

***Table A3.1**: Primer used to identify a specific fungal genera. The table shows a list at which different genetic markers that were used to identify a specific fungal genera down to species lever.*

Genetic markers	Aureobasidium	Ganoderma	Aspergillus	Cladosporium	Mortierella	Alternaria	Penicillium
Genetic markers	ITS *LSU* *RPB2*(Bolyen et al.)	ITS TEF1-α(v11) *RPB2*(v11)	ITS *BT2* Cal	ITS Cal TEF1-α(Bolyen et al.)	ITS TEF1-α(Bolyen et al.) RPB1	ITS *BT2* Cal	ITS *BT2* Cal

RPB2(Bolyen et al.)

Table A3.2: PCR reactions for different primers. A list of PCR reagents for differen and their respective volumues for each genetic marker.

Genetic markers	**Reagents**	**Volume**
ITS	10 x DreamTaqBuffer	2.5
	Water	18.875
	dNTPs mix 2 mM	0.5
	Forward	0.5
	Reverse	0.5
	5 U/µL DreamTaq DNA polymerase	0.125
	DNA template	2
CAL *RPB2*(v11) *RPB2*(Bolyen et al.) TEF1-α(v11) RPB1	10 x DreamTaqBuffer	2.5
	Water	17.875
	dNTPs mix 2 mM	0.5
	Forward	0.5
	Reverse	0.5
	5 U/µL DreamTaq DNA Polymerase	0.125
	DNA template	3

Table A3.3*: PCR conditions for genetic markers. Genetic markers shown with cycle stages, time, temperature and cycle number.*

Genetic markers	**Cycle stages**	**Time**	**Temperature** (Cº)	**Cycles** (x)
	First denaturation	3 min	95	

ITS: *Ganoderma* *Aspergillus* *Mortierella/* *Absidia* *Penicillium*	Denaturation	45 sec	95	10
	Annealing	45 sec	60 –50 (meltdown)	
	Extension	90 sec	72	
	Denaturation	45 sec	95	25
	Annealing	45 sec	50	
	Extension	90 sec	72	
	Final extension	7 min	72	
	Hold	Infinite	4	
ITS: *Aurobasidium* *Cladosporium* *Alternaria*	First denaturation	3 min	94	
	Denaturation	45 sec	94	35
	Annealing	45 sec	50	
	Extension	90 sec	72	
	Final extension	6 min	72	
	Hold	Infinite	4	
cal *rpb2*(v11) *rpb2*(Bolyen et al.)	First denaturation	3 min	95	
	Denaturation	1 min	95	35
	Annealing	1 min	55	
	Extension	2 min	72	
	Final extension	10 min	72	
	Hold	Infinite	4	
tef1-α (v11)	First denaturation	3 min	95	
	Denaturation	50 sek	95	40
	Annealing	50 sek	48	
	Extension	50 sek	72	
	Final extension	7 min	72	
	Hold	Infinite	4	
rpb1: Cladosporium	First denaturation	3 min		
	Denaturation	1 min	95	35
	Annealing	1 min	95	
	Extension	2 min	59	

	Final extension	10 min	72		
	Hold	Infinite	72		
rpb1: *Mortierella/ Absidia*	First denaturation	3 min	95		
	Denaturation	1 min	95		35
	Annealing	1 min	52.2		
	Extension	2 min	72		
	Final extension	10 min	72		
	Hold	Infinite	4		
LSU *tef1-α* (Bolyen et al.): *Mortierella/ Absidia*	First denaturation	3 min	94		
	Denaturation	45	94	35	
	Annealing	45	52		
	Extension	90	72		
	Final extension	6	72		
	Hold	Infinite	4		
tef1-α(Bolyen et al.) *Cladosporium*	First denaturation	3 min	94		
	Denaturation	45 sek	94	30	
	Annealing	30 sek	52		
	Extension	90 sek	72		
	Final extension	6 min	72		
	Hold	Infinite	4		
bt2	First denaturation	5 min	95		
	Denaturation	95 sek	95	35	
	Annealing	20 sek	58		
	Extension	30 sek	72		
	Final extension	6 min	72		
	Hold	Infinite	4		

Appendix 4: Growing fungi on plastic

Table A4.1: *LDPE piece sample number overview.*

Fungi	***Aureobasidium sp.***		***Ganoderma sp.***		***Aspergillus sp.***		***Cladosporium sp.***		***Mortierella sp.***		***Alternaria sp.***		***Penicillium sp.***		***Control***	
	Uv	***Not-UV***	***Uv***	***Not-UV***	***Uv***	***Not-UV***	***Uv***	***Not-UV***	***Uv***	***Not-UV***	***Uv***	***Not-UV***	***Uv***	***Not-UV***	***Uv***	***Not-UV***
MSM with Glucose	*1a*	*1b*	*2a*	*2b*	*3a*	*3b*	*4a*	*4b*	*5a*	*5b*	*6a*	*6b*	*7a*	*7b*	*8a*	*8b*
MSM without glucose	*9a*	*9b*	*10a*	*10b*	*11a*	*11b*	*12a*	*12b*	*13a*	*13b*	*14a*	*14b*	*15a*	*15b*	*16a*	*16b*
Soil	*17a*	*17b*	*18a*	*18b*	*19a*	*19b*	*20a*	*20b*	*21a*	*21b*	*22a*	*22b*	*23a*	*23b*	*24a*	*24b*

Appendix 5: Analysing plastic

Table A5.1: Fixation solution recipe

Step	**Description**
1	Mix 50 ml of 4% paraformaldehyde with 25 ml 0.1 M PIPES buffer.
2	Add 5 ml 25% glutaraldehyde
3	Add 20 ml distilled H_2O

Procedure A5.2: Pre dehydration procedure. The performed with stirring.

Step	**Description**
1	Remove liquid (fixation mix) from samples and add 0.05 PIPES buffer, pH 7. Let the buffer stay for 10 minutes and repeat the step two more times.
2	Remove liquid (buffer) from samples and add ethanol. Let the ethanol stay for 10 minutes. Repeat this step with 30%, 50%, 70%, 90% and 96% ethanol
3	Remove liquid(ethanol) from samples and add 100% ethanol. Let the ethanol stay for 10 minutes and repeat the step two more times.

Appendix results

Appendix 6: Sample collection

Table A6.1: *Platic wrap sample information. The information is based on information from This sample information is the information used as metadata for the bioinformatic part in metabarcoding.*

sample-id	Countrypart	Age	Area_conditions	Grass_treatment
1	Western country	10	Grassland	Formic_acid
2	Western country	Unknown	Grassland	Unknown
3	Eastern country	Unknown	Grassland	Unknown
4	Eastern country	3	Grassland	Natural_silage
5a	Eastern country	7	Grassland	Unknown
5b	Eastern country	7	Grassland	Unknown
5c	Eastern country	7	Grassland	Unknown
5d	Eastern country	7	Grassland	Unknown
6	Western country	10	Under_roof	Unknown
7	Western country	7	Under_roof	Unknown
8a	Western country	10	Under_roof	Natural_silage
8b	Western country	10	Grassland	Natural_silage
9a	Eastern country	30	Forest	Untreated

9b	Eastern country	7	Forest	Formic_acid
9c	Eastern country	10	Forest	Formic_acid
10a	Western country	2	Forest	Unknown
10b	Western country	8	Forest	Unknown
10c	Western country	8	Forest	Unknown
11a	Eastern country	10	Under_roof	Unknown
11b	Eastern country	10	Grassland	Natural_silage
11c	Eastern country	10	Grassland	Natural_silage
12a	Western country	15	Berry_farming	Unknown
12b	Western country	28	Grassland	Unknown
13	Trøndelag	10	Forest	Unknown
14	Western country	7	Under_roof	Acid
15	Western country	10	Forest	Acid
16	Eastern country	1	Grassland	Unknown

Appendix 8: Cultivation and isolation of plastic degrading fungi

A8.1: *The seven selected genera isolated.*

Isolate	Morfological identification	Isolated from
1	*Aureobasidium*	Eastern Norway(S11a)
2	*Ganoderma*	NVI Mycoteket

3	*Aspergillus*	Western Norway (S7)
4	*Cladosporium*	Eastern Norway (S4)
5	*Mortierella*	Eastern Norway (5d)
6	*Alternaria*	Eastern Norway (11)c
7	*Penicillium*	Western Norway (12a)

Table A8.2: *NanoDrop measurement after DNA extraction. From left, column one shows the fungal identity based on microscopy, while column two shows the measured DNA concentration based on wavelength absorbance. The third column show the absorbance relationship between DNA and proteins, while the fourth column shows the absorbance relationship between DNA and organic compounds.*

Fungi	ng/ul	A260/A280	A260/A230
Aureobasidium	194.4	2.17	2.11
Ganoderma	111.1	2.13	1.52
Aspergillus	47	2.14	1.07
Cladosporium	16.1	2.06	0.62
Mortierella	5.1	3.1	0.27
Alternaria	63.6	2.14	1.3
Penicillium	11.1	2.32	0.49

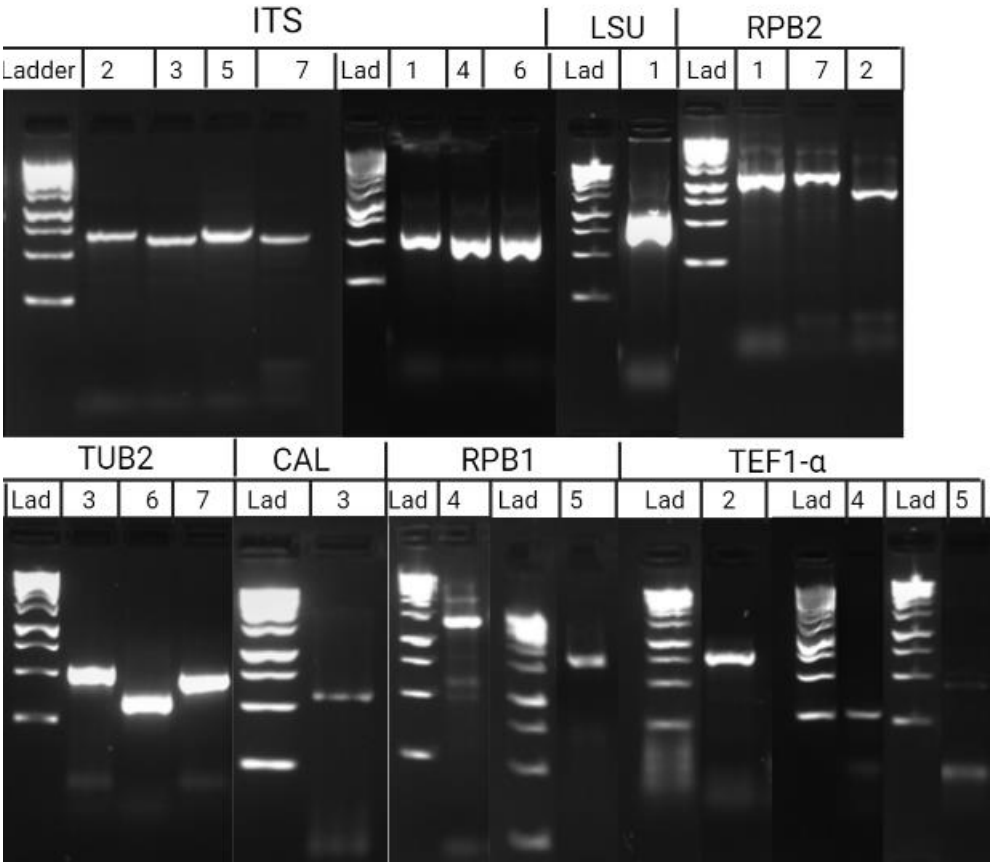

Figure A8.3*: Agarose gel electrophoresis of isolated fungi. The figure shows Agarose gel electrophoresis results after PCR amplification with different primers for different isolates. The primers used were ITS, LSU, RPB2, BT2, CAL, RPB1 and TEF1-α. The isolates used were the mikroscopicly identified Aureobasidium Sp (v11), Ganoderma Sp (Bolyen et al.), Aspergillus Sp (**3**), Cladosporium Sp (**4**), Mortierella Sp (**5**), Alternaria Sp (**6**) and Penicillium (**7**). Lad stands for 1 kB ladder. The ladder intensity does not represent the concentration. Picture was taken with Azure c150 Gel Imaging System (Azure Biosystems, Dublin, California, United States).*

Table A8.4: *NSM and number of repicates. The most fittting NSM values identifyed through MEGA 11 and the number of replicates used in gitbash to make a phylogenetic tree for each fungal isolate.*

Isolate genus	**NSM**	**Number of replicates**
Aureobasidium	TN93+G+I	640
Ganoderma	HKY+G+I	320
Aspergillus	K80+G+I	1000
Cladosporium	K80+G	1000

Absidia	HKY+G+I	768
Alternaria	K80+G	1000
Penicillium	TN93+G+I	512

Appendix 19: Growing fungi on plastic

***Table A9.1**: Wettability measurements. The table shows the water droplet angle on the LDPE measured before and after UV radiation. The angle reduction after radiation is calculated in the last column.*

Plastic ID	**Before UV-radiation (B_f)(º)**	**After UV-radiation (A_f) (º)**	**Reduction (A_f - B_f) (º)**
1a	97.575	71.63	-25.95
2a	91.625	68.20	-23.43
3a	90.825	70.23	-20.60
4a	90.625	76.43	-14.20
5a	95.25	73.55	-21.70
6a	92.7	72.35	-20.35
7a	87.1	72.63	-14.48
8a	94.575	73.35	-21.23
9a	91.85	68.48	-23.38
10a	91.75	71.88	-19.88
11a	90	63.03	-26.98
12a	98.875	73.50	-25.38
13a	94.675	66.95	-27.73
14a	88.575	66.78	-21.80
15a	97.375	69.78	-27.60
16a	93.65	75.80	-17.85
17a	91.475	72.08	-19.40
18a	94.975	72.23	-22.75
19a	97.25	70.33	-26.93
20a	93.075	71.75	-21.33
21a	96.8	68.60	-28.20

22a	91.275	74.53	-16.75
23a	88.825	66.73	-22.10
24a	94.8	70.78	-24.03
25a	98.15	68.48	-29.68
26a	96.725	68.75	-27.98
27a	97.35	66.13	-31.23

Table A9.2*: OD values of samples grown In MSM with glucose. *= outlier.*

Day	**1a**	**1b**	**2a**	**2b**	**3a**	**3b**	**4a**	**4b**	**5a**	**5b**	**6a**	**6b**	**7a**	**7b**	**8a**	**8b**
2	0	0	0	0	0	0	0	0	0*	0	0	0	0	0	0	0
7	0.103	0.119	0.004	0.004	0.014	0.012	0.01	0.007	0.053	0.006	0.001	-0,001	0,003	0,006	0	0
14	1.326	1.474	0.001	0.013	0.015	0.008	0.001	-0.002	0.059	0.015 *	0.051	0.024	0.009	0.022	0	0
21	1.281	2.003	0.001	0.001	0.049	0.034	0.002	0.005	0.006 *	0.003	0.049	0.025	0.012	0.904 *	0.007	0.004
28	0.848	1.237	0	0	0.053	0.03	0.006	0.002	0.056	0.001	0.045	0.026	0.015	0.075	0	0.01 *
35	0.747	0.845	0.114 *	0	0.169	0.035	0.025	0.007	0.056	0.001	0,055	0,035	0,014	0,08	0,001	0,001
42	1.512	1.683	0.003	0.003	0.194	0.099	0.22 *	0.004	0.056	0	0.057	0.081	0.036	0.321	-0.002	-0.002
49	1.077	0.538	0.001	0	0.185	0.062	0.041	0.014	0.059	0.008	0.406 *	0.177	0.028	0.125	0.008	0.007
56	0.98	0.61	0.00	0.09 *	0.09	0.04	0.04	0.02	0.06	0.00	0.09	0.18	0.04	0.31	0.00	0.00
63	2.341 *	1.056	0.013	0.013	0.147	0.083	0.071	0.033	0.054	0.001	0.101	0.201	0.027	0.259	0.046 *	0.006
70	1.038	0.77	0.024	0.009	0.164	0.097	0.08	0.043	0.054	0.001	0.17	0.133	0.045	0.09	0.004	0.006
76	1.667	0.685	0.001	0	0.155	0.064	0.033	0.173 *	0.058	0.005	0.118	0.171	0.043	0.205	0.001	0
88	1.215	0.855	0	0.007	0.114	0.071	0.225 *	0.111	0.054	0	0.1	0.176	0.035	0.132	0	0

***Table A9.3**: OD values of samples grown In MSM without glucose. *= outlier.*

Day	9a	9b	10a	10b	11a	11b	12a	12b	13a	13b	14a	14b	15a	15b	16a	16b
2	0	0	0	0	0	0	0	0	0	0	0	0	0	0	0	0
7	0.003	0.004	0.001	0.003	0	0.001	0	0.001	0.002	0.001	0.002	0.001	0.002	0.002	0.001	0.002
14	0.014	0.006	0.007	0.009	0.006	0.001	0.021	0.009	0.006 *	0	0	0.008	0.012	0.003	0.005	0.006 *
21	0.015	0.016	0.013	0.027	0.01	0.018	0.014	0.014	0.002	0.003	0.003	0.011	0.017	0.004	0.004	0.002
28	0.012	0.009	0.013	0.12	0.15 *	0.003	0.014	0.013	0.001	0.014 *	0.001	0.03	0.014	0.002	0.002	0.002
35	0.017	0.017	0.018	0.251 *	0.019	0	0.018	0.02	0.002	0.001	0	0.013	0.129 *	0.002	0	0.001
42	0.015	0.015	0.031	0.018	0.018	0.001	0.017	0.015	0.002	0.004	0.003	0.016	0.033	0.004	0.002	0.002
49	0.019	0.021	0.039	0.028	0.023	0.014	0.024	0.023	0.003	0.003	0.003	0.19 *	0.026	0.002	0.003	0.002
56	0.021	0.024	0.052	0.026	0.022	0.010	0.025	0.032	0.001	0.006	0.024 *	0.039	0.024	0.006	0.046 *	0.00
63	0.036	0.035	0.045	0.029	0.029	0.005	0.052 *	0.021	0.004	0.008	0.001	0.02	0.037	0.008	0.001	0.003
70	0.038	0.047	0.047	0.031	0.029	0.003	0.021	0.035	0	0	0	0.016	0.029	0.001	0.003	0
76	0.039	0.041	0.036	0.034	0.029	0.005	0.018	0.02	0	0	0	0.018	0.029	0.003	0.001	0
88	0.042	0.041	0.035	0.045	0.032	0.043 *	0.023	0.025	0.003	0.002	0.002	0.036	0.039	0.008	0.003	0.003

***Table A9.4**: pH values of samples grown In MSM with glucose. *= outlier.*

Day	1a	1b	2a	2b	3a	3b	4a	4b	5a	5b	6a	6b	7a	7b	8a	8b
2	4.704 *	4.704 *	4.704	4.704 *	4.704 *	4.704 *	4.704 *	4.704 *	4.704 *	4.704 *	4.704 *	4.704 *	4.704 *	4.704 *	4.704 *	4.704 *
7	3.056	4.248	3.01	4.291	2.851	2.924	4.096	4.471	4.246	4.308	4.384	4.337	3.566	3.196	4.681 *	4.427
14	2.88	3.081	4.109	4.121	2.74	2.732	3.492	3.54	3.245	4.261	3.387	3.344	3.112	2.767	4.258	4.28
21	2.858	2.875	3.992	4.017	2.821	2.82	3.227	3.247	3.32	4.335	3.247	3.335	2.946	2.814	4.299	4.32

28	2.905	2.894	3.941	3.955	2.887	2.864	3.002	3.037	3.356	4.35	3.266	3.35	2.886	2.875	4.32	4.34
35	2.789	2.779	3.666	3.832	2.792	2.784	2.82	2.839	3.289	4.308	3.13	3.196	2.773	2.831	4.329	4.384
42	2.809	2.819	3.617	3.757	2.806	2.778	2.825	2.826	3.289	4.281	3.083	3.114	2.795	2.838	4.246	4.277
49	2.81	2.757	3.553	3.711	2.795	2.77	2.792	2.798	3.267	4.22	2.955	2.941	2.73	2.772	4.202	4.221
56	2.809	2.787	3.503	3.66	2.788	2.788	2.833	2.836	3.302	4.249	2.937	2.936	2.759	2.82	4.231	4.23
63	2,847	2,796	3,485	3,713	2,686	2,697	2,776	2,912	3,471	4,373	2,894	2,831	2,658	2,704	4,286	4,266
70	2,4	2,3	2,25*	3,53	2,55	2,55	2.56	2.39	3.07	4.14	2.45	2.35	2.65	2.45	4.16	4.18
76	2.49	2.34	3.05	3.4	2.56	2.55	2.49	2.51	3.06	4.15	2.61	2.67	2.44	2.5	4.2	4.22
88	2.65	2.38	2.97	3.28	2.4	2.4	2.38	2.53	2.9	4.32	2.54	2.53	2.37	2.47	4.13	4.1

Table A9.5*: pH values of samples grown In MSM without glucose. *= outlier.*

Day	**9a**	**9b**	**10a**	**10b**	**11a**	**11b**	**12a**	**12b**	**13a**	**13b**	**14a**	**14b**	**15a**	**15b**	**16a**	**16b**
2	5.623	5.623	5.623	5.623	5.623	5.623	5.623	5.623	5.623	5.623	5.623	5.623	5.623	5.623	5.623	5.623
7	5.427	5.463	5.473	5.461	5.487	5.467	5.489	5.508	5.489	5.492	5.573	5.592	5.566	5.561	5.539	5.533
14	5.409	5.475	5.473	5.464	5.464	5.469	5.435	5.442	5.471	5.486	5.457	5.439	5.446	5.45	5.453	5.457
21	5.533	5.558	5.559	5.543	5.55	5.552	5.54	5.525	5.557	5.56	5.559	5.547	5.541	5.549	5.541	5.549
28	5.544	5.586	5.579	5.56	5.573	5.57	5.563	5.554	5.586	5.576	5.572	5.563	5.558	5.575	5.548	5.559
35	5.635	5.637	5.634	5.613	5.62	5.645	5.629	5.608	5.636	5.641	5.693	5.641	5.625	5.645	5.624	5.626
42	5.537	5.553	5.268	5.47	5.525	5.545	5.532	5.515	5.518	5.539	5.551	5.543	5.532	5.556	5.532	5.535
49	5.502	5.514	5.296	5.473	5.495	5.504	5.485	5.477	5.498	5.498	5.502	5.498	5.5	5.521	5.468	5.485
56	5.493	5.393	5.297	5.452	5.471	5.495	5.446	5.442	5.48	5.488	5.484	5.477	5.46	5.508	5.431	5.48
63	5.436	5.526	5.399	5.608	5.543	5.593	5.565	5.58	5.59	5.615	5.556	5.566	5.541	5.593	5.56	5.59*
70	5.36	5.46	5.36	5.53	5.5	5.61	5.43	5.49	5.56	5.46	5.36	5.41	5.5	5.58	5.43	5.48

76	5.39	5.38	5.29	5.48	5.46	5.54	5.46	5.59	5.68	5.58	5.37	5.54	5.49	5.44	5.4	5.57
88	5.49	5.47	5.35	5.34 *	5.42	5.55	5.3 *	5.4	5.47	5.4	5.38	5.35	5.39	5.45	5.43	5.5

Table A9.6: Contamination control at the end of the experiment. The table shows which of the samples that was contaminated (Cont.).

Sample	1a	2a	3a	4a	5a	6a	7a	8a
Cont.	None	none	None	Fungi	Fungi	None	None	Fungi
Sample	1b	2b	3b	4b	5b	6b	7b	8b
Cont.	None	none	None	Fungi	Fungi	None	None	Fungi
Sample	9a	10a	11a	12a	13a	14a	15a	16a
Cont.	None	Bakteria	None	None	Fungi	None	None	Fungi
Sample	9b	10b	11b	12b	13b	14b	15b	16b
Cont.	None	Bacteria	None	None	Fungi	Fungi and bacteria	None	Fungi
Sample	17a	18a	19a	20a	21a	22a	23a	24a
Cont.	None	None	None	None	Fungi	None	None	Fungi
Sample	17b	18b	19b	20b	21b	22b	23b	24b
Cont.	None	None	None	None	Bacteria	None	None	Fungi

Norges miljø- og biovitenskapelige universitet
Noregs miljø- og biovitskapelege universitet
Norwegian University of Life Sciences

Postboks 5003
NO-1432 Ås
Norway